Abstract

Subdivision schemes are recursive methods for generating smooth functions from discrete data. These schemes have received considerable attention in the last decades because they allow designs of efficient, local, and hierarchical modeling algorithms in a wide range of applications related to computer-aided geometric design, computer graphics, and the recent area of interest like fractional calculus. A subdivision starts with a set of initial control points and then recursively generates denser control points by a linear combination of nodes of a lower refinement level.

Spline functions and subdivision schemes are strongly linked. To be more specific, several authors widely discussed smooth subdivision schemes based on polynomial splines in the literature. Accordingly, we have devoted this Ph.D. thesis to providing an in-depth theoretical and practical study of subdivision schemes based on non-polynomial splines, i.e., cycloidal splines. Namely, we have considered the splines spanned by polynomials and trigonometric or hyperbolic functions.

This Ph.D. thesis is divided into two parts: The first section is about hyperbolic algebraic splines. Indeed, uniform algebraic hyperbolic B-splines of any degree k have been examined. Then, for each arbitrary order k, we established a general formula for the refinement equations. The subdivision schemes are established using these refinement equations. Finally, we provided a new multiresolution technique for curves of general topology to introduce a new inverse subdivision scheme connected with algebraic hyperbolic B-splines of order $k = 3$. Numerical results back up theoretical conclusions.

We proposed a new algebraic trigonometric Hermite interpolation operator in the second part. This operator interpolates the function values and the first derivative values at the break-points of a partition. The considered Hermite interpolating splines give an optimal convergence order and produce linear polynomials and trigonometric functions. Hence, quadrature rules with endpoint corrections are provided based on integrating the considered Hermite interpolating splines. These rules are employed to solve the 1-D Fredholm integral equations numerically. The error bound is examined, and numerical examples of the proposed interpolating splines' performance are provided.

Keywords: Uniform algebraic hyperbolic B-splines, Uniform algebraic trigonometric B-splines, Subdivision scheme, Reverse subdivision scheme, Multiresolution Analysis, Wavelets, Hermite spline interpolation, Quadrature rule, Fredholm integral equation.

Mohamed Ajeddar

A study of non-polynomial splines and their Numerical applications

2021/2022

جامعة الحسن الأول
UNIVERSITÉ HASSAN 1ER

Université Hassan 1er
Centre d'Études Doctorales en Sciences et Techniques & Sciences Médicales

كلية العلوم و التقنيات سطات
FACULTÉ DES SCIENCES ET TECHNIQUES SETTAT

Faculté des Sciences et Techniques Settat

THÈSE DE DOCTORAT

Pour l'obtention de grade de Docteur en Sciences et Techniques

Formation Doctorale : Mathématiques, Informatique et Applications

Spécialité : Mathématiques Appliquées

Sous le thème

A study of non-polynomial splines and their Numerical applications

Présentée par :

Mohamed Ajeddar

Soutenue le : 31 Mars 2022 à 10h à la Faculté des Sciences et Techniques de Settat devant le jury composé de :

Mr. Mohammed Zakkari	**PES**	**Faculté des Sciences et Techniques, Settat**	**Président**
Mr. Mohammed Louzar	**PES**	**Faculté des Sciences et Techniques, Settat**	**Rapporteur**
Mr. Aziz Ikemakhen	**PES**	**Faculté des Sciences et Techniques, Marrakech**	**Rapporteur**
Mr. Mohammed Mestari	**PES**	**Ecole Normale Supérieure de l'Enseignement Technique, Mohammedia**	**Rapporteur**
Mr. Mohamed Abdou El Omary	**PES**	**Faculté des Sciences et Techniques, Settat**	**Examinateur**
Mr. Abdellah Lamnii	**PES**	**École Normal Supérieure, Tétouan**	**Co-Directeur de thèse**
Mr. Abdelghani Ben Tahar	**PES**	**Faculté des Sciences et Techniques, Settat**	**Directeur de thèse**

Année Universitaire : 2021/2022

Remerciement

Cette thèse a été effectuée au département de Mathématiques et Informatique de la Faculté des sciences et techniques Settat, au sein du Laboratoire de Mathématiques, Informatique et Sciences de l'Ingénieur (MISI).

Avant tous, je remercie ALLAH, le tout puissant, le miséricordieux, de m'avoir donné la santé et tout dont je nécessitais pour l'accomplissement de cette thèse.

Je tiens tout d'abord à remercier très vivement mon encadrant de thèse le Professeur Abdellah Lamnii, Professeur de l'enseignement supérieur, d'avoir accepté d'encadrer mes travaux de recherche. Il m'a encouragé à me "jeter" dans le monde des fonctions splines et ondelettes. Je lui exprime ma plus profonde reconnaissance de m'avoir accompagné pendant les années de préparation de cette thèse. Il a toujours apporté sa rigueur scientifique à certains points-clés de ce travail. Je lui suis particulièrement reconnaissant de me soutenir tout en m'accordant sa confiance et une grande liberté d'action. Il m'a aidé à progresser dans ma réflexion grâce à ses conseils, son esprit critique et sa disponibilité. Il m'a toujours considéré comme ami et collègue et non plus comme son éléve. Ces quelques lignes ne sauraient lui exprimer totalement ma reconnaissance. J'espère que notre collaboration continuera puisqu'il est réellement stimulant d'échanger des idées et mener un projet en ta compagnie.

J'adresse mes sincères remerciements à tous les membres du jury pour l'intérêt qu'ils ont bien voulu porter à ce travail de thèse:

- Je remercie de tout coeur Pr. Mohamed Louzar, Pr. Mohammed Mestari et Pr. Aziz Ikemakhen pour avoir accepté de rapporter cette thèse, de leur intérêt pour mon travail, ainsi que pour leurs remarques positives et encourageantes.

- C'est avec grand plaisir que je remercie Pr. Mohammed Zakkari qui m'a fait l'honneur de présider le jury de cette thèse. Je suis aussi très reconnaissant envers le Pr. Mohamed Abdou El Omary et le Pr. Abdelghani Ben Tahar pour leur participation à mon jury. C'est pour moi un grand honneur de partager mon travail avec eux.

Les plus sincères remerciements s'adressent à Salah Eddarhgani qui m'a accompagné professionnellement, et amicalement durant toute cette période. Ensuite je tiens aussi à remercier mes amis et mes collègues qui m'ont apporté leur aide et qui m'ont soutenu moralement tout au long de ces années d'études.

Enfin, je tiens à exprimer mes derniers remerciements aux personnes qui me sont les plus chères, mes parents, mes frères ainsi que mes sœurs pour leurs soutien pendant ces longues années d'études, et sans qui rien de tout ceci n'aurait été possible. C'est à cette charmante et solide famille que je dédie cette thèse.

Merci à tous ces gens et à ceux qui ont contribué de près ou de loin pour que ce travail voit le jour.

Abstract

Subdivision schemes are recursive methods for generating smooth functions from discrete data. These schemes have received considerable attention in the last decades because they allow designs of efficient, local, and hierarchical modeling algorithms in a wide range of applications related to computer-aided geometric design, computer graphics, and the recent area of interest like fractional calculus. A subdivision starts with a set of initial control points and then recursively generates denser control points by a linear combination of nodes of a lower refinement level.

Spline functions and subdivision schemes are strongly linked. To be more specific, several authors widely discussed smooth subdivision schemes based on polynomial splines in the literature. Accordingly, we have devoted this Ph.D. thesis to providing an in-depth theoretical and practical study of subdivision schemes based on non-polynomial splines, i.e., cycloidal splines. Namely, we have considered the splines spanned by polynomials and trigonometric or hyperbolic functions.

This Ph.D. thesis is divided into two parts: The first section is about hyperbolic algebraic splines. Indeed, uniform algebraic hyperbolic B-splines of any degree k have been examined. Then, for each arbitrary order k, we established a general formula for the refinement equations. The subdivision schemes are established using these refinement equations. Finally, we provided a new multiresolution technique for curves of general topology to introduce a new inverse subdivision scheme connected with algebraic hyperbolic B-splines of order $k = 3$. Numerical results back up theoretical conclusions.

We proposed a new algebraic trigonometric Hermite interpolation operator in the second part. This operator interpolates the function values and the first derivative values at the break-points of a partition. The considered Hermite interpolating splines give an optimal convergence order and produce linear polynomials and trigonometric functions. Hence, quadrature rules with endpoint corrections are provided based on integrating the considered Hermite interpolating splines. These rules are employed to solve the 1-D Fredholm integral equations numerically. The error bound is examined, and numerical examples of the proposed interpolating splines' performance are provided.

Keywords: Uniform algebraic hyperbolic B-splines, Uniform algebraic trigonometric B-splines, Subdivision scheme, Reverse subdivision scheme, Multiresolution Analysis, Wavelets, Hermite spline interpolation, Quadrature rule, Fredholm integral equation.

Contents

List of Figures

List of Tables

General introduction

During the last three decades, the problem of interpolation or approximation of data has been the subject of several research works. As a result, various approaches have been developed in this domain. Currently, several researchers are interested in developing these methods. So far, bezier models, polynomial and trigonometric B-splines provide an appropriate approach to interpolation/approximation problems.

The most commonly used curve types in Computer Aided Geometric Design (CAGD) for interpolating point sets are parametric curves such as polynomial splines, Bézier curves, and B-spline curves. B-spline functions have been introduced for the first time by Schoenberg in 1946. Since its introduction, univariate splines approximation has become popular in applications of numerical calculations and has been the subject of thousands of research papers and several books. Today, B-splines functions are universally known as a powerful tool in the theory of approximation and interpolation. Moreover, B-splines have become basic tools in many application domains such as data fitting, numerical integration, differentiation, numerical solutions of integral and differential equations, design and surface software, data compression, image analysis, signal processing. Thanks to their analytical definition as piecewise polynomials, these functions have several interesting properties such as smoothness, compact support, the partition of unity and stable evaluations.

A new class of parametric curves called Bézier curves was introduced by the engineers Pierre Bézier and Paul de Casteljau in the French automobile industry. These curves are expressed in Bernstein form and controlled by a sequence of control points. By moving these points, we can modify the shape of the curve. P. de Casteljau designed a recursive method to evaluate Bézier curves called De Casteljau's algorithm. In addition to this feature, Bézier curves possess significant affine invariance, endpoint interpolation, convex hull property, variation diminishing property. These curves have been used to solve planar and spatial interpolation problems see, e.g., [85]. The Bézier curves were extended to well-known B-spline curves, which are piecewise polynomials defined by a sequence of control points and a knot vector.

B-spline curves have similar properties as Bézier curves and provide more flexibility than the latter. These curves are a powerful tool to represent free-form shapes, and they have been used extensively to solve interpolation and approximation problems. Trigonometric and hyperbolic B-spline curves with shape parameters are

equally important and useful for modeling in CAGD like classical B-spline curves. This thesis introduces the quadratic and cubic trigonometric B-spline curves using new cubic basis functions with shape parameter $\alpha \in [0, 4]$. All geometric characteristics of the proposed B-spline curves are similar to the classical B-spline. Still, the shape-adjustable is an additional quality that the classical B-spline curves do not hold. The properties of these bases are similar to the classical B-spline bases and have been delineated. In addition, this thesis concentrates on constructing orthogonal wavelets with compact support and high-order scaling functions. The rationale behind this construction is that orthogonality gives the wavelets and scaling functions certain advantages. The most desirable benefit of orthogonality is that it provides a fast and efficient way to decompose signals into coefficients as well as to reconstruct the signal from its coefficients. Therefore, this property can help speed up and reduce the cost of data processing.

A fundamental problem of geometric modeling is the definition and generation of smooth curves and surfaces specified by a small set of control points. One class of solutions is based on subdivision: an iterative replacement of coarser representations of a curve or surface by finer representations. The notion of subdivision scheme was introduced in 1974 by G. Chaikin [21] in the context of computer-aided design (CAD). Algorithms for generating subdivision curves are often specified in terms of iterated matrix multiplication. Each multiplication maps a globally indexed sequence of points representing a coarser curve approximation onto a longer sequence representing a more refined approximation. Unfortunately, this use of matrices and indices obscure the local and stationary character of typical subdivision rules. On the other hand, The subdivision is a smoothing technique, but its reverse can generate a rough approximation at high energy. Thus, after a few iterations of the inversion process, it is generally challenging to find a correspondence between the coarse points' overall structure and the original ones. However, the proposed smooth reverse subdivision approach preserves the origin curve's overall design, making it a better candidate for wavelet construction.

This thesis presents the subdivision scheme for B-splines curves as an alternative to the classical methods using the analytical definition of spline curves and the general formula of refinement equation for B-splines. Contrary to the classical techniques, it is based on a relation that allows building and increasing the number of control points from initial points. By repeating this process, the number of control points is doubled at each iteration, which allows the B-spline curve to be approached at a finer and finer resolution, which explains the subdivision scheme for the relation between two levels of resolution. Furthermore, we have constructed non-stationary subdivision schemes called "Smooth Reverse Subdivision" based on trigonometric and hyperbolic B-splines for order 3. As the matrix corresponding to the generalized subdivision scheme of order 3 is not a square matrix, by using the same method introduced in [21] we compute the expression of the inverse scheme of order 3. Using the multiresolution theory, we propose the wavelets corresponding

to the generalized scheme of order 3.

Integral equations are of great scientific interest. They are among the most important branches of mathematics. It is known that they affect various areas of applied mathematics and physics. In practice, most models constructed from engineering physics and biology problems are best treated when presented in the form of integral equations. Integral equation methods are particularly well adapted to computational problems in the case of infinite spaces or when the boundaries are mobile or unknown. These methods are also very accurate. Historically, the solution of boundary problems has been the origin of the systematic development of the theory of integral equations, creating a fruitful interaction between these two branches of mathematics. Fredholm (1866-1927) studied the method for solving integral equations of the second kind, he gave the first general solution of the Dirichlet problem. In this thesis, we study the existence and uniqueness of the approximate solution of the Fredholm integral equation of second type

$$f(x) - \int_a^b K(x,t)f(t)dt = g(x), \tag{0.0.1}$$

where the function $f(x)$, is the unknown function to be determined on $[a,b]$, while $g : [a,b] \to \mathbb{R}$ and $K : [a,b] \times [a,b] \to \mathbb{R}$ are known functions, a and b are constants.

Since it is not always possible to solve integral equations analytically, numerical methods must be used to determine approximate numerical solutions. For example, the numerical solution of a Fredholm integral equation of the form (2.3.3) is considered in a large body of literature; some of the most well-known approximation techniques are based upon interpolation, quadrature, projection, and collocation are covered in [8, 13, 40, 46]. The two most popular numerical methods for solving this equation are the projection and Nyström methods. In the Nyström methods, also known as quadrature methods, the quadrature formulas are used to approximate the exact integral in the equation. While in the projection methods, the quadrature formulas are used to approximate integrals in the linear system matrix to be solved.

The numerical methods developed in this thesis are based upon the widely used Nyström method [71]. We start by recalling Nyström's original method for solving an integral equation that assumes that the kernel function is continuous. Then we apply quadrature formulas based on Hermite spline interpolation to the solution of a class of Fredholm equations using Nyström's methods. The aim is to improve the order of convergence obtained by Nyström's original method. Finally, explicit results for the trigonometric splines of the interpolants are provided.

Outlined of the thesis

In Chapter 2, we begin by studying the uniform B-splines generated over the space spanned by $\{\sinh(\alpha x), \cosh(\alpha x), x^{k-3}, \ldots, x, 1)\}$, with multiplied nodes on the borders to adjust the curves and to avoid getting incomplete curves at the borders,

then, we prove the main result of this paper which is the refinement equation of UAH B-splines of k^{th} order. Moreover, we study the linear subdivision schemes which play a fundamental role in the construction of curves. By using the definition of UAH B-spline curves and the matrix formula of refinement equation for B-splines we present a simple technique that allows one to construct subdivision scheme of UAH B-spline curves. It is well known that the subdivision approach for calculating curves is fast with the B-splines model. Then, we construct the inverse subdivision scheme associated with the quadratic UAH B-spline by following the method introduced in [24], thus, when the uniform subdivision scheme is applied to the decimated curve, a good approximation to the original curve is achieved. The errors between the reconstructed and original polygons are stored so that we can reconstruct the original polygon exactly. Our approach is much simpler, as applications include lossy and lossless compression as well as multiresolution editing.

Chapter 3 is divided into two parts. In the first one, we construct orthogonal wavelet-based on trigonometric splines of order three. The second and in the same way we construct orthogonal wavelets based on quadratic hyperbolic splines with uniform, simple knot sequences. Then, we give the different steps of computer implementation, and finally, we present a test example by using knot sequences uniform.

In Chapter 4, we give a general and simple approach for constructing a composite Hermite interpolation method that reproduces the space of algebraic trigonometric functions. As an application of these operators, we define quadrature rules with a high degree of accuracy. More precisely, the approach we describe in this chapter produces an approximation method known as Hermite interpolation; its principal advantage lies in the flexibility and simplicity of this approach. Also, it provides a direct construction without solving any system of linear equations, which makes this approach very convenient in practice. Moreover, it is locally, and the interpolant's value depends only on the function's values and its first derivative at the data points. Finally, it has a relatively small norm at infinity, so it is a near-optimal approximant.

We conclude by presenting a summary of our approach's contributions, performances, and limitations and some perspectives of this analysis, and other possible future research directions for this work in wavelet analysis of seismic data and the resolution of integral equations.

Chapter 1

Preliminaries

Contents

This first chapter aims to familiarize the reader of this thesis with the main concepts and useful tools such as B-spline curves, wavelets, and integral equations. In addition, we are interested in the parametric model, and the subdivision curve model since these are the geometric models that are currently the most used in CAD, and which are also the models most used in CAO, and which are also the models used for the work of this thesis.

1.1 Polynomial splines

Let $I = [a, b]$ be a bounded interval in $\mathbb{R}$, n a non negative integer and let $U = \{u_0 = a < u_1 < \ldots < u_n = b\}$ be an uniform partition of I. For a given positive

integer $d \geq 2$. The space of polinomial splines of degree d is defined by

$$\Theta_d(I,U) = \{f \in C^{d-1}([a,b]) \ : f(x)/_{[u_j,u_{j+1}]} \in P_d, j = 0,\ldots,n-1\},$$

Any spline of degree d on a given knot sequence can be expressed as a unique linear combination of B-splines of the same degree. This expression is given by

$$f(x) = \sum_{\lambda=0}^{d} a_\lambda x^\lambda + \sum_{\nu=1}^{n-1} b_\nu (x-u_\nu)_+^d, \tag{1.1.1}$$

with

$$(x-u_\nu)_+^d = \begin{cases} (x-u_\nu)^d & \text{si } x \geq u_\nu, \\ 0 & \text{otherwise.} \end{cases}$$

Corollary 1.1.1. *$\Theta_d(I,U)$ is a vector space with dimension $n+d$ and*

$$\{f_0,\ldots,f_d,g_{d,1},\ldots,g_{d,n-1}\}$$

is a basis of this space with,

$$\begin{cases} f_j = x^j, & j = 0,\ldots,d, \\ g_{d,j} = (x-u_\nu)_+^d, & \nu = 0,\ldots,n-1. \end{cases}$$

In effect $dim(\Theta_d(I,U)) = dim(P_d)+dim\ (span\{(x-u_\nu)_+^d\}) = (d+1)+(n-1) = d+n$ with $\nu = 1,...,(n-1)$.

The previous basis is of a theoretical nature and is not suitable for an actual calculation because it leads to unacceptable numerical errors. In order to remedy this problem Isaac Jacob Schönberg [74] has to construct a new basis of the space $\Theta_d(I,U)$ with bounded and minimal support, more precisely it is necessary to introduce additional knots to the right of b and to the left of a.

Definition 1.1.1. For a given knot sequence $\{u_{-d} < u_{-d+1} < ... < u_{n+d}\}$ such that $u_i \leq u_{i+1}$ for $0 \leq i \leq n-1$. B-spline basis functions of arbitrary degree d can be recursively constructed by means of the Cox-de Boor formula [37]

$$B_{i,d}(x) = \frac{x-u_i}{u_{i+d}-u_i} B_{i,d-1}(x) + \frac{u_{i+d+1}-x}{u_{i+d+1}-u_{i+1}} B_{i+1,d-1}(x), \tag{1.1.2}$$

for all real numbers x, with

$$B_{i,0}(x) = \begin{cases} 1, & x \in [x_i, x_{i+1}[, \\ 0, & otherwise. \end{cases}$$

Remark 1. 1. If the knots are equidistantly distributed over the domain of the spline, the spline is called uniform.

2. The knots $\{u_0, u_1, u_2, \ldots, u_n\}$ are called interior nodes.

3. The knots $\{u_{-d} < \ldots < u_{-1}, u_{n+1} < \ldots < u_{n+d}\}$ are called extreme nodes.

4. We say that a knot has multiplicity R if it appears R times in the knot sequence. Knots of multiplicity one, two, and three are also called simple, double, and triple knots.

5. If the knot sequence is uniform and also a subset of $\mathbb{Z}$, i.e. a sequence of integers, the spline is referred to as a cardinal spline. This review will put extra focus on cardinal and uniform B-splines because their form has many advantages such as efficient evaluation and regularization.

Note that the convention of B-splines being left continuous is used. In the case of repeating knots, the denominators can have a value of zero. In these circumstances, "0/0" is presumed to be zero. Sometimes in literature, a B-spline basis function is also characterized by its order, which is equal to its degree raised by one, such that a first-order B-spline equals a zero degree B-spline. In this thesis, the B-splines will only be characterized by their degree d. The naming of B-splines by degree follows the naming convention of polynomials, e.g, B-splines of degree one are linear B-splines, degree two are quadratic B-splines, degree three are cubic B-splines, and so on. As d tends to infinity, the centralized cardinal B-spline converges to the probability density function of the standard normal distribution [80]. The following example shows that linear B-splines are quite simple.

Example 1.1.1. Using the recurrence formula (1.1.2), we obtain the splines of degree 1 are defined as follows

$$B_{i,1}(x) = \begin{cases} \dfrac{x - u_i}{u_{i+1} - u_i}, & x \in [u_i, u_{i+1}[, \\ \dfrac{u_{i+2} - x}{u_{i+2} - u_{i+1}}, & x \in [u_{i+1}, u_{i+2}[, \\ 0, & \text{otherwise.} \end{cases}$$

By applying the recurrence relation (4.5.2) twice, we obtain an explicit expression for a generic polynomial quadratic B-spline,

$$B_{i,2}(x) = \begin{cases} \dfrac{(x - u_i)^2}{(u_{i+1} - u_i)(u_{i+2} - u_i)}, & x \in [u_i, u_{i+1}[, \\ \dfrac{(x - u_i)(u_{i+2} - x)}{(u_{i+2} - u_i)(u_{i+2} - u_{i+1})} + \dfrac{(x - u_{i+1})(u_{i+3} - x)}{(u_{i+2} - u_{i+1})(u_{i+3} - u_{i+1})}, & x \in [u_{i+1}, u_{i+2}[, \\ \dfrac{(u_{i+3} - x)^2}{(u_{i+3} - u_{i+1})(u_{i+3} - u_{i+2})}, & x \in [u_{i+2}, u_{i+3}[, \\ 0, & \textit{otherwise.} \end{cases}$$

The cubic B-splines with support $[u_i, u_{i+4}]$ are defined as follows

$$B_{i,3}(x) = \begin{cases} \dfrac{(x-u_i)^3}{(u_{i+3}-u_i)(u_{i+2}-u_i)(u_{i+1}-u_i)}, & x \in [u_i, u_{i+1}[, \\ \dfrac{(x-u_i)^2(u_{i+2}-x)}{(u_{i+3}-u_i)(u_{i+2}-u_i)(u_{i+2}-u_{i+1})} + \dfrac{(x-u_i)(u_{i+3}-x)(x-u_{i+1})}{(u_{i+3}-u_{i+1})(u_{i+3}-u_i)(u_{i+2}-u_{i+1})} \\ \quad + \dfrac{(u_{i+4}-x)(x-u_{i+1})^2}{(u_{i+4}-u_{i+1})(u_{i+3}-u_{i+1})(u_{i+2}-u_{i+1})}, & x \in [u_{i+1}, u_{i+2}[, \\ \dfrac{(x-u_i)(u_{i+3}-x)^2}{(u_{i+3}-u_{i+2})(u_{i+3}-u_{i+1})(u_{i+3}-u_i)} + \dfrac{(u_{i+4}-x)(u_{i+3}-x)(x-u_{i+1})}{(u_{i+4}-u_{i+1})(u_{i+3}-u_{i+1})(u_{i+3}-x_{i+2})} \\ \quad + \dfrac{(u_{i+4}-x)^2(x-u_{i+2})}{(u_{i+4}-u_{i+2})(u_{i+4}-u_{i+1})(u_{i+3}-u_{i+2})}, & x \in [u_{i+2}, u_{i+3}[, \\ \dfrac{(u_{i+4}-x)^3}{(u_{i+4}-u_{i+1})(u_{i+4}-u_{i+2})(u_{i+4}-u_{i+3})}, & x \in [u_{i+3}, u_{i+4}[, \\ 0, & otherwise. \end{cases}$$

1.1.1 Properties of the B-spline functions

The B-spline functions $B_{i,d}$ defined using the procedure described above are polynomials of degree d. There are several important features of the basis functions that are pointed out by Hughes et al. [20].

1. B-spline functions form a partition of unity, i.e.

$$\sum_{i=R-d}^{R} B_{i,d}(x) = 1 \; for \; x \in [u_R, u_{R+1}[, \tag{1.1.3}$$

$$\sum_{i=-d+1}^{n-1} B_{i,d}(x) = 1. \tag{1.1.4}$$

2. The basis functions are interpolatory at the end points of the knot vector, such that:

$$B_{i,d}(u_1) = \delta_{i,1} \quad and \quad B_{i,d}(u_{n+d+1}) = \delta_{i,n},$$

where, δ is the Kronecker symbol.

3. The support of each $B_{i,d}$ is compact and contained in $[u_i, u_{i+d+1}]$. The supports of the functions are growing with increasing polynomial degree. In fact, the support will cover exactly $(d+2)$ knots. Note however that some of these knots may be equal and thus have knot multiplicity greater than one. In these cases, the support will not go over $(d+1)$ knot spans, which is the maximum support it can have.

4. Each B-spline function is nonnegative over the entire domain, that is: $B_{i,d}(x) \geq 0$ for all $u_i \leq x \leq u_{i+d+1}$. which means that all the coefficients of a mass matrix computed from a B-spline basis are also nonnegative, which can be useful for mass lumping schemes [20].

5. The B-spline functions indeed form a basis for the space of polynomials of degree less than or equal to d, $\mathbb{P}_d$. That is, they are all linearly independent i.e.
$$\sum_{i=1}^{n} \alpha_i B_{i,d}(x) = 0 \Leftrightarrow \alpha_i = 0, \quad \forall i = 1, 2, \ldots, n. \tag{1.1.5}$$

6. The B-spline function $B_{i,d}(u_i)$ is of regularity C^{d-R} at each knot of multiplicity R. When the multiplicity of a knot is exactly d, the basis function is interpolatory.

1.1.2 Derivatives of B-spline functions

The derivatives of B-spline functions are represented in terms of lower-order B-spline basis, as it comes directly from the recursive definition given in equations (1.1.2). Thus, the first derivative of the i-th B-spline basis function of degree d is given by

$$B'_{i,d}(x) = \frac{d}{u_{i+d} - u_i} B_{i,d-1}(x) - \frac{d}{u_{i+d+1} - u_{i+1}} B_{i+1,d-1}(x). \tag{1.1.6}$$

Proof. The proof can be done by induction on d.
For $d = 1$, $\quad B_{i,1}(x) = \dfrac{x - u_i}{u_{i+1} - u_i} B_{i,0}(x) + \dfrac{u_{i+2} - x}{u_{i+2} - u_{i+1}} B_{i+1,0}(x)$.
So that: $B'_{i,1}(x) = \dfrac{1}{u_{i+1} - u_i} B_{i,0}(x) - \dfrac{1}{u_{i+2} - u_{i+1}} B_{i+1,0}(x)$.
Now assume that the result is true up to order d,

$$\begin{aligned} B'_{i,d+1}(x) =& \frac{1}{u_{i+d+1} - u_i} B_{i,d}(x) + \frac{x - u_i}{u_{i+d+1} - u_i} B'_{i,d}(x), \\ & - \frac{1}{u_{i+d+2} - u_{i+1}} B_{i+1,d}(x) + \frac{u_{i+d+2} - x}{u_{i+d+2} - u_{i+1}} B'_{i+1,d}(x). \end{aligned}$$

We apply the recurrence hypothesis for $B'_{i,d}(x)$ and $B'_{i,d+1}(x)$; we will have

$$\begin{aligned} B'_{i,d+1}(x) =& \frac{1}{u_{i+d+1} - u_i} B_{i,d}(x) + \frac{x - u_i}{u_{i+d+1} - u_i} \\ & \left[\frac{d}{u_{i+d} - u_i} B_{i,d-1}(x) - \frac{d}{u_{i+d+1} - u_{i+1}} B_{i+1,d-1}(x) \right] \\ & - \frac{1}{u_{i+d+2} - u_{i+1}} B_{i+1,d}(x) + \frac{u_{i+d+2} - x}{u_{i+d+2} - u_{i+1}} \\ & \left[\frac{d}{u_{i+d+1} - u_{i+1}} B_{i+1,d-1}(x) - \frac{d}{u_{i+d+2} - u_{i+2}} B_{i+2,d-1}(x) \right], \\ =& \frac{1}{u_{i+d+1} - u_i} B_{i,d}(x) - \frac{1}{u_{i+d+2} - u_{i+1}} B_{i+1,d}(x) \\ & + \frac{d\,(x - u_i)}{(u_{i+d+1} - u_i)\,(u_{i+d} - u_i)} B_{i,d-1}(x) \end{aligned}$$

$$+ d\left[\frac{u_{i+d+2}-x}{(u_{i+d+2}-u_{i+1})(u_{i+d+1}-u_{i+1})} - \frac{u_{i+d+2}-x}{(u_{i+d+1}-u_i)(u_{i+d+1}-u_{i+1})}\right]$$
$$B_{i+1,d-1}(x) - d\frac{x-u_i}{(u_{i+d+2}-u_{i+1})(u_{i+d+2}-u_{i+2})}B_{i+2,d-1}(x).$$

On the other hand

$$\frac{u_{i+d+2}-x}{u_{i+d+2}-u_{i+1}} - \frac{x-u_i}{u_{i+d+1}-u_i} = \frac{u_{i+d+1}-x}{u_{i+d+1}-u_i} - \frac{x-u_{i+1}}{u_{i+d+2}-u_{i+1}}.$$

So, we have

$$\begin{aligned}
B'_{i,d+1}(x) =& \frac{1}{u_{i+d+1}-u_i}B_{i,d}(x) - \frac{1}{u_{i+d+2}-u_{i+1}}B_{i+1,d}(x) + \frac{d}{u_{i+d+1}-u_i} \\
& \left[\frac{x-u_i}{u_{i+d}-u_i}B_{i,d-1}(x) + \frac{u_{i+d+1}-x}{u_{i+d+1}-u_{i+1}}B_{i+1,d-1}(x)\right] - \frac{d}{u_{i+d+2}-u_{i+1}} \\
& \left[\frac{x-u_{i+1}}{u_{i+d+1}-u_{i+1}}B_{i+1,d-1}(x) + \frac{u_{i+d+2}-x}{u_{i+d+2}-u_{i+2}}B_{i+2,d-1}(x)\right]B_{i+2,d-1}(x), \\
=& \frac{1}{u_{i+d+1}-u_i}B_{i,d}(x) - \frac{1}{u_{i+d+2}-u_{i+1}}B_{i+1,d}(x) + \frac{d}{u_{i+d+1}-u_i}B_{i,d}(x) \\
& - \frac{d}{u_{i+d+2}-u_{i+1}}B_{i+1,d}(x), \\
=& \frac{d+1}{u_{i+d+1}-u_i}B_{i,d}(x) - \frac{d+1}{u_{i+d+2}-u_{i+1}}B_{i+1,d}(x).
\end{aligned}$$

The proof is complete. □

1.2 Uniform algebraic trigonometric B-splines (UAT B-splines)

In this section, we are briefly going to learn about the concept of UAT B-splines and to understand a certain number of definitions and fundamental properties of the UAT B-splines. We also give some B-spline figures to confirm a certain number of properties such as positivity, partition of the unit and support. The following notations are used throughout the entire work.
Let ℓ be a positive integer greater than or equal to 2, and $m_\ell = 2^\ell$, then we put

$$\Phi^\ell = \{\phi_i^\ell = a + ih_\ell, \quad i = 0, \ldots, m_\ell\}, \tag{1.2.1}$$

where $h_\ell = \dfrac{b-a}{m_\ell}$ the set of knots that subdivide the interval $I = [a, b]$ uniformly.

Definition 1.2.1. Let $\tilde{s}(x)$ be a piecewise function restricted to the space

$$\Gamma_k = \text{span}\{1, x, x^2, \ldots, x^{k-3}, \cos(\alpha x), \sin(\alpha x)\}, \tag{1.2.2}$$

for each subinterval $[\phi_j, \phi_{j+1}], j = 0, \ldots, m_\ell - 1$. If $\tilde{s}(x)$ is $(k - R - 1)$ times continuously differentiable at a knot ϕ_i^ℓ of multiplicity R, we call it an algebraic trigonometric spline of order k.

Let $S_k([a, b], \Phi^\ell)$ be the collection of all algebraic trigonometic splines of order k defined over Φ^ℓ. Furthermore, it can be easily checked that $S_k([a, b], \Phi^\ell)$ is a linear space.

Definition 1.2.2. A set of basis functions $N_{i,k}^{[\alpha,\ell]}$ of the space S_k is defined as follows

$$N_{0,2}^{[\alpha,\ell]}(x) = \begin{cases} \dfrac{\alpha h_\ell \sin(\alpha x)}{2(1-\cos(\alpha h_\ell))}, & x \in [0, h_\ell[, \\ \dfrac{\alpha h_\ell \sin(\alpha(2h_\ell - x))}{2(1-\cos(\alpha h_\ell))}, & x \in [h_\ell, 2h_\ell[, \\ 0, & otherwise, \end{cases} \tag{1.2.3}$$

and

$$N_{i,2}^{[\alpha,\ell]}(x) = N_{0,2}^{[\alpha,\ell]}(x - \phi_i^\ell),$$

where $\alpha > 0$ is the tension parameter. Next, for $k \geq 3$, $N_{i,k}^{[\alpha,\ell]}$ is defined recursively by

$$N_{i,k}^{[\alpha,\ell]}(x) = \frac{1}{h_\ell} \int_{x-h_\ell}^{x} N_{i,k-1}^{[\alpha,\ell]}(t)dt, \tag{1.2.4}$$

and

$$N_{i,k}^{[\alpha,\ell]}(x) = N_{0,k}^{[\alpha,\ell]}(x - \phi_i^\ell).$$

Example 1.2.1. Using formula (4.2.2) we obtain explicit expressions of trigonometric B-splines $N_{0,3}^{[\alpha,\ell]}$ and $N_{0,4}^{[\alpha,\ell]}$. Indeed, by invoking (4.2.1), we infer that

$$N_{0,3}^{[\alpha,\ell]}(x) = \frac{1}{h_\ell} \int_{x-h_\ell}^{\phi} N_{0,2}^{[\alpha,\ell]}(t)dt.$$

If $x \in [0, h_\ell]$ we have $t \in [-h_\ell, h_\ell]$, and

$$\begin{aligned} N_{0,3}^{[\alpha,\ell]}(x) &= \frac{1}{h_\ell} \int_{x-h_\ell}^{0} 0dt + \frac{1}{h_\ell} \int_{0}^{x} \frac{\alpha h_\ell \sin(\alpha t)}{2(1-\cos(\alpha h_\ell))} dt, \\ &= \frac{1-\cos(\alpha x)}{4\sin^2\left(\frac{\alpha h_\ell}{2}\right)}. \end{aligned}$$

If $x \in [h_\ell, 2h_\ell]$ we have $t \in [0, 2h_\ell]$, furtheremore

$$\begin{aligned} N_{0,3}^{[\alpha,\ell]}(x) &= \frac{1}{h_\ell} \int_{\phi-h_\ell}^{h_\ell} \frac{\alpha h_\ell \sin(\alpha t)}{2(1-\cos(\alpha h_\ell))} dt + \frac{1}{h_\ell} \int_{h_\ell}^{x} \frac{\alpha h_\ell \sin(\alpha(2h_\ell - t))}{2(1-\cos(\alpha h_\ell))} dt, \\ &= \frac{-2\cos(\alpha h_\ell) + \cos(\alpha(2h_\ell - x)) + \cos(\alpha(x - h_\ell))}{4\sin^2\left(\frac{\alpha h_\ell}{2}\right)}. \end{aligned}$$

If $x \in [2h_\ell, 3h_\ell]$ we obtain $t \in [h_\ell, 3h_\ell]$ and

$$\begin{aligned} N_{0,3}^{[\alpha,\ell]}(x) &= \frac{1}{h_\ell}\int_{x-h_\ell}^{2h_\ell} \frac{\alpha h_\ell \sin(\alpha(2h_\ell - t))}{2(1-\cos(\alpha h_\ell))}dt + \frac{1}{h_\ell}\int_{2h_\ell}^{x} 0dt, \\ &= \frac{1-\cos(\alpha(3h_\ell - x))}{4\sin^2\left(\frac{\alpha h_\ell}{2}\right)}. \end{aligned}$$

Finally the UAT B-spline $N_{0,3}^{[\alpha,\ell]}$ is given by

$$N_{0,3}^{[\alpha,\ell]}(x) = \begin{cases} \dfrac{1-\cos(\alpha x)}{4\sin^2\left(\frac{\alpha h_\ell}{2}\right)}, & x \in [0, h_\ell[, \\ \dfrac{-2\cos(\alpha h_\ell) + \cos(\alpha(2h_\ell - x)) + \cos(\alpha(x - h_\ell))}{4\sin^2\left(\frac{\alpha h_\ell}{2}\right)}, & x \in [h_\ell, 2h_\ell[, \\ \dfrac{1-\cos(\alpha(3h_\ell - x))}{4\sin^2\left(\frac{\alpha h_\ell}{2}\right)}, & x \in [2h_\ell, 3h_\ell[. \\ 0, & otherwise. \end{cases}$$

In the same way we find the UAT B-spline $N_{0,4}^{[\alpha,\ell]}(x)$

$$N_{0,4}^{[\alpha,\ell]}(x) = \begin{cases} \dfrac{\alpha x - \sin(\alpha x)}{2\alpha h_\ell - 2\alpha h_\ell \cos(\alpha h_\ell)}, & x \in [0, h_\ell[, \\ \dfrac{-2\alpha h_\ell + 2\sin(\alpha(h_\ell - x)) + \sin(\alpha(2h_\ell - x)) + 2\alpha(x - h_\ell)\cos(\alpha h_\ell) + \alpha x}{2\alpha h_\ell(\cos(\alpha h_\ell) - 1)}, & x \in [h_\ell, 2h_\ell[, \\ \dfrac{-2\alpha h_\ell + \sin(\alpha(2h_\ell - x)) + 2\sin(\alpha(3h_\ell - x)) + 2\alpha(x - 3h_\ell)\cos(\alpha h_\ell) + \alpha x}{4\alpha h_\ell \sin^2\left(\frac{\alpha h_\ell}{2}\right)}, & x \in [2h_\ell, 3h_\ell[, \\ -\dfrac{\alpha(x - 4h_\ell) + \sin(\alpha(4h_\ell - x))}{4\alpha h_\ell \sin^2\left(\frac{\alpha h_\ell}{2}\right)}, & x \in [3h_\ell, 4h_\ell[, \\ 0, & otherwise. \end{cases}$$

In Figure 1.1, we present graphical behavior of the graphs of the UAT B-splines of order 2, 3 and 4, and the effect of the shape parameter α. With the blue curves represents $N_{0,2}^{[\alpha,\ell]}(x)$, the red curves represents $N_{0,3}^{[\alpha,\ell]}(x)$ and the yellow curves represents $N_{0,4}^{[\alpha,\ell]}(x)$. In [34], M. E. Fang et al. proved that all the desirable properties of classical polynomial B-splines carry over to the generalized UAT B-splines of order k. In this section, we mention only the most remarkable ones such as

Property 1.2.1. The family $N_{i,k}^{[\alpha,\ell]}, i = 0, \ldots, m_\ell - k$ generates the space $S_k([a,b], \Phi^\ell)$. Moreover, we have

1. Local support: $\text{supp}\left(N_{i,k}^{[\alpha,\ell]}\right) = [\phi_i^\ell, \phi_{i+k}^\ell]$.
2. Positivity: $N_{i,k}^{[\alpha,\ell]}(x) \geq 0$ for all $\phi_i^\ell \leq x \leq \phi_{i+k}^\ell$.
3. Derivative: $\left(N_{i,k}^{[\alpha,\ell]}(x)\right)' = \dfrac{1}{h_\ell}\left(N_{i,k-1}^{[\alpha,\ell]}(x) - N_{i+1,k-1}^{[\alpha,\ell]}(x)\right)$.

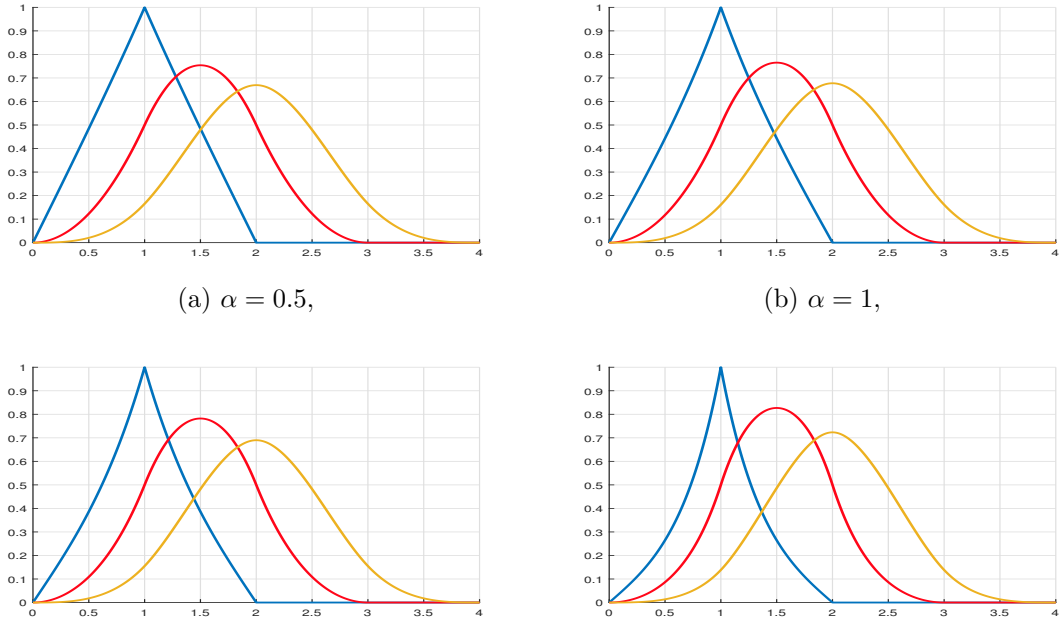

(a) $\alpha = 0.5$, (b) $\alpha = 1$,

(c) $\alpha = 1.5$, (d) $\alpha = 2$.

Figure 1.1 – UAT B-spline functions of order 2,3 and 4, with $\alpha = 0.5, 1, 1.5, 2$.

4. Partition of unity: $\sum_{i \in \mathbb{Z}} N_{i,k}^{[\alpha,\ell]}(x) = 1$, for all $k \geq 2$ and $\forall x \in \mathbb{R}$.

5. Linear independence globally: $N_{i,k}^{[\alpha,\ell]}(x)$, $i = 0, \ldots, m_\ell$ are linearly independent on $(-\infty, +\infty)$.

1.3 Curves B-splines and subdivision

1.3.1 Parametric Curves

In parametric modeling, curves are described intuitively as a continuous deformation of a line segment. By varying a parameter u along this line, a corresponding point along the curve, $\mathcal{C}(x)$, can be found. In practice, it is more intuitive to manipulate a curve using a set of points rather than a mathematical formula. Therefore, parametric curves are usually represented as affine combinations of a set of points called control points. To formalize the representation of a curve $\mathcal{C}(x)$ based on its control points $P_0, P_1, \ldots, P_n$, a set of basis functions $B_i(x)$ with the affinity property [14] is necessary. For example, Bézier curves of degree d

$$C_d(x) = \sum_{i=0}^{d} P_i \mathcal{B}_{i,d}(x), \quad 0 \leq t \leq 1, \tag{1.3.1}$$

are created by an affine combination of control points using Bernstein polynomials

$$\mathcal{B}_{i,d}(x) = \begin{pmatrix} d \\ i \end{pmatrix} x^i (1-x)^{d-i} \text{ where } \begin{pmatrix} d \\ i \end{pmatrix} = \frac{d!}{i!(d-i)!}. \tag{1.3.2}$$

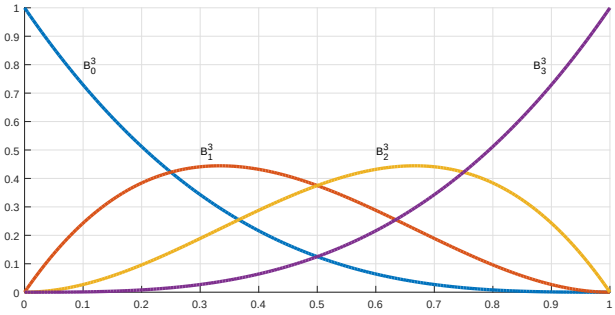

Figure 1.2 – Bernstein basis for $d = 3$.

The choice of the interval $[0, 1]$ is not a restriction because the Bézier curves are invariant by an affine transformation of the parametrization domain.
In Bézier curves, the degree d of the basis functions is coupled with the number of control points. Therefore, adding more control points increases the degree of these polynomials, making them expensive to compute. Also, because the Bernstein polynomials are non-zero over the entire parametric domain, changing one of the control points affects the whole curve. These problems can be solved using a careful selection of piecewise polynomial functions or splines.

1.3.2 UAT B-spline curves

Now we are going to introduce the notion of B-spline curves associated with the above family $N_{i,k}^{\alpha}$, $i = 0, \ldots, m_\ell - k$. It can be easily seen that these functions B-splines are suitable for geometric modeling because of the good properties they possess. A B-spline curve is a piecewise polynomial function expressed with respect to a set of B-spline basis functions. The maximum allowable cross-segment continuity is equal to the order of the B-spline minus two (C^2 in the case of cubic B-splines), and the minimum is C^1, which implies that the two adjacent segments are disjoint. The basis functions are chosen to have the minimal possible support subject to their piecewise polynomial nature and the specified cross-segment continuity. However, in practical geometric modeling applications, the span of parameter x is always restricted to a finite interval such as $[\phi_0^\ell, \phi_{m_\ell}^\ell]$. To do this, we denote by $\mathcal{C}_k$. The B-spline curves of order $k \geq 3$, thus,

$$\mathcal{C}_k(x) = \sum_{i=0}^{m_\ell - k} c_i N_{i,k}^{[\alpha,\ell]}(x), \tag{1.3.3}$$

where $C^k = [c_0^\ell, c_1^\ell, \ldots, c_{m_\ell - k}^\ell]$ stands for the control polygon. As the polynomial B-spline curves, $\mathcal{C}_k$ has the following properties derived directly from the UAT B-spline basis properties.

1. Convex hull property: $\mathcal{C}_k$ lies inside the convex hull of the corresponding control polygon. It follows from the non-negativity and partition of unity of the UAT B-splines basis.

2. Geometric invariance: The shape of UAT B-spline curves is independent of the choice of coordinate system because $\mathcal{C}_k$ is an affine combination of the control points.

3. Local control property: Local adjustment can be made without disturbing the rest of the curve because change of one control points will alter at most k segments of the original UAT B-spline curves of order k.

4. Derivative:
$$\frac{d\mathcal{C}_k(t)}{dt} = \frac{1}{h_\ell} \sum_{i=1}^{m_\ell - k} \Delta c_i N_{i,k-1}^{\alpha}(t, h_\ell),$$
where $\Delta c_i = c_i - c_{i-1}$.

The α-tension parameter plays a crucial role and has a significant impact on both the visual and geometric properties of the UAT B-spline curves. In Figure 1.3, we give the numerical examples of trigonometric B-spline curves with different values of tension parameter α. According to these values, it seems that when α increases, the UAT B-spline curve converges towards the initial polygon. In order to get a good approximation, it is necessary to use a small step size of refinement. But the problem, in this case, is the cost of manipulation.

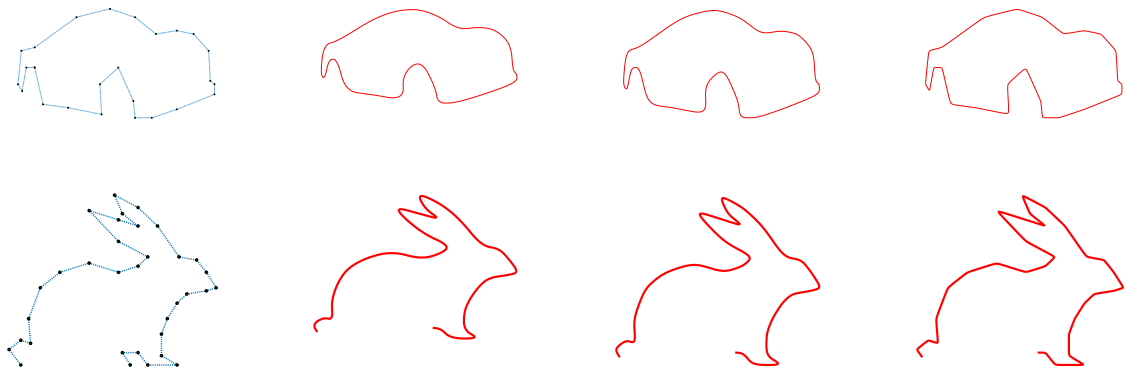

(e) Control polygon. (f) $\alpha = 1.5$. (g) $\alpha = 2.5$. (h) $\alpha = 3.5$.

Figure 1.3 – UAT B-spline curves with different values of tension parameter α.

1.3.3 Subdivision

In recent years, the subdivision has emerged as a major geometric modeling technique. Algorithms for generating subdivision curves are often specified in terms of iterated matrix multiplication. Each multiplication maps a globally indexed sequence of points representing a coarser curve approximation onto a longer sequence representing a more refined approximation. Unfortunately, this use of matrices and indices obscure the local and stationary character of typical subdivision rules. Subdivision curves are defined using discrete operations applied on a set of coarse points to produce a set of fine points. These operations can be used to approximate different types of curves, such as Bezier and B-spline curves.
Chaikin introduced discrete operations for curve subdivision in 1974 (see [21]). Given a coarse control polygon $\{P_1, P_2, \ldots, P_n\}$, he presented the following subdivision masks

$$\begin{cases} F_{j-1} &= \frac{3}{4}P_{i-1} + \frac{1}{4}P_i, \\ F_j &= \frac{1}{4}P_{i-1} + \frac{3}{4}P_i, \end{cases} \tag{1.3.4}$$

to find fine points $\{F_1, F_2, \ldots, F_{2n}\}$. The repetitive application of the Chaikin masks to a coarse curve will converge to a quadratic B-spline curve. The convergence of the limit curve in the Chaikin subdivision is the result of the scheme's corner-cutting behavior [29]. Lane and Riesenfeld [48] introduced a general derivation form for B-spline subdivision schemes using a duplication followed by a few averaging steps that involve two direct neighbors. Using this technique, the cubic B-spline subdivision masks may be found as

$$\begin{cases} F_{j-1} &= \frac{1}{2}P_{i-1} + \frac{1}{2}P_i, \\ F_j &= \frac{1}{8}P_{i-1} + \frac{3}{4}P_i + \frac{1}{8}P_{i+1}. \end{cases} \tag{1.3.5}$$

A subdivision matrix can represent the process of applying subdivision masks to the coarse points. For closed curves, this matrix has a circular structure. For example, the matrix form of cubic B-spline subdivision for closed curves has the following banded structure.

$$P^T = \begin{pmatrix} \frac{1}{2} & \frac{1}{8} & 0 & 0 & 0 & \frac{1}{8} & \frac{1}{2} & \frac{3}{4} \\ \frac{1}{2} & \frac{3}{4} & \frac{1}{2} & \frac{1}{8} & 0 & 0 & 0 & \frac{1}{8} \\ 0 & \frac{1}{8} & \frac{1}{2} & \frac{3}{4} & \frac{1}{2} & \frac{1}{8} & 0 & 0 \\ 0 & 0 & 0 & \frac{1}{8} & \frac{1}{2} & \frac{3}{4} & \frac{1}{2} & \frac{1}{8} \end{pmatrix}. \tag{1.3.6}$$

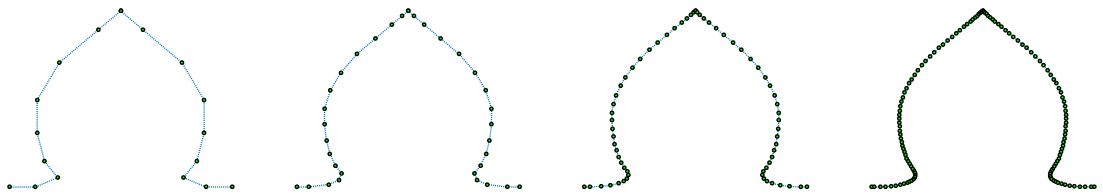

Figure 1.4 – An open curve throughout its three stages of cubic polynomial B-spline subdivision.

The columns of this matrix contain a regular, repeating set of values $\left(\frac{1}{8}, \frac{1}{2}, \frac{3}{4}, \frac{1}{2}, \frac{1}{8}\right)$ known as filter values. These filter values are shifted by two at each column because of the mid-point knot insertion. The subdivision masks appear on the rows of this matrix. Applying these masks on the coarse points doubles the number of points at each step see Figure 1.5. For open curves, some extraordinary masks need to be found for interpolating the first and the last points (boundaries) in a smooth manner. These extraordinary masks occur due to the multiple knots used at the ends of the knot sequence in B-spline curves to interpolate boundaries. For example, to handle the boundaries in cubic B-spline open curve subdivision, four extra rows appear at each end of the matrix P.

$$P = \begin{bmatrix} 1 & 0 & 0 & 0 & 0 & 0 & 0 & 0 \\ \frac{1}{2} & \frac{1}{2} & 0 & 0 & 0 & 0 & 0 & 0 \\ 0 & \frac{3}{4} & \frac{1}{4} & 0 & 0 & 0 & 0 & 0 \\ 0 & \frac{3}{16} & \frac{11}{16} & \frac{1}{8} & 0 & 0 & 0 & 0 \\ 0 & 0 & \frac{1}{2} & \frac{1}{2} & 0 & 0 & 0 & 0 \\ 0 & 0 & \frac{1}{8} & \frac{3}{4} & \frac{1}{8} & 0 & 0 & 0 \\ 0 & 0 & 0 & \frac{1}{2} & \frac{1}{2} & 0 & 0 & 0 \\ 0 & 0 & 0 & \frac{1}{8} & \frac{3}{4} & \frac{1}{8} & 0 & 0 \\ 0 & 0 & 0 & 0 & \frac{1}{2} & \frac{1}{2} & 0 & 0 \\ 0 & 0 & 0 & 0 & \frac{1}{8} & \frac{11}{16} & \frac{3}{16} & 0 \\ 0 & 0 & 0 & 0 & 0 & \frac{1}{4} & \frac{3}{4} & 0 \\ 0 & 0 & 0 & 0 & 0 & 0 & \frac{1}{2} & \frac{1}{2} \\ 0 & 0 & 0 & 0 & 0 & 0 & 0 & 1 \end{bmatrix}. \tag{1.3.7}$$

These extra-ordinary rows have symmetric arrangements near the boundaries. The interior rows contain the regular subdivision masks of the cubic B-spline.

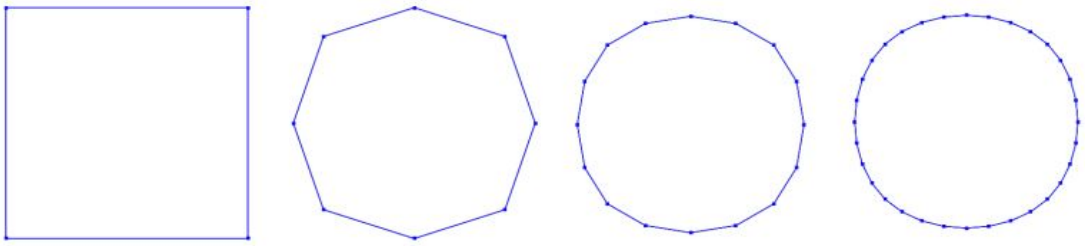

Figure 1.5 – A closed curve throughout its three stages of cubic polynomial B-spline subdivision.

1.4 Multiresolution analysis and orthogonal wavelets

1.4.1 Multiresolution analysis

S. G. Mallat and Y. Meyer, in 1986, introduced the concept of multiresolution analysis as a tool for constructing orthonormal wavelet bases [61, 62]. This notion came to be included in the framework of multiscale approaches for which the work of Haar (1909), Franklin, and Littlewood-Paley in functional analysis are pioneers. To introduce this notion, we will need to recall the concept of a Reisz basis which is "weaker" than the concept of an orthonormal basis but often suffisant for obtaining interesting results. The multiresolution analysis allows decomposing mono or multidimensional signals on an orthonormal basis of scale functions and on the basis of wavelet functions. Therefore, this orthonormal wavelet family by multiresolution analysis reduces to nothing any redundancy.
In this section, we shortly introduce wavelet bases on the real line generated by one wavelet and by one scaling function. With this motivation, we set out to construct orthogonal wavelets systems built upon B-spline, a well-known class of functions. To set up the theoretical background, we start with the definitions of Riesz basis and Multiresolution Analysis.

Definition 1.4.1. (Reisz base)
Let $\mathbb{H}$ be a Hilbert space with inner product $< .,. >$, and norm $\|.\| =< .,. >^{1/2}$. A family $(e_\lambda)_{\lambda\in\mathbb{Z}^+}$ is called a Riesz basis of a Hilbert space $\mathbb{H}$, if and only if it spans $\mathbb{H}$, i.e. all finite linear combinations of the e_λ are dense in $\mathbb{H}$, and if there exist constants A, B such that $0 < A \leq B$ and

$$A\sum_{\lambda=1}^{n}|f_\lambda|^2 \leq \left\|\sum_{\lambda=1}^{n} f_\lambda e_\lambda\right\|^2 \leq B\sum_{\lambda=1}^{n}|f_\lambda|^2. \tag{1.4.1}$$

The constants A, B are called Riesz bounds.
In this case the family $(e_\lambda)_{\lambda\in\mathbb{Z}^+}$ verifying inequality (2.3.1) is said to be H-stable.

It is well known that any orthonormal basis satisfies (2.3.1) with $A = B = 1$. Riesz bases have many useful properties of orthonormal bases without requiring orthonormality. The condition (2.3.1) can be interpreted as ensuring stability of the reconstruction of an arbitrary element $f \in \mathbb{H}$ from its coefficients $\{f_\lambda\}$ in the sense that small roundoff errors in the computation of the coefficients f_k can not lead to a large error in the reconstruction. The main properties of multiresolution analysis are summarized in the following theorem.

Definition 1.4.2. (Multiresolution analysis)
A multiresolution analysis is an ordered pair $(\{V_j, j \in \mathbb{Z}\}, \phi)$, where $\{V_j, j \in \mathbb{Z}\}$ is a sequence of closed linear subspaces of $L^2(\mathbb{R})$ such that:
AMR.1:

$$\ldots \subset V_2 \subset V_1 \subset V_0 \subset V_{-1} \subset V_{-2} \subset \ldots; \tag{1.4.2}$$

AMR.2:

$$\lim_{j \to +\infty} V_j = \bigcap_{j=-\infty}^{j=+\infty} V_j = \{0\}; \tag{1.4.3}$$

AMR.3:

$$f(.) \in V_j \Leftrightarrow f(\frac{\cdot}{2}) \in V_{j+1}; \tag{1.4.4}$$

AMR.4:

$$\forall (j,k) \in \mathbb{Z}^2, \quad f(.) \in V_j \Leftrightarrow f(. - 2^j k) \in V_j; \tag{1.4.5}$$

AMR.5:

$$\lim_{j \to -\infty} V_j = \overline{\bigcup_{j=-\infty}^{j=+\infty} V_j} = L^2(\mathbb{R}); \tag{1.4.6}$$

AMR.6:

There exists φ such that the family $\varphi(. - k)_{k \in \mathbb{Z}}$ is a Reisz basis of V_0.

The function φ is called the scaling function or the wavelet father. 2^j is called scale factor, it is the inverse of the resolution 2^{-j}.

Comment:

- The embedding of the spaces $\{V_j, j \in \mathbb{Z}\}$ is the one used by I. Daubechies and some authors. However, most authors use a reverse order. Then, V_j represents the space in which the function is approximated at the 2^{-j} resolution.
- The equality (4.3.1) reflects that the approximation of a function to a particular resolution 2^{-j} contains all the information necessary to construct a coarser resolution 2^{-j}.
- The equality (4.3.2) implies that if the resolution is too weak, i.e. if 2^{-j} tends to 0, we lose all the details. At minimum resolution, all information is lost.

– The property (1.4.4) implies that the dilation by a factor of 2, "enlarges" the details by a factor of 2, we have an approximation to a coarser resolution.

– The property (4.3.4) states that the space Vj is invariant for any length translation proportional to 2-j.

– The equality (4.3.5) implies that when j tends to $-\infty$ the approximation converges to the signal: at infinite resolution, we reproduce the all signal.

The multiresolution approximation can be illustrated on a simple example of human vision as follows: each space V_j must be seen as the set of photographs that can be taken at a certain distance, if the distance for V_{j-1} is "smaller", we see more detail and the approximation is better and inversely. The figure (1.7) shows the "behavior" of the multiresolution analysis on a landscape.

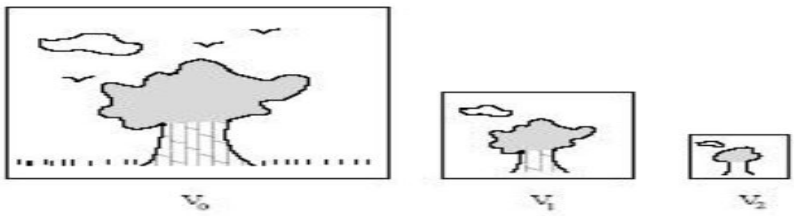

Figure 1.6 – Representation of a landscape in multiresolution analysis [15].

The multiresolution analysis behaves like a microscope which, depending on the resolution, can increase or decrease the details and is therefore called a mathematical "microscope".

1.4.2 Construction of orthogonal wavelet bases

Splines have become the standard mathematical tool for representing smooth shapes in computer graphics and geometric modeling. Wavelets have been introduced more recently but are now well established in mathematics and applied sciences like signal processing and numerical analysis. The two concepts are closely related as splines provide some of the most important examples of wavelets. The purpose of this paragraph, is to recall the main properties of orthogonal wavelets for applications. The original objective of wavelet theory is to construct orthogonal bases of $L^2(\mathbb{R})$ note $\{\psi_i, i \in \mathbb{Z}^+\}$, i.e., consisting of the translates and dilates of a single function, preferably localized and regular. To this end we consider W_{j-1} be the orthogonal complement of V_{j-1} in V_j and the following direct sum decomposition can be formed

$$\begin{aligned} V_j &= V_{j-1} \oplus W_{j-1}, \\ &= V_{j-2} \oplus W_{j-2} \oplus W_{j-1}, \\ &\vdots \\ &= V_{-j} \bigoplus_{i=-j}^{j-1} W_i. \end{aligned} \tag{1.4.7}$$

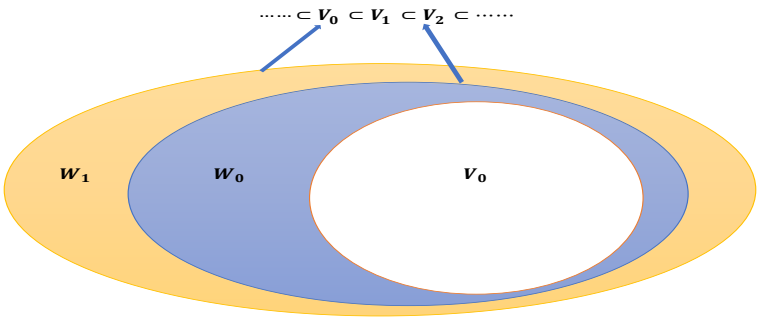

Figure 1.7 – The spaces W_j.

The decomposition of the space V_j is the basis of an analysis of wavelets. The objects we will manipulate (curves or surfaces) are elements of this space. Let $\tau^{\ell-1} = \{\tau_i^{\ell-1} = \phi_{2i-1}^{\ell}\}_{i=1}^{m_{\ell-1}}$ be a new knots sequences where $\Phi^{\ell} = \Phi^{\ell-1} \cup \tau^{\ell-1}$. The construction of minimally supported wavelets is reduced to the problem of finding minimal intervals that can support a wavelet, and we show that the total number of such intervals agrees exactly with the dimension of W. If we denote by $d_{\phi^l}(i)$ the multiplicity on the right (resp. $g_{\phi^l}(i)$ on the left) of ϕ_i^{ℓ} i.e. $d_{\phi^\ell}(i) = max\{j \in \mathbb{N} : \phi_i^{\ell} = \phi_{i+j-1}^{\ell}\}$ and $g_{\phi^\ell}(i) = max\{j \in \mathbb{N} : \phi_i^{\ell} = \phi_{i-j+1}^{\ell}\}$. Then we have the following proposition

Theorem 1.4.1. *Let $\tau_i^{\ell-1} \in \tau^{\ell-1}$, then there exists a wavelet $\psi_{i,\ell-1} \in W_{\ell-1}$ with minimal support $[\phi_{l_i}^{\ell}, \phi_{r_i}^{\ell}]$, where ℓ_i is the largest integer that verifies*

$$Card\{j : \tau_j^{\ell-1} \in (\phi_{\ell_i}^{\ell}, \tau_i^{\ell-1}], \quad j < i\} + d_{\phi^\ell}(\ell_i) = k. \tag{1.4.8}$$

Then, r_i is the smallest integer that verifies

$$Card\{j : \tau_j^{\ell-1} \in [\tau_i^{\ell-1}, \phi_{r_i}^{\ell}), \quad j > i\} + g_{\phi^\ell}(r_i) = k. \tag{1.4.9}$$

According to this Theorem, there exists for each $\tau_i^{\ell-1}$, $i = 1, \ldots, m_{\ell-1}$ one wavelet $\psi_{i,\ell-1} \in W_{\ell-1}$ with minimal support. In the next figure, we give the graph of the most popular wavelets.

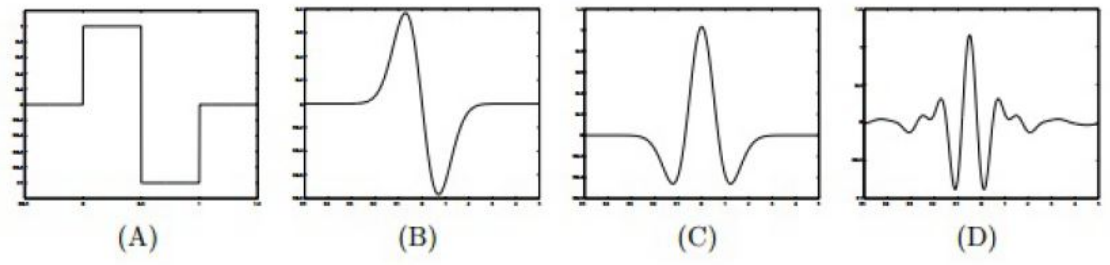

Figure 1.8 – (A) Haar wavelet ; (B) Gaussian first derivative wavelet ; (C) Sombrero wavelet ; (D) Meyer wavelet.

1.5 Integral equations

An integral equation is an equation in which an unknown function appears under one or more integral signs. J. Fourier $(1768 - 1830)$ is the first mathematician who discovered this kind of integral equation due to the fact that he obtained the formula of the Fourier transformation. Moreover, we can interpret the inversion formula as providing the inverse operator of the Fourier integral operator. Thus, the theory of integral equations has been an active research domain in applied mathematics and mathematical physics. Since this kind of equation is very well conditioned to numerical approximation, these methods have become an essential tool for investigating various fundamental scientific problems that were difficult or impossible to solve in the past.
The integral equation we are interested in in this work is a Fredholm equation of the second kind.

$$f(x) - \int_a^b K(x,t)f(t)dt = g(x), \tag{1.5.1}$$

where the function $f(x)$, is the unknown function while $g(x)$ and $K(x,t)$ are known functions, a and b are constants.
For simplicity, (4.5.6) can be written in symbolic form as

$$f - \mathcal{K}f = g. \tag{1.5.2}$$

where, $\mathcal{K}$ is the Fredholm integral operator with kernel K, defined by

$$\mathcal{K}f(x) = \int_a^b K(x,t)f(t)dt. \tag{1.5.3}$$

Depending on the complexity of the operator $\mathcal{K}$, equation (4.2.3) becomes difficult or impossible to solve. We then content with an approximate solution using numerical methods to solve the integral equations. Precisely in this part, we approximate the operator $\mathcal{K}$ by a degenerate kernel operator $\mathcal{K}_\ell$, derived from the Nyström method [60].

1.5.1 Nyström's methods

The Nyström method, also called the quadrature method, consists in applying the numerical methods of calculating integrals to obtain a linear system. It is nothing else than the approximation of the kernel K by an operator of finite dimension, i.e., a matrix. This method is totally discrete, so it provides the first efficient way to solve a numerical equation.
In the Nyström method the action of the integral operator $\mathcal{K}$ in (4.2.3) is approximated by the numerical operator $\mathcal{K}_\ell$ such that

$$\mathcal{K}_\ell f(x) = \sum_{i=0}^{m_\ell} \omega_i f(\phi_i^\ell) K(x, \phi_i^\ell), \tag{1.5.4}$$

which represents an $(m_\ell + 1)$ node quadrature rule with weights ω_i, and nodes ϕ_i^ℓ. Using (4.3.3), the approximate solution $f(x)$ of the Fredholm linear integral equations (4.5.6) satisfies the discrete equation

$$f_\ell = g + \sum_{i=0}^{m_\ell} \omega_i f(\phi_i^\ell) K(x, \phi_i^\ell), \quad x \in [a, b], \tag{1.5.5}$$

that has the corresponding symbolic form

$$f_\ell - \mathcal{K}_\ell f_\ell = g, \tag{1.5.6}$$

which is an $m_\ell \times m_\ell$ linear system for the nodal values $f_\ell(\phi_i^\ell)$, $i = 0, \ldots, m_\ell$, of the approximate solution. That is, (1.5.6) can be written in matrix-vector form as

$$(\mathbf{I}_\ell - \mathbf{K}_\ell) Z_\ell = G_\ell,$$

wherein, for $i = 0, \ldots, m_\ell$, we have

$$\{Z_\ell\}_i = f_\ell(\phi_i^\ell),\ \{G_\ell\}_i = g_\ell(\phi_i^\ell),\ \{\mathbf{K}_\ell\}_{i,j} = \omega_j K(\phi_i^\ell, \phi_j^\ell),$$

and $\mathbf{I}_\ell$ is the $m_\ell \times m_\ell$ identity matrix. To determine the approximate solution, the system matrix in (1.5.6) must be inverted. It is, therefore, useful to understand the linear algebra of the sub-matrices within that system. This method will be used in chapter 3 to solve Fredholm's integral equation using the quadrature and Hermite interpolation methods by the quadratic B splines.

Chapter 2

Smooth reverse subdivision of uniform algebraic hyperbolic B-splines curves

Contents

2.1 Introduction

In this chapter, we start with an introduction of uniform hyperbolic algebraic B-splines. generated over the space spanned by $\{\sinh(\alpha x), \cosh(\alpha x), x^{k-3}, \ldots, x, 1\}$, in which k is an integer larger than or equal to 3 and α is a tension parameter. The principal objective of this chapter is to apply this mathematical model of UAH B-splines to construct a general formula of the refinement equation for any given order k. Using the matrix version of this equation, we have also constructed the subdivision formula for UAH B-splines curves. In order to introduce a new reverse subdivision framework, entitled "Smooth Reverse Subdivision" associated with the cubic UAH B-splines, by continuing this process, we present a new multiresolution

technique for general topology curves. We illustrate our results by numerical experiments.

The results obtained in this chapter are presented in the research article [6], in collaboration with abdellah lamnii.

2.2 Uniform algebraic hyperbolic B-splines (UAH B-splines)

The UAH B-splines introduced in this chapter coincide with a particular case of the well-known hyperbolic spline functions. For instance, the hyperbolic interpolation spline built by Kvasov [42] is a special case of UAH B-splines. In the literature, there are a lot of papers devoted to constructing hyperbolic spline functions. For example. In the work of Kulikov and Makaro [41], a class of minimal hyperbolic splines and their properties are demonstrated. Sakai and Usmani [68] generated B-splines bases for hyperbolic and trigonometric splines by using a convolution process of an exponential function. They also provided an application of a hyperbolic spline of degree 4 to a numerical solution of a simple perturbation problem. Xu [84] established an implicit recurrence relation to derive explicit recursive algorithms for the computation of Tchebycheff B-splines. Based on the ideas and the results of Ron [64], Dahmen and Micchelli [23], made a thorough study of exponential splines and describe an application of E-splines to the Hilbert function for linear diophantine equations. It is well known that one can develop a nice spline theory based on cardinal exponential polynomials for constructing the hyperbolic polynomial B-splines (e.g., see Unser and Blu [79] and references therein). Many basis splines functions exist with a similar construction based on exponential, trigonometric or hyperbolic functions (see for example [49, 51, 55]). Moreover, B-spline's straightforward generalization is given in Zakharov[82], employing exponential functions with the strang-fix conditions.
Using the same notation as we defined in section 1.2, the space of uniform algebraic hyperbolic splines of order k is defined by

$$\mathcal{S}_k([a,b],\Phi^\ell)=\{s\in C^{k-2}([a,b])\ : s|_{[\phi_j^\ell,\phi_{j+1}^\ell]}\in\Delta_k\},\tag{2.2.1}$$

where $\Delta_k = span\{\sinh(\alpha x),\cosh(\alpha x),x^{k-3},\ldots,x,1\}$.
A basis of this space is $\{M_{i,k}^{[\alpha,\ell]},\ i\in\mathcal{I}\}$ with $\mathcal{I}=\{1,2,\ldots,m_\ell-k\}$, with these notation, $\text{supp}(M_{i,k}^{[\alpha,\ell]})=[\phi_i^\ell,\phi_{i+k}^\ell]$ and $\mathcal{I}_i=\{i,\ldots,i+k\}$ is the set of interiors knots in the support of $M_{i,k}^{[\alpha,\ell]}$. As usual, we add multiple knots at the the extremities of the interval $[a,b]$ such that $\phi_{-k}^\ell=\ldots=\phi_0^\ell=a$ and $\phi_{m_\ell}^\ell=\ldots=\phi_{m_\ell+k}^\ell=b$ (see [31],

for instance).
According to [49], in the following, we define UAH B-spline basis functions of order $k = 2$,

$$M_{0,2}^{[\alpha,\ell]}(x) = \begin{cases} \dfrac{\alpha h_\ell \sinh(\alpha x)}{2(\cosh(\alpha h_\ell) - 1)}, & x \in [0, h_\ell[, \\ \dfrac{\alpha h_\ell \sinh(\alpha(2h_\ell - x))}{2(\cosh(\alpha h_\ell) - 1)}, & x \in [h_\ell, 2h_\ell[, \\ 0, & otherwise, \end{cases} \tag{2.2.2}$$

and

$$M_{i,2}^{[\alpha,\ell]}(x) = M_{0,2}^{[\alpha,\ell]}(x - \phi_i^\ell),$$

Next, for $k \geq 3$, $M_{i,k}^{[\alpha,\ell]}$ are recursively defined by

$$M_{i,k}^{[\alpha,\ell]}(x) = \frac{1}{h_\ell} \int_{x-h_\ell}^{x} M_{i,k-1}^{[\alpha,\ell]}(t)dt, \tag{2.2.3}$$

The UAH B-splines $M_{i,k}^{[\alpha,\ell]}(x)$, for $i = 0, \ldots, m_\ell - k$ have interesting properties similar to those of the classical polynomial B-splines see [34, 43].

Property 2.2.1. The above family $M_{i,k}^{[\alpha,\ell]}, i = 0, \ldots, m_\ell - k$ generates the space $S_k([a, b], \Phi^\ell)$. Moreover, the following properties hold

1. Positivity: $\forall x \in [\phi_i^\ell, \phi_{i+k}^\ell]$ we have $M_{i,k}^{[\alpha,\ell]}(x) \geq 0$.
2. Derivative: $\left(M_{i,k}^{[\alpha,\ell]}(x)\right)' = \dfrac{1}{h_\ell}\left(M_{i,k-1}^{[\alpha,\ell]}(x) - M_{i+1,k-1}^{[\alpha,\ell]}(x)\right)$.
3. Partition of unity: $\sum_{i\in\mathbb{Z}} M_{i,k}^{[\alpha,\ell]}(x) = 1$, for all $k \geq 2$ and $\forall x \in \mathbb{R}$.
4. Linear independence globally: $M_{i,k}^{[\alpha,\ell]}(x)$, $i = 0, ..., m_\ell$ are linearly independent on $(-\infty, +\infty)$.

In Figure 2.1, we present the graphs of the UAH B-splines of order 2, 3 and 4, with different values of α. With the red curves represents $\alpha = 0.5$, the blue curves represents $\alpha = 1$ and the black curves represents $\alpha = 2$.

2.3 Refinement equation

A fundamental property of the basic B-splines functions is that each of them can be written as a linear combination of copies of it. Indeed, in the following theorem we are going to prove that the hyperbolic B-spline of order k satisfy the refinement equation. This procedure subdivides a hyperbolic B-spline associated with h_ℓ in a scaled and contracted copies of it associated with $h_{\ell+1}$ as follows.

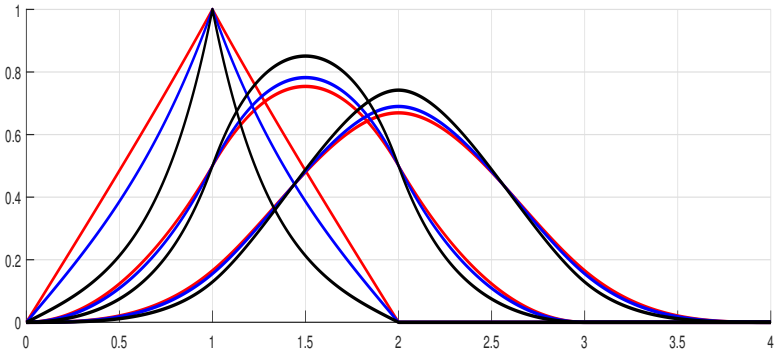

Figure 2.1 – UAH B-splines of order 2,3 and 4, with different values of α.

Theorem 2.3.1. *Let $M_{i,k}^{[\alpha,\ell]}(x)$ and $M_{i,k}^{[\alpha,\ell+1]}(x)$ represent the UAH B-splines of order $k \geq 2$ defined by knots Φ^{ℓ} and $\Phi^{\ell+1}$ respectively. Then, for all $i = 0, \ldots, m_{\ell} - k$, $M_{i,k}^{[\alpha,\ell]}(x)$ is defined by:*
If k is even, with $k = 2n$,

$$M_{i,k}^{[\alpha,\ell]}(x) = \sum_{j=0}^{n-1} \lambda_j^{[k,\ell]} \left(M_{2i+j,k}^{[\alpha,\ell+1]}(x) + M_{2i+k-j,k}^{[\alpha,\ell+1]}(x) \right) + \lambda_n^{[k,\ell]} M_{2i+n,k}^{[\alpha,\ell+1]}(x),$$

where

$$\lambda_0^{[k,\ell]} = \frac{\lambda_0^{[2,\ell]}}{2^{k-2}}, \lambda_j^{[k,\ell]} = \frac{\lambda_{j-1}^{[k-1,\ell]} + \lambda_j^{[k-1,\ell]}}{2}, \; j = 1, \ldots, n-1, \lambda_n^{[k,\ell]} = \lambda_{n-1}^{[k-1,\ell]}. \qquad (2.3.1)$$

If k is odd, with $k = 2n + 1$,

$$M_{i,k}^{[\alpha,\ell]}(x) = \sum_{j=0}^{n} \lambda_j^{[k,\ell]} \left(M_{2i+j,k}^{[\alpha,\ell+1]}(x) + M_{2i+k-j,k}^{[\alpha,\ell+1]}(x) \right),$$

where

$$\lambda_0^{[k,\ell]} = \frac{\lambda_0^{[2,\ell]}}{2^{k-2}}, \quad \lambda_j^{[k,\ell]} = \frac{\lambda_{j-1}^{[k-1,\ell]} + \lambda_j^{[k-1,\ell]}}{2}, \quad j = 1, \ldots, n. \qquad (2.3.2)$$

With $\lambda_0^{[2,\ell]} = \dfrac{1}{1 + \cosh(\alpha \frac{h_\ell}{2})}$ *and* $\lambda_1^{[2,\ell]} = \dfrac{2\cosh(\alpha \frac{h_\ell}{2})}{1 + cosh(\alpha \frac{h_\ell}{2})}$.

Proof. The proof can be done by induction on k. Indeed, for $k = 2$ according to the relationship (4.2.1), we deduce that $M_{i,2}^{[\alpha,\ell]}(x)$ can be written in the form

$$M_{i,2}^{[\alpha,\ell]}(x) = \lambda_0^{[2,\ell]} M_{2i,2}^{[\alpha,\ell+1]}(x) + \lambda_1^{[2,\ell]} M_{2i+1,2}^{[\alpha,\ell+1]}(x) + \lambda_2^{[2,\ell]} M_{2i+2,2}^{[\alpha,\ell+1]}(x).$$

Since $M_{i,2}^{[\alpha,\ell]}$ is symmetric, we obtain $\lambda_0^{[2,\ell]} = \lambda_2^{[2,\ell]}$.

Consequently, it suffices to compute $\lambda_0^{[2,\ell]}$ and $\lambda_1^{[2,\ell]}$, as a result we get

$$M_{i,2}^{[\alpha,\ell]}(x) = \begin{cases} \lambda_0^{[2,\ell]} M_{2i,2}^{[\alpha,\ell+1]}(x), & x \in [ih_\ell, (2i+1)\frac{h_\ell}{2}], \\ \lambda_0^{[2,\ell]} M_{2i,2}^{[\alpha,\ell+1]}(x) + \lambda_1^{[2,\ell]} M_{2i+1,2}^{[\alpha,\ell+1]}(x), & x \in [(2i+1)\frac{h_\ell}{2}, (2i+2)\frac{h_\ell}{2}], \end{cases}$$

with a simple computation we get $\lambda_0^{[2,\ell]} = \dfrac{1}{1+\cosh(\alpha\frac{h_\ell}{2})}$ and $\lambda_1^{[2,\ell]} = \dfrac{2\cosh(\alpha\frac{h_\ell}{2})}{1+\cosh(\alpha\frac{h_\ell}{2})}$.
Similarly, for $k=3$, $M_{i,3}^{[\alpha,\ell]}(x)$ can be written as

$$M_{i,3}^{[\alpha,\ell]}(x) = \lambda_0^{[3,\ell]} M_{2i,3}^{[\alpha,\ell+1]}(x) + \lambda_1^{[3,\ell]} M_{2i+1,3}^{[\alpha,\ell+1]}(x) + \lambda_2^{[3,\ell]} M_{2i+2,3}^{[\alpha,\ell+1]}(x) + \lambda_3^{[3,\ell]} M_{2i+3,3}^{[\alpha,\ell+1]}(x).$$

According to the symmetry of B-splines $M_{i,3}^{\alpha}, i = 0, \ldots, m_\ell - k$ we have $\lambda_0^{[3,\ell]} = \lambda_3^{[3,\ell]}$ and $\lambda_1^{[3,\ell]} = \lambda_2^{[3,\ell]}$. Moreover

$$M_{i,3}^{[\alpha,\ell]}(x) = \begin{cases} \lambda_0^{[3,\ell]} M_{2i,3}^{[\alpha,\ell+1]}(x), & x \in [ih_\ell, \dfrac{(2i+1)h_\ell}{2}], \\ \lambda_0^{[3,\ell]} M_{2i,2}^{[\alpha,\ell+1]}(x) + \lambda_1^{[3,\ell]} M_{2i+1,3}^{[\alpha,\ell+1]}(x), & x \in [\dfrac{(2i+1)h_\ell}{2}, (i+1)h_\ell], \end{cases} \tag{2.3.3}$$

On the other hand, we exploit the formula (4.2.2) to compute $M_{0,3}^{[\alpha,\ell]}$.
So,

$$M_{0,3}^{[\alpha,\ell]}(x) = \begin{cases} \dfrac{\cosh(\alpha x) - 1}{4\sinh^2(\frac{\alpha h_\ell}{2})}, & x \in [0, h_\ell[, \\ -\dfrac{\cosh(\alpha(x-h_\ell)) + \cosh(\alpha(2h_\ell - x)) - 2\cosh(\alpha h_\ell)}{2(\cosh(\alpha h_\ell) - 1)}, & x \in [h_\ell, 2h_\ell[, \\ \dfrac{\cosh(\alpha(3h_\ell - x)) - 1}{4\sinh^2(\frac{\alpha h_\ell}{2})}, & x \in [2h_\ell, 3h_\ell[, \\ 0, & otherwise. \end{cases} \tag{2.3.4}$$

Then, by (2.3.3) and (2.3.4), we obtain

$$\lambda_0^{[3,\ell]} = \frac{\lambda_0^{[2,\ell]}}{2}, \quad \lambda_1^{[3,\ell]} = \frac{\lambda_0^{[2,\ell]} + \lambda_1^{[2,\ell]}}{2}.$$

Now, suppose this proposition holds for $k-1$, where $k \geq 4$.
If $k-1$ is even such as $k-1 = 2n$, then k is odd, therefore

$$M_{i,k-1}^{[\alpha,\ell]}(x) = \sum_{j=0}^{n-1} \lambda_j^{[k-1,\ell]} \left(M_{2i+j,k-1}^{[\alpha,\ell+1]}(x) + M_{2i+k-1-j,k-1}^{[\alpha,\ell+1]}(x) \right) + \lambda_n^{[k-1,\ell]} M_{2i+n,k-1}^{[\alpha,\ell+1]}(x).$$

Using equation (4.2.2) we have

$$\begin{aligned} M_{i,k}^{[\alpha,\ell]}(x) &= \frac{1}{h_\ell}\int_{x-h_\ell}^{x} M_{i,k-1}^{[\alpha,\ell]}(t)dt, \\ &= \frac{1}{h_\ell}\int_{x-\frac{h_\ell}{2}}^{x} M_{i,k-1}^{[\alpha,\ell]}(t)dt + \frac{1}{h_\ell}\int_{x-h_\ell}^{x-\frac{h_\ell}{2}} M_{i,k-1}^{[\alpha,\ell]}(t)dt, \\ &= I_1(x,h_\ell) + I_2(x,h_\ell), \end{aligned}$$

where

$$\begin{aligned} I_1(x,h_\ell) &= \frac{1}{h_\ell}\int_{x-\frac{h_\ell}{2}}^{x} M_{i,k-1}^{[\alpha,\ell]}(t)dt, \\ &= \frac{1}{2}\left(\sum_{j=0}^{n-1}\lambda_j^{[k-1,\ell]}\left(M_{2i+j,k}^{[\alpha,\ell+1]}(x) + M_{2i+k-1-j,k}^{[\alpha,\ell+1]}(x)\right) + \lambda_n^{[k-1,\ell]}M_{2i+n,k}^{[\alpha,\ell+1]}(x)\right), \end{aligned}$$

and

$$\begin{aligned} I_2(x,h_\ell) &= \frac{1}{h_\ell}\int_{x-h_\ell}^{x-\frac{h_\ell}{2}} M_{i,k-1}^{[\alpha,\ell]}(t)dt, \\ &= \frac{1}{2}\left(\sum_{j=0}^{n-1}\lambda_j^{[k-1,\ell]}\left(M_{2i+j+1,k}^{[\alpha,\ell+1]}(x) + M_{2i+k-j,k}^{[\alpha,\ell+1]}(x)\right) + \lambda_n^{[k-1,\ell]}M_{2i+n+1,k}^{[\alpha,\ell+1]}(x)\right). \end{aligned}$$

Finally we obtain

$$\begin{aligned} M_{i,k}^{[\alpha,\ell]}(x) &= \sum_{j=0}^{n-1}\frac{\lambda_j^{[k-1,\ell]}}{2}\left[M_{2i+j,k}^{[\alpha,\ell+1]}(x) + M_{2i+k-j,k}^{[\alpha,\ell+1]}(x)\right] + \frac{\lambda_n^{[k-1,\ell]}}{2}\left[M_{2i+n,k}^{[\alpha,\ell+1]}(x) + M_{2i+n+1,k}^{[\alpha,\ell+1]}(x)\right] \\ &\quad + \sum_{j=0}^{n-1}\frac{\lambda_j^{[k-1,\ell]}}{2}\left[M_{2i+j+1,k}^{[\alpha,\ell+1]}(x) + M_{2i+k-1-j,k}^{[\alpha,\ell+1]}(x)\right], \\ &= \sum_{j=0}^{n-1}\frac{\lambda_j^{[k-1,\ell]}}{2}\left[M_{2i+j,k}^{[\alpha,\ell+1]}(x) + M_{2i+k-j,k}^{[\alpha,\ell+1]}(x)\right] + \frac{\lambda_n^{[k-1,\ell]}}{2}\left[M_{2i+n,k}^{[\alpha,\ell+1]}(x) + M_{2i+n+1,k}^{[\alpha,\ell+1]}(x)\right] \\ &\quad + \sum_{j=1}^{n}\frac{\lambda_{j-1}^{[k-1,\ell]}}{2}\left[M_{2i+j,k}^{[\alpha,\ell+1]}(x) + M_{2i+k-j,k}^{[\alpha,\ell+1]}(x)\right], \\ &= \sum_{j=1}^{n}\frac{\lambda_{j-1}^{[k-1,\ell]} + \lambda_j^{[k-1,\ell]}}{2}\left[M_{2i+j,k}^{[\alpha,\ell+1]}(x) + M_{2i+k-j,k}^{[\alpha,\ell+1]}(x)\right] \\ &\quad + \frac{\lambda_0^{[k-1,\ell]}}{2}\left[M_{2i,k}^{[\alpha,\ell+1]}(x) + M_{2i+k,k}^{[\alpha,\ell+1]}(x)\right], \\ &= \sum_{j=0}^{n}\lambda_j^{[k,\ell]}\left[M_{2i+j,k}^{[\alpha,\ell+1]}(x) + M_{2i+k-j,k}^{[\alpha,\ell+1]}(x)\right], \end{aligned}$$

with

$$\lambda_0^{[k,\ell]} = \frac{\lambda_0^{[2,\ell]}}{2^{k-2}} \quad , \quad \lambda_j^{[k,\ell]} = \frac{\lambda_{j-1}^{[k-1,\ell]} + \lambda_j^{[k-1,\ell]}}{2}, \quad j = 1, \dots, n.$$

Similarly, we can prove that, if $k-1$ is odd we have

$$M_{i,k}^{[\alpha,\ell]}(x) = \sum_{j=0}^{n-1} \lambda_j^{[k,\ell]} \left[M_{2i+j,k}^{[\alpha,\ell+1]}(x) + M_{2i+k-j,k}^{[\alpha,\ell+1]}(x) \right] + \lambda_n^{[k,\ell]} M_{2i+n,k}^{[\alpha,\ell+1]}(x),$$

where

$$\lambda_0^{[k,\ell]} = \frac{\lambda_0^{[2,\ell]}}{2^{k-2}}, \quad \lambda_j^{[k,\ell]} = \frac{\lambda_{j-1}^{[k-1,\ell]} + \lambda_j^{[k-1,\ell]}}{2}, \; j = 1, \dots, n-1, \quad \lambda_n^{[k-1,\ell]} = \lambda_{n-1}^{[k-1,\ell]}.$$

The proof is complete. □

We will see later on the importance of this equation. In figure 2.2, we introduce the refinement equation associated with the UAH B-spline of order 3 and 4.

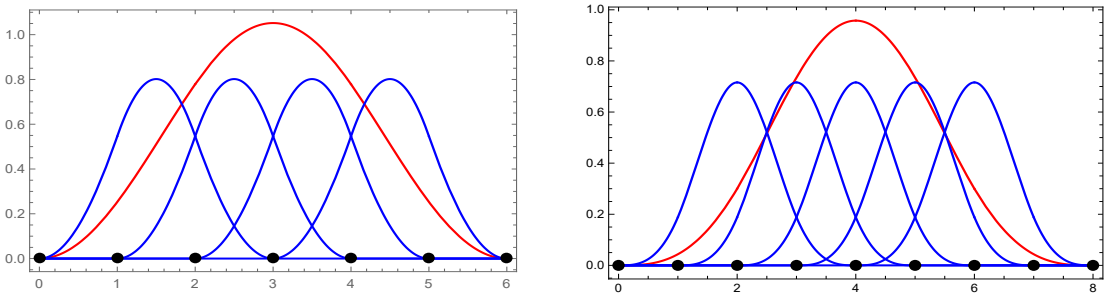

(a) Quadratic UAH B-splines. (b) Cubic UAH B-splines.

Figure 2.2 – UAH B-spline curves and refinement equation.

Remark 2. We can prove the generalized refinement equation similarly for UAT B splines which is defined in section 1.2. In effect, in this case, the value of $\lambda_0^{[2,\ell]}$ and $\lambda_1^{[2,\ell]}$ are given by

$$\begin{cases} \lambda_0^{[2,\ell]} = \dfrac{1}{1+\cos(\alpha h_{\ell+1})}, \\ \lambda_1^{[2,\ell]} = \dfrac{2\cos(\alpha h_{\ell+1})}{1+cos(\alpha h_{\ell+1})}. \end{cases}$$

2.3.1 Refinement matrices

According to the previous theorem, we can represent this refinement equation in matrix form as follows.

Corollary 2.3.1. *The UAH B-splines* $M_\ell^k = (M_{0,k}^{[\alpha,\ell]}(x), M_{1,k}^{[\alpha,\ell]}(x), \dots, M_{m_\ell-k,k}^{[\alpha,\ell]}(x))^T$

satisfy the following generalized refinement equation

$$M_\ell^k = P_k M_{\ell+1}^k, \tag{2.3.5}$$

where P_k *is* $(m_\ell - k + 1) \times (m_{\ell+1} - k + 1)$ *refinement matrix defined as*

- *Case* k *even* $(n = \dfrac{k}{2})$*:*

$$P_k = \begin{pmatrix}
\lambda_0^{[k,\ell]} & \lambda_1^{[k,\ell]} & \cdots & \lambda_{n-1}^{[k,\ell]} & \lambda_n^{(k)} & \lambda_{n-1}^{[k,\ell]} & \cdots & \lambda_1^{[k,\ell]} & \lambda_0^{[k,\ell]} & 0 & \cdots & & & & 0 \\
0 & 0 & \lambda_0^{[k,\ell]} & \lambda_1^{[k,\ell]} & \cdots & \lambda_{n-1}^{[k,\ell]} & \lambda_n^{[k,\ell]} & \lambda_{n-1}^{[k,\ell]} & \cdots & \lambda_1^{[k,\ell]} & \lambda_0^{[k,\ell]} & 0 & \cdots & & 0 \\
0 & 0 & 0 & 0 & \lambda_0^{[k,\ell]} & \lambda_1^{[k,\ell]} & \cdots & \lambda_{n-1}^{[k,\ell]} & \lambda_n^{[k,\ell]} & \lambda_{n-1}^{[k,\ell]} & \cdots & \lambda_1^{[k,\ell]} & \lambda_0^{[k,\ell]} & 0 & \cdots & 0 \\
\vdots & & & & \ddots & \ddots & & \ddots & \ddots & \ddots & \ddots & \ddots & \ddots & & & \vdots \\
 & & & & & \ddots & \ddots & & \ddots & \ddots & \ddots & \ddots & \ddots & \ddots & & \\
0 & \cdots & & & 0 & \lambda_0^{[k,\ell]} & \lambda_1^{[k,\ell]} & \cdots & \lambda_{n-1}^{[k,\ell]} & \lambda_n^{[k,\ell]} & \lambda_{n-1}^{[k,\ell]} & \cdots & \lambda_1^{[k,\ell]} & \lambda_0^{[k,\ell]} & 0 & 0 \\
0 & \cdots & & & & 0 & 0 & \lambda_0^{[k,\ell]} & \lambda_1^{[k,\ell]} & \cdots & \lambda_{n-1}^{[k,\ell]} & \lambda_n^{[k,\ell]} & \lambda_{n-1}^{[k,\ell]} & \cdots & \lambda_1^{[k,\ell]} & \lambda_0^{[k,\ell]}
\end{pmatrix},$$

- *Case* k *odd* $(n = \dfrac{k-1}{2})$*:*

$$P_k = \begin{pmatrix}
\lambda_0^{[k,\ell]} & \lambda_1^{[k,\ell]} & \cdots & \lambda_n^{[k,\ell]} & \lambda_n^{[k,\ell]} & \lambda_{n-1}^{[k,\ell]} & \cdots & \lambda_1^{[k,\ell]} & \lambda_0^{[k,\ell]} & 0 & \cdots & & & & 0 \\
0 & 0 & \lambda_0^{[k,\ell]} & \lambda_1^{[k,\ell]} & \cdots & \lambda_n^{[k,\ell]} & \lambda_n^{[k,\ell]} & \lambda_{n-1}^{[k,\ell]} & \cdots & \lambda_1^{[k,\ell]} & \lambda_0^{[k,\ell]} & 0 & \cdots & & 0 \\
0 & 0 & 0 & 0 & \lambda_0^{[k,\ell]} & \lambda_1^{[k,\ell]} & \cdots & \lambda_{n-1}^{[k,\ell]} & \lambda_n^{[k,\ell]} & \lambda_n^{[k,\ell]} & \cdots & \lambda_1^{[k,\ell]} & \lambda_0^{[k,\ell]} & 0 & \cdots & 0 \\
\vdots & & & & \ddots & \ddots & & \ddots & \ddots & \ddots & \ddots & \ddots & \ddots & & & \\
 & & & & & \ddots & \ddots & & \ddots & \ddots & \ddots & \ddots & \ddots & \ddots & & \\
0 & \cdots & & & 0 & \lambda_0^{[k,\ell]} & \lambda_1^{[k,\ell]} & \cdots & \lambda_n^{[k,\ell]} & \lambda_n^{[k,\ell]} & \lambda_{n-1}^{[k,\ell]} & \cdots & \lambda_1^{[k,\ell]} & \lambda_0^{[k,\ell]} & 0 & 0 \\
0 & \cdots & & & & 0 & 0 & \lambda_0^{[k,\ell]} & \lambda_1^{[k,\ell]} & \cdots & \lambda_n^{[k,\ell]} & \lambda_n^{[k,\ell]} & \lambda_{n-1}^{[k,\ell]} & \cdots & \lambda_1^{[k,\ell]} & \lambda_0^{[k,\ell]}
\end{pmatrix}.$$

Where $\lambda_i^{[k,\ell]}$, $i = 0, \ldots, n$ *are given in* (2.3.1) *and* (4.3.1).

2.4 Subdivision formula for UAH B-splines curves

The notion of the subdivision is present in many areas of applied mathematics, it was introduced for the first time in 1947 by de Rham. Its re-invention in 1974 by Chaikin made them available as part of computer-aided design (CAD). Today, a variety of techniques for building a subdivision curve have been developed in the literature. The first scheme constructed allowed to approach the B-spline curves (Catmull, et al. [16] and Doo, et al. [25]). Then, in 1980 Lane and Riesenfeld [48] proposed an algorithm for the subdivision of uniform B-spline curves with arbitrary order. Therefore in 1987, an interpolating scheme, which conserves the initial points, was developed by Dyn et al. [27] and Dubuc [28]. After that, in 1991, Cavaretta et al. [17] and Dyn [26] propose a general theory and techniques of convergence studies, strongly inspired by the construction of the refinement equation in wavelet multiresolution analysis. In 2016, Siddiqi et al. [69] introduced binary approximat-

ing non-stationary subdivision schemes using hyperbolic B-spline with the ability of reproduction of parabolas and hyperbolas. One can also find various other subdivision schemes that are special cases of these three classes of B-splines (Morin et al., 2001; Jena et al., 2002; Lu et al., 2002; Zhang et al., 2005; Zhang and Krause, 2005).

In this section, we shall discuss the subdivision formula for UAH B-spline curves. This procedure subdivides a UAH B-spline curve associated with h_ℓ in a scaled and contracted copies of itself associated with $h_{\ell+1}$. More precisely, we present the explicit matrix form of the generalized subdivision scheme of this type of B spline, afterward illustrating some numerical examples of the application of this scheme in generating limit curves.

Corollary 2.4.1. *Let $\mathcal{C}_k$ be a hyperbolic algebraic B-spline curve of order $k \geq 3$ with interval size h_ℓ and control polygon $C^\ell = [c_0^\ell, c_1^\ell, c_2^\ell, \cdots, c_{m_\ell-k}^\ell]$, $m_\ell \geq k$, that is,*

$$\mathcal{C}_k(t) = \sum_{i=0}^{m_\ell-k} c_i^\ell M_{i,k}^{[\alpha,\ell]}(t).$$

The curve $\mathcal{C}_k$ can also be represented by the refined knots $\phi^{\ell+1}$ as:

$$\mathcal{C}_k(t) = \sum_{i=0}^{m_{\ell+1}-k} c_i^{\ell+1} M_{i,k}^{[\alpha,\ell+1]}(t) = C^\ell P_k M_{\ell+1}^k, \tag{2.4.1}$$

where P_k is the refinement matrix given by (4.3.2) and $C^{\ell+1} = (c_0^{\ell+1}, c_1^{\ell+1}, \cdots, c_{m_{\ell+1}-k}^{\ell+1})$ is the new control polygon given by the following form

$$C^{\ell+1} = C^\ell P_k. \tag{2.4.2}$$

The construction of a B-spline curve starts with a base level polygonal mesh C^ℓ. A refinement scheme is then applied to this curve. This process takes that mesh and subdivides it, creating new vertices. Finally, the positions of the new vertices in the generated curve $C^{\ell+1}$ are computed based on the positions of nearby old vertices by applying the refinement matrix P_k.

The curves generated by this subdivision scheme have C^{k-1} continuity differential. However, the curves constructed by subdivision methods can be decomposed without introducing any details. By using a multiresolution analysis, this problem can be solved. Indeed, a multiresolution analysis decomposes a function into a coarse approximation of the function plus some details. Thus, multiresolution encapsulates two processes: decomposition (reverse subdivision plus detail representation) and reconstruction (subdivision plus detail correction). Currently, such multiresolution analysis tools are being applied to curve editing and compression.

2.4.1 Numerical example

In Figure 2.3, we present a numerical example of UAH B-spline curves, we consider two different curves, and we illustrate four subdivision steps with order $k = 3$ and tension parameter set to $\alpha = 0.5$. At each iteration, we use (4.3.5) and we obtain new control points, which enhance the shape precision of the curves and eventually converge to the original initial curve. Our proposed method is straightforward and easy to manipulate, moreover digitally, it is less computational compared to the current techniques available in the literature.

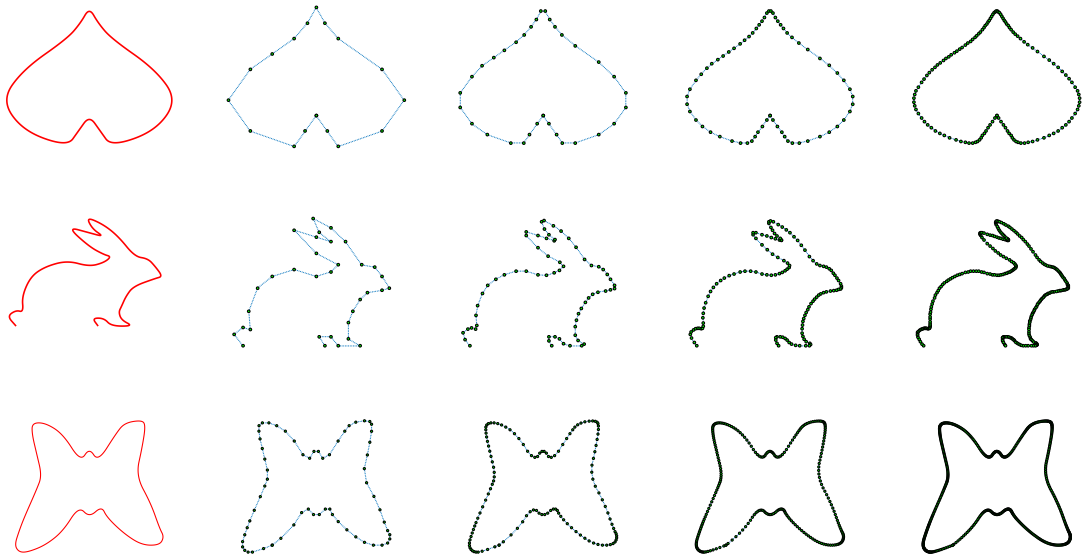

(k) B-spline curve. (l) initial polygon. (m) Smoothed once. (n) Smoothed twise. (o) Smoothed thrice.

Figure 2.3 – Tree steps of subdivision curves with $k = 3$ and $\alpha = 0.5$.

2.5 Reverse subdivision of quadratic UAH B-spline curve

The subdivision is a smoothing technique, but its reverse can generate a rough approximation at high energy. Thus, after a few iterations of the inversion process, it is generally challenging to find a correspondence between the coarse points' overall structure and the original ones. However, the proposed smooth reverse subdivision approach preserves the origin curve's overall design, making it a better candidate for wavelet construction. The reverse scheme was introduced in many papers see for instance [24] where the authors present a reverse Chaikin algorithm and [66, 67] where Javad Sadeghi, Faramarz F. Samavati present smooth reverse subdivision, based on a least squares problem. The reverse subdivision is a very important task in several applications for curves and surfaces. A well-known example of the

application of reverse subdivision is the removal of noise from curves. For instance, Foster et al. [35] use reverse subdivision to remove and filter artifacts and noises from silhouettes extracted from polygonal meshes. This approach was also used by Mundermann et al. [56] to reduce the number of vertices in the raw data of a digitized leaf in their work on modeling lobed leaves.

This section aims to find an explicit mathematical method of uniform reverse subdivision associated with polygonal curves, and it's about extracting the different formulas from the control polygon points $C^\ell = [c_i^\ell, i = -2, ..., m_\ell - 1]^T$ at step ℓ by using that of the step $\ell + 1$. For convenience of discussion, we first define the quadratic UHA B-splines. From (4.2.2) we have

$$M_{0,3}^{[\alpha,\ell]}(x) = \begin{cases} \dfrac{\cosh(\alpha x) - 1}{4\sinh^2(\frac{\alpha h_\ell}{2})}, & x \in [\phi_0^\ell, \phi_1^\ell[, \\ -\dfrac{\cosh(\alpha(x - h_\ell)) + \cosh(\alpha(2h_\ell - x)) - 2\cosh(\alpha h_\ell)}{2(\cosh(\alpha h_\ell) - 1)}, & x \in [\phi_1^\ell, \phi_2^\ell[, \\ \dfrac{\cosh(\alpha(3h_\ell - x)) - 1}{4\sinh^2(\frac{\alpha h_\ell}{2})}, & x \in [\phi_2^\ell, \phi_3^\ell[, \\ 0, & otherwise. \end{cases} \tag{2.5.1}$$

and

$$M_{i,3}^{[\alpha,\ell]}(x) = M_{0,3}^{[\alpha,\ell]}(x - \phi_i^\ell).$$

Then, the respective left and right hand side boundary hyperbolic UAH B-splines are

$$M_{-2,3}^{[\alpha,\ell]}(x) = \begin{cases} \dfrac{\cosh(\alpha(h_\ell - x)) - 1}{\cosh(\alpha h_\ell) - 1}, & x \in [\phi_0^\ell, \phi_1^\ell[, \\ 0, & otherwise. \end{cases}$$

$$M_{-1,3}^{[\alpha,\ell]}(x) = \begin{cases} \dfrac{2\cosh(\alpha h) - 2\cosh(\alpha(h - x)) - \cosh(\alpha x) + 1}{4\sinh^2\left(\frac{\alpha h_\ell}{2}\right)}, & x \in [\phi_0^\ell, \phi_1^\ell[, \\ \dfrac{\sinh^2\left(\alpha h - \frac{\alpha x}{2}\right)}{2\sinh^2\left(\frac{\alpha h_\ell}{2}\right)}, & x \in [\phi_1^\ell, \phi_2^\ell[, \\ 0, & otherwise. \end{cases}$$

$$M_{m_\ell-2,3}^{[\alpha,\ell]}(x) = \begin{cases} \dfrac{\cosh\left(\alpha\left(\left(m_\ell - 2\right)h_\ell - x\right)\right) - 1}{4\sinh^2\left(\frac{\alpha h_\ell}{2}\right)}, & x \in \left[\phi_{m_\ell-2}^\ell, \phi_{m_\ell-1}^\ell\right[, \\ 1 - \cosh\left(\alpha\left(m_\ell h_\ell - x\right)\right) & \\ \dfrac{-2\cosh\left(\alpha\left(x - \left(m_\ell - 1\right)h\right) + 2\cosh\left(\alpha h_\ell\right)\right.}{4\sinh^2\left(\frac{\alpha h_\ell}{2}\right)}, & x \in \left[\phi_{m_\ell-1}^\ell, \phi_{m\ell}^\ell\right[\\ 0, & \text{otherwise}, \end{cases}$$

$$M_{m_\ell-1,3}^{[\alpha,\ell]}(x) = \begin{cases} \dfrac{\cosh(\alpha(x - (m_\ell - 1)h_\ell)) - 1}{\cosh(\alpha h_\ell) - 1}, & x \in [\phi_{m_\ell-1}^\ell, \phi_{m_\ell}^\ell[, \\ 0, & otherwise. \end{cases}$$

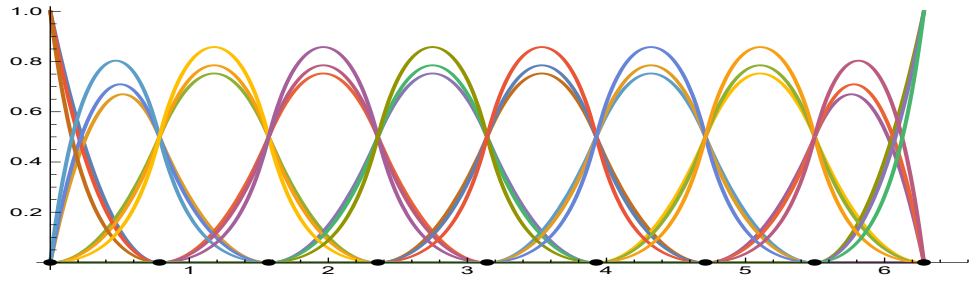

Figure 2.4 – The UAH B-splines $M_{i,3}^{[\alpha,\ell]}(x)$ with $\alpha = 0.5, 1, 2$.

Corollary 2.5.1. *The UAH B-splines* $M_{i,3}^{[\alpha,\ell]}$, $i = -2, \ldots, m_\ell - 1$ *satisfy the following refinement equation*

$$M_{\ell-1}^3 = P_3 M_\ell^3, \tag{2.5.2}$$

where the refinement matrix P_3 *of size* $(m_{\ell-1}+2) \times (m_\ell+2)$. *More precisely, the entries* $(p_{i,j})$ *of* P_3 *are all equal to zero except*

- $p_{1,1} = 1$ *and* $p_{1,2} = \lambda_0^{[2,\ell]}$,
- $p_{2,2} = 1 - \lambda_0^{[2,\ell]}$, $p_{2,3} = \lambda_1^{[3,\ell]}$ *and* $p_{2,4} = \lambda_0^{[3,\ell]}$,
- $p_{i,2i-3} = p_{i,2i} = \lambda_0^{[3,\ell]}$ *and* $p_{i,2i-2} = p_{i,2i-1} = \lambda_1^{[3,\ell]}$, *for* $i = 3, \cdots, m_{\ell-1}$,
- $p_{m_{\ell-1}+1,m_\ell-1} = \lambda_0^{[3,\ell]}$, $p_{m_{\ell-1}+1,m_\ell} = \lambda_1^{[3,\ell]}$ *and* $p_{m_{\ell-1}+1,m_\ell+1} = 1 - \lambda_0^{[2,\ell]}$,
- $p_{m_{\ell-1}+2,m_\ell+1} = \lambda_0^{[2,\ell]}$ *and* $p_{m_{\ell-1}+2,m_\ell+2} = 1$.

For the reverse subdivision problem, we have two types of polygons to calculate the position of a single point in the original: where the first represent the weak resolution and the second represent the correction. This cannot be guaranteed in the general case. As in [24], the solution is to take the average of the two positions and store the error vectors. Then by using (4.3.5), we have,

$$\begin{cases} c_{-2}^{\ell+1} & = c_{-2}^{\ell}, \\ c_{-1}^{\ell+1} & = \lambda_0^{[2,\ell+1]} c_{-2}^{\ell} + (1 - \lambda_0^{[2,\ell]}) c_{-1}^{\ell}, \\ c_{2i}^{\ell+1} & = \lambda_1^{[3,\ell+1]} c_{i-1}^{\ell} + \lambda_0^{[3,\ell+1]} c_i^{\ell}, \qquad i = 0, ..., m_\ell - 2, \\ c_{2i+1}^{\ell+1} & = \lambda_0^{[3,\ell+1]} c_{i-1}^{\ell} + \lambda_1^{[3,\ell+1]} c_i^{\ell}, \qquad i = 0, ..., m_\ell - 2, \\ c_{m_{\ell+1}-2}^{\ell+1} & = (1 - \lambda_0^{[2,\ell]}) c_{m_\ell-2}^{\ell} + \lambda_0^{[2,\ell+1]} c_{m_\ell-1}^{\ell}, \\ c_{m_{\ell+1}-1}^{\ell+1} & = c_{m_\ell-1}^{\ell}. \end{cases} \tag{2.5.3}$$

By solving the system (2.5.3), we get the formulas to compute the points C^ℓ according to the points $C^{\ell+1}$. The first two points and the last two points are given by

$$\begin{cases} c^\ell_{-2} & = c^{\ell+1}_{-2}, \\ c^\ell_{-1} & = 2\delta^{\ell+1}c^{\ell+1}_{-2} + (1-2\delta^{\ell+1})c^{\ell+1}_{-1}, \\ c^\ell_{m_\ell-2} & = (1-2\delta^{\ell+1})c^{\ell+1}_{m_{\ell+1}-2} + 2\delta^{\ell+1}c^{\ell+1}_{m_{\ell+1}-1}, \\ c^\ell_{m_\ell-1} & = c^{\ell+1}_{m_{\ell+1}-1}, \end{cases} \tag{2.5.4}$$

where $\delta^{\ell+1} = \dfrac{-1}{2}\text{sech}\,(\alpha h_{\ell+1})$.

Remark 1. when this technique is based on the UAT B splines introduced in section 1.2, the value of $\delta^{\ell+1}$ is equal to

$$\delta^{\ell+1} = \frac{-1}{2}\sec\,(\alpha h_{\ell+1})$$

Then, the forward reverse subdivision schemes step becomes:
for $i = 1, \cdots, m_{\ell-1} - 2$ we have

$$\begin{cases} c^\ell_{i-1} & = (1-\delta^{\ell+1})c^{\ell+1}_{2i} + \delta^{\ell+1}c^{\ell+1}_{2i+1}, \\ c^\ell_{i} & = \delta^{\ell+1}c^{\ell+1}_{2i} + (1-\delta^{\ell+1})c^{\ell+1}_{2i+1}, \end{cases} \tag{2.5.5}$$

in particular

$$\begin{cases} c^\ell_{-2} & = (1-\frac{1}{2}\delta^{\ell+1})c^{\ell+1}_{-2} + \frac{1}{2}\delta^{\ell+1}c^{\ell+1}_{-1}, \\ e^\ell_{-2} & = \frac{1}{2}\delta^{\ell+1}c^{\ell+1}_{-2} - \frac{1}{2}\delta^{\ell+1}c^{\ell+1}_{-1}, \end{cases}$$

$$\begin{cases} c^\ell_{-1} & = \frac{3}{2}\delta^{\ell+1}c^{\ell+1}_{-2} + (1-\frac{3}{2}\delta^{\ell+1})c^{\ell+1}_{-1}, \\ e^\ell_{-1} & = \frac{1}{2}\delta^{\ell+1}c^{\ell+1}_{-2} - \frac{1}{2}\delta^{\ell+1}c^{\ell+1}_{-1}. \end{cases}$$

Consequently, for $i = 0, ..., m_\ell - 3$,

$$\begin{cases} c^\ell_{i} & = \dfrac{\delta^{\ell+1}}{2}\left(c^{\ell+1}_{2i} - c^{\ell+1}_{2i+1} - c^{\ell+1}_{2i+2} + c^{\ell+1}_{2i+3}\right) + \dfrac{1}{2}\left(c^{\ell+1}_{2i+1} + c^{\ell+1}_{2i+2}\right), \\ e^\ell_{i} & = \dfrac{\delta^{\ell+1}}{2}\left(c^{\ell+1}_{2i} - c^{\ell+1}_{2i+1} + c^{\ell+1}_{2i+2} - c^{\ell+1}_{2i+3}\right) + \dfrac{1}{2}\left(c^{\ell+1}_{2i+1} - c^{\ell+1}_{2i+2}\right). \end{cases} \tag{2.5.6}$$

Therefore,

$$\begin{cases} c^{\ell}_{m_\ell-2} &= (1-\frac{3}{2}\delta^{\ell+1})c^{\ell+1}_{m_{\ell+1}-2}+\frac{3}{2}\delta^{\ell+1}c^{\ell+1}_{m_{\ell+1}-1},\\ e^{\ell}_{m_\ell-2} &= -\frac{1}{2}\delta^{\ell+1}c^{\ell+1}_{m_{\ell+1}-2}+\frac{1}{2}\delta^{\ell+1}c^{\ell+1}_{m_{\ell+1}-1}, \end{cases}$$

$$\begin{cases} c^{\ell}_{m_\ell-1} &= \frac{1}{2}\delta^{\ell+1}c^{\ell+1}_{m_{\ell+1}-2}+(1-\frac{1}{2}\delta^{\ell+1})c^{\ell+1}_{m_{\ell+1}-1},\\ e^{\ell}_{m_\ell-1} &= -\frac{1}{2}\delta^{\ell+1}c^{\ell+1}_{m_{\ell+1}-2}+\frac{1}{2}\delta^{\ell+1}c^{\ell+1}_{m_{\ell+1}-1}. \end{cases}$$

So, the scheme (2.5.3) becomes, for $i=0,...,m_\ell-2$

$$\begin{cases} c^{\ell+1}_{-2} &= c^{\ell}_{-2}+e^{\ell}_{-2},\\ c^{\ell+1}_{-1} &= \lambda_0^{[2,\ell+1]}\left(c^{\ell}_{-2}-e^{\ell}_{-2}\right)+(1-\lambda_0^{[2,\ell+1]})\left(c^{\ell}_{-1}+(1-4\delta^{\ell+1})e^{\ell}_{-1}\right),\\ c^{\ell+1}_{2i} &= \lambda_1^{[3,\ell+1]}(c^{\ell}_{i-1}-e^{\ell}_{i-1})+\lambda_0^{[3,\ell+1]}(c^{\ell}_{i}+e^{\ell}_{i}),\\ c^{\ell+1}_{2i+1} &= \lambda_0^{[3,\ell+1]}(c^{\ell}_{i-1}-e^{\ell}_{i-1})+\lambda_1^{[3,\ell+1]}(c^{\ell}_{i}+e^{\ell}_{i}),\\ c^{\ell+1}_{m_{\ell+1}-2} &= (1-\lambda_0^{[2,\ell+1]})\left(c^{\ell}_{m_\ell-2}+(1-4\delta^{\ell+1})e^{\ell}_{m_\ell-2}\right)+\lambda_0^{[2,\ell+1]}\left(c^{\ell}_{m_\ell-1}-e^{\ell}_{m_\ell-1}\right),\\ c^{\ell+1}_{m_{\ell+1}-1} &= c^{\ell}_{m_\ell-1}+e^{\ell}_{m_\ell-1}, \end{cases} \tag{2.5.7}$$

where $e^{\ell}_i,\ i=-2,...,m_\ell-1$ called details.

This reverse subdivision problem related to subdivision curves joins the problem of approximating a set of points or segments by smooth parametric curves such as B-Splines. Besides, a subdivision curve does not have a parametric formulation and, therefore, cannot be evaluated at any curvilinear abscissa. Note that this disadvantage can be resolved by different techniques, such as the one used here. Indeed, this technique helps to obtain an optimal set of coarse initial polygon points that have minimal subdivision error and minimum overall energy, for example, see Figures 2.6 and 2.5. On the other hand, the reverse subdivision plays an essential role in real applications, especially in:

- The simplification of curves: By using inverse subdivision, the size of a subdivision curve can be reduced. Indeed, the compression of the size given its geometry allows its transmission by the network [81, 50].
- The reconstruction of a parametric curve/surface by inverse subdivision: In the context of C.A.O, for example, to obtain continuous surfaces from imported discrete mesh data [50, 63].
- The multiresolution representation of a subdivision model: The subdivision process increases by the resolution of the subdivision mesh, and, conversely,

the reverse subdivision decreases by the resolution of the mesh. For graphic outputs or in animation films, smooth meshes are used when they are close and coarse meshes when they are far away.

- The deformation of a mesh by the subdivision: Reverse subdivision also makes it possible to reconstruct a new coarse mesh from a distorted subdivision mesh [33].

2.5.0.1 Numerical example

Here we present some examples to illustrate how the proposed technique of inverted subdivision schemes can be used in the approximation of curves. Indeed, Figures 2.6 and 2.5 shows a closed and an open UAH B-splines curves with four levels of smooth reverse subdivision.

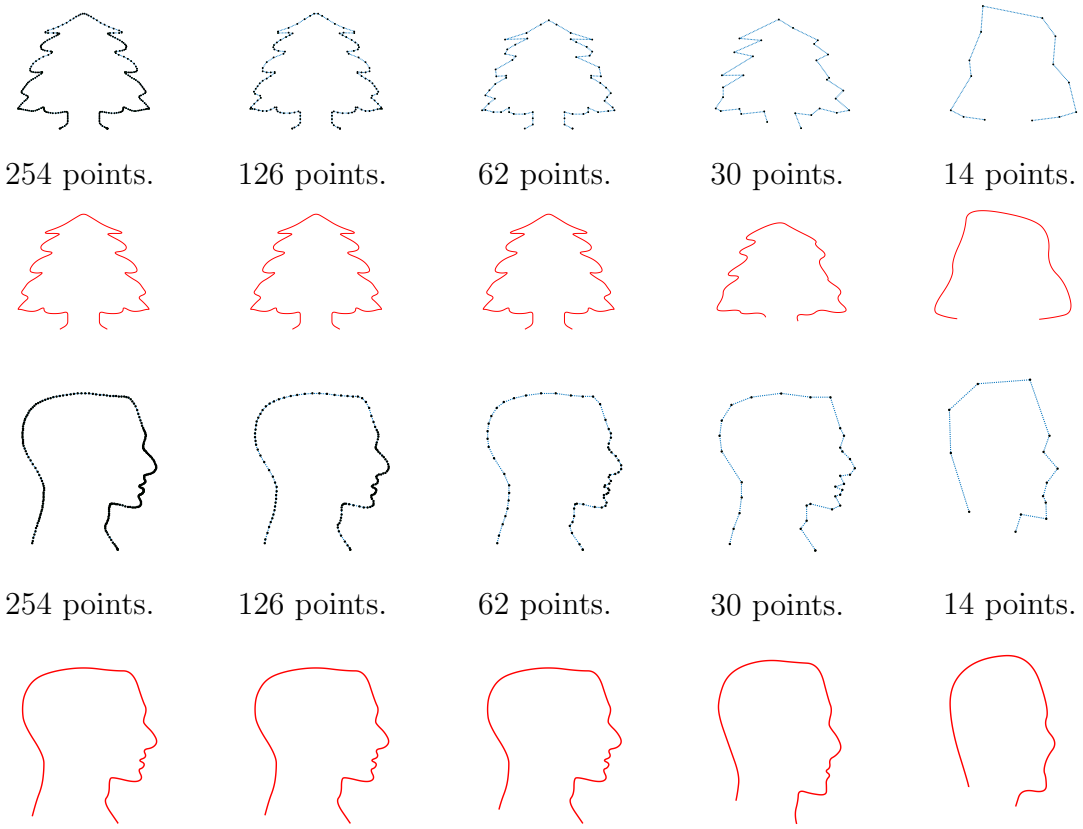

Figure 2.5 – An open curve with 254 points and its three levels of local quadratic B-spline smooth reverse subdivision.

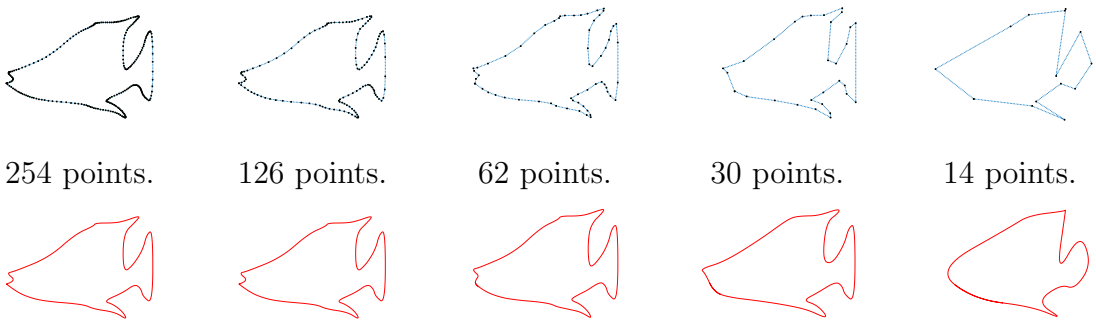

Figure 2.6 – A closed curve with 254 points and its four levels of local quadratic B-spline smooth reverse subdivision.

2.6 Multiresolution and reverse subdivision

based on the reverse subdivision technique. For example, Samavati and Bartels [35] are the first researchers. They used the notion of reverse subdivision method for constructing multiresolution representation and studied its application to derive local reverse subdivision filters using local linear conditions [14]. Reference [67], Sadeghi et al. developed a full multiresolution representation based on reverse subdivision to create a good and smooth approximation of the original control points. In [24], Mohamed F. Hassan and Neil A. Dodgson presented a reverse Chaikin algorithm that generates a multiresolution representation of any line chain.

In this subsection, by following the method introduced in [24], we present the UAH-spline wavelets associated with UAH splines of order three. In a multiresolution representation a set of fine points $\mathcal{C}^\ell$ is decomposed to a set of coarse points $\mathcal{C}^{\ell-1}$ and some wavelet coefficients $E^{\ell-1}$ called details. The decomposition is done using analysis filter matrices A_ℓ and B_ℓ as $C^{\ell-1} = A_\ell C^\ell$ and $E^{\ell-1} = B_\ell C^\ell$ where the filters matrix A_ℓ and B_ℓ of size $(m_{\ell-1}+2) \times (m_\ell + 2)$. According to (4.4.1), it is easy to find that:

$$A_\ell = \frac{1}{2}\begin{pmatrix}
2-\delta^\ell & \delta^\ell & 0 & \cdots & & & & & & & 0 \\
3\delta^\ell & 2-3\delta^\ell & 0 & \cdots & & & & & & & 0 \\
0 & 0 & \delta^\ell & 1-\delta^\ell & 1-\delta^\ell & \delta^\ell & 0 & \cdots & & & 0 \\
0 & 0 & 0 & 0 & \delta^\ell & 1-\delta^\ell & 1-\delta^\ell & \delta^\ell & 0 & \cdots & 0 \\
\vdots & & & & \ddots & \ddots & \ddots & \ddots & & & \vdots \\
0 & \cdots & 0 & \delta^\ell & 1-\delta^\ell & 1-\delta^\ell & \delta^\ell & 0 & 0 & 0 & 0 \\
0 & & & \cdots & 0 & \delta^\ell & 1-\delta^\ell & 1-\delta^\ell & \delta^\ell & 0 & 0 \\
0 & & & & & & & \cdots & 0 & 2-3\delta^\ell & 3\delta^\ell \\
0 & & & & & & & \cdots & 0 & \delta^\ell & 2-\delta^\ell
\end{pmatrix}$$

$$B_\ell = \frac{1}{2}\begin{pmatrix}
\delta^\ell & -\delta^\ell & 0 & \cdots & & & & & & & 0 \\
\delta^\ell & -\delta^\ell & 0 & \cdots & & & & & & & 0 \\
0 & 0 & \delta^\ell & 1-\delta^\ell & \delta^\ell-1 & -\delta^\ell & 0 & \cdots & & & 0 \\
0 & 0 & 0 & 0 & \delta^\ell & 1-\delta^\ell & \delta^\ell-1 & -\delta^\ell & 0 & \cdots & 0 \\
\vdots & & & & \ddots & \ddots & \ddots & \ddots & & & \vdots \\
0 & \cdots & 0 & \delta^\ell & 1-\delta^\ell & \delta^\ell-1 & -\delta^\ell & 0 & 0 & 0 & 0 \\
0 & & & \cdots & 0 & \delta^\ell & 1-\delta^\ell & \delta^\ell-1 & -\delta^\ell & 0 & 0 \\
0 & & & & & & & \cdots & 0 & -\delta^\ell & \delta^\ell \\
0 & & & & & & & \cdots & 0 & -\delta^\ell & \delta^\ell
\end{pmatrix}$$

Similarly, if we write the synthesis step as:

$$C^\ell = \mathcal{P}_\ell C^{\ell-1} + Q_\ell E^{\ell-1}.$$

Then the wavelet synthesis filters, $\mathcal{P}_\ell$ and Q_ℓ where $dim(Q_\ell) = (m_\ell+2)\times(m_{\ell-1}+2)$ are derived from (4.5.1) as $\mathcal{P}_\ell = P_3$ and the matrix Q_ℓ is defined as follows:
The entries $(q_{i,j})$ of Q_ℓ are all equal to zero except

- $q_{1,1} = 1$ and $q_{2,1} = -\lambda_0^{[2,\ell]}$,
- $q_{2,2} = (1-\lambda_0^{[2,\ell]})(1-4\delta^\ell)$, $q_{3,2} = -\lambda_1^{[3,\ell]}$ and $q_{4,2} = -\lambda_0^{[3,\ell]}$,
- $q_{2j-3,j} = \lambda_0^{[3,\ell]}$, $q_{2j-2,j} = \lambda_1^{[3,\ell]}$, $q_{2j-1,j} = -\lambda_1^{[3,\ell]}$ and $q_{2j,j} = -\lambda_0^{[3,\ell]}$, for $j = 3, \cdots, m_{\ell-1}$,
- $q_{m_\ell-1,m_{\ell-1}+1} = -\lambda_0^{[3,\ell]}$, $q_{m_\ell,m_{\ell-1}+1} = -\lambda_1^{[3,\ell]}$ and $q_{m_\ell+1,m_{\ell-1}+1} = (1-\lambda_0^{[2,\ell]})(1-4\delta^\ell)$,
- $q_{m_\ell+1,m_{\ell-1}+2} = -\lambda_0^{[2,\ell]}$ and $q_{m_\ell+2,m_{\ell-1}+2} = 1$.

The advantage of this reverse Chaikin method over other wavelet methods is computation speed, both the analysis and the synthesis filters are sparse, whereas in many wavelet methods, the analysis filters, A_ℓ and B_ℓ, are dense, thus requiring quadratic rather than a linear time to perform the analysis (reverse subdivision) step naïvely, or else requiring the solution of a linear system [70]. Using the matrix Q_ℓ, we deduce that the elements $\Psi_{i,\ell-1},\ i = -2, \ldots, m_{\ell-1}-1$ of the base UAH B-wavelets are given by the following theorem.

Theorem 2.6.1. *For all $i = -2, ..., m_{\ell-1}-1$, the UAH B-wavelettes $\Psi_{i,\ell-1}$ is given*

by

$$\begin{cases} \Psi_{-2,\ell-1} & = M^{[\alpha,\ell]}_{-2,3}(x) + \boldsymbol{r}_0(h_\ell) M^{[\alpha,\ell]}_{-1,3}(x), \\ \Psi_{-1,\ell-1} & = \boldsymbol{r}_1(h_\ell) M^{[\alpha,\ell]}_{-1,3}(x) + \boldsymbol{r}_2(h_\ell) M^{[\alpha,\ell]}_{0,3}(x) - r_3(h_\ell) M^{[\alpha,\ell]}_{1,3}(x), \\ \Psi_{m_{\ell-1}-2,\ell-1} & = -\boldsymbol{r}_3(h_\ell) M^{[\alpha,\ell]}_{m_\ell-4,3}(x) + \boldsymbol{r}_2(h_\ell) M^{[\alpha,\ell]}_{m_\ell-3,3}(x) + \boldsymbol{r}_1(h_\ell) M^{[\alpha,\ell]}_{m_\ell-2,3}(x), \\ \Psi_{m_{\ell-1}-1,\ell-1} & = \boldsymbol{r}_0(h_\ell) M^{[\alpha,\ell]}_{m_\ell-2,3}(x) + M^{[\alpha,\ell]}_{m_\ell-1,3}(x), \end{cases} \tag{2.6.1}$$

and for $i = 0, \ldots, m_{\ell-1} - 3$,

$$\Psi_{i,\ell-1} = \boldsymbol{r}_3(h_\ell) \left(M^{[\alpha,\ell]}_{2i,3}(x) - M^{[\alpha,\ell]}_{2i+3,3}(x) \right) + \boldsymbol{r}_2(h_\ell) \left(M^{[\alpha,\ell]}_{2i+2,3}(x) - M^{[\alpha,\ell]}_{2i+1,3}(x) \right),$$

where the expressions of $(\boldsymbol{r}_j(h_\ell))_{0\le j\le 3}$, *are as follows:*
$\boldsymbol{r}_0(h_\ell) = -\lambda_0^{[2,\ell]}$, $\boldsymbol{r}_1(h_\ell) = (1-\lambda_0^{[2,\ell]})(1-4\delta^\ell)$, $\boldsymbol{r}_2(h_\ell) = -\lambda_1^{[3,\ell]}$ *and* $\boldsymbol{r}_3(h_\ell) = -\lambda_0^{[3,\ell]}$.

Remark 3. As it was noticed in [47], the formulae of $(\mathbf{r}_j(h_\ell))_{0\le j\le 3}$ given above are not appropriate for small values of h_ℓ. In order to remedy that inconvenience, we use their following Taylor expansions:

$$\begin{aligned} \mathbf{r}_0(h_\ell) &= -\frac{1}{2} + \frac{\alpha^2 h_\ell^2}{32} - \frac{1}{768}\alpha^4 h_\ell^4 + O(h_\ell^6), \\ \mathbf{r}_1(h_\ell) &= \frac{3}{2} - \frac{13\alpha^2 h_\ell^2}{32} + \frac{133\alpha^4 h_\ell^4}{768} + O(h_\ell^6), \\ \mathbf{r}_2(h_\ell) &= -\frac{3}{4} - \frac{\alpha^2 h_\ell^2}{64} + \frac{\alpha^4 h_\ell^4}{1536} + O(h_\ell^6), \\ \mathbf{r}_3(h_\ell) &= -\frac{1}{4} + \frac{\alpha^2 h_\ell^2}{64} - \frac{\alpha^4 h_\ell^4}{1536} + O(h_\ell^6). \end{aligned}$$

Remark 4. when this technique is based on the UAT B splines introduced in section 1.2, the value of $\mathbf{r}_i(h_\ell)$ is equal to

$$\begin{aligned} \mathbf{r}_0(h_\ell) &= -\frac{1}{2} - \frac{\alpha^2 h_\ell^2}{32} - \frac{\alpha^4 h_\ell^4}{768} + O(h_\ell^6), \\ \mathbf{r}_1(h_\ell) &= \frac{3}{2} + \frac{\alpha^2 h_\ell^2}{32} + \frac{\alpha^4 h_\ell^4}{768} + O(h_\ell^6), \\ \mathbf{r}_2(h_\ell) &= -\frac{3}{4} + \frac{\alpha^2 h_\ell^2}{64} + \frac{\alpha^4 h_\ell^4}{1536} + O(h_\ell^6), \\ \mathbf{r}_3(h_\ell) &= -\frac{1}{4} - \frac{\alpha^2 h_\ell^2}{64} - \frac{\alpha^4 h_\ell^4}{1536} + O(h_\ell^6). \end{aligned}$$

Remark 5. For the Taylor expansions of $\mathbf{r}_2(h_\ell)$ and $\mathbf{r}_3(h_\ell)$ the first digit corresponds exactly to the result found by Mohamed F. Hassan and Neil A. Dodgson in 2005, for more information see [24].

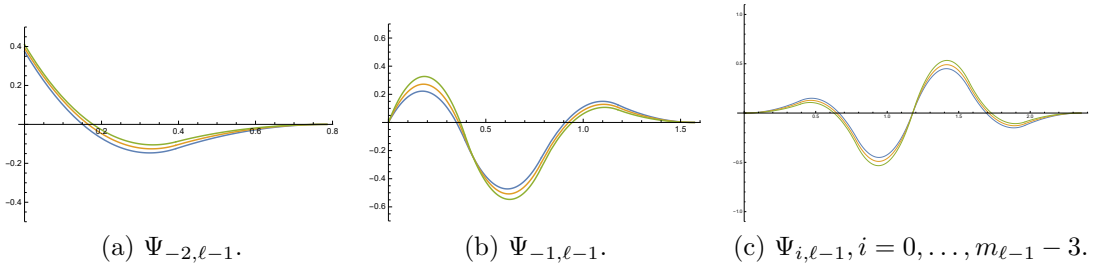

(a) $\Psi_{-2,\ell-1}$. (b) $\Psi_{-1,\ell-1}$. (c) $\Psi_{i,\ell-1}, i = 0, \ldots, m_{\ell-1} - 3$.

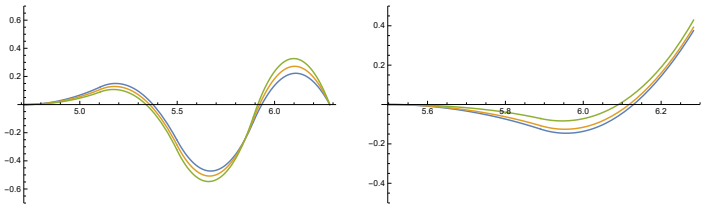

(d) $\Psi_{m_{\ell-1}-2,\ell-1}$. (e) $\Psi_{m_{\ell-1}-1,\ell-1}$.

Figure 2.7 – Graphs of UAH B-spline wavelets for $\alpha = 0.5, 1, 2$.

2.7 Conclusion

In this work, we have constructed a new formula of the refinement equation for any given order k of UAH B-splines. Then, we have presented a smooth reverse subdivision approach based on quadratic UAH B-splines. A multiresolution representation is also being studied to develop interesting applications based on a smooth reverse subdivision approach.

Chapter 3

Hyperbolic and trigonometric B-splines orthogonal wavelets

Contents

3.1 Introduction

Splines have become the standard mathematical tool for representing smooth shapes in computer graphics and geometric modeling. Wavelets have been introduced more recently but are now well established both in mathematics and in applied sciences like signal processing and numerical analysis. In this chapter, by using trigonometric and hyperbolic splines, we investigate mutually orthogonal spline wavelet spaces on uniform partitions of a bounded interval $[a, b]$, addressing the existence, uniqueness, and construction of bases of minimally supported spline wavelets. This new construction has many good properties, such as orthogonality, symmetry, and continuity, which are important for wavelet transforms and practical applications.

3.2 Quadratic UAT B-spline orthogonal wavelets

The most widely used curves are B-spline curves (Hoschek and Lasser, 1993), particularly the quadratic and cubic B-spline curves. Piecewise curves with three consecutive control points for each curve segment are flexible and can be used conveniently.

The quadratic trigonometric algebraic curve with C^1 continuity is introduced by [38]. It holds the basic properties of classical B-spline curves. Han [39] added cubic trigonometric B-spline curves on the uniform and non-uniform knots with shape parameters to the literature. Analogous to the quadratic B-spline curves, this chapter aims to present practical piecewise trigonometric curves generated by the space $S_k([a,b],\Phi^\ell)$ introduced in definition 1.2.1 and to construct the associated orthogonal spline wavelet.
Let now V_ℓ be the space of quadratic UAT B-splines associated with subdivision Φ^ℓ.

$$V_\ell = \{f \in C([a,b]) \ : f|_{[\phi_i^\ell,\phi_{i+1}^\ell]} \in \{1,\cos(\alpha t),\sin(\alpha t)\},\ i=0,\dots,m_\ell-1\}, \quad (3.2.1)$$

The dimension of V_ℓ is $m_\ell+2$. Then, the UAT B-spline of order three based on the uniformly spaced knots $(0,h_l,2h_l,3h_l)$ are given by

$$N_{i,3}^{[\alpha,\ell]}(t) = N_{0,3}^{[\alpha,\ell]}(t-\phi_i^\ell),$$

where

$$N_{0,3}^{[\alpha,\ell]}(t) = \begin{cases} \dfrac{1-\cos(\alpha t)}{4\sin^2\left(\frac{\alpha h_\ell}{2}\right)}, & t \in [\phi_0^\ell,\phi_1^\ell[, \\ \dfrac{-2\cos(\alpha h_\ell)+\cos(\alpha(2h_\ell-t))+\cos(\alpha(t-h_\ell))}{4\sin^2\left(\frac{\alpha h_\ell}{2}\right)}, & t \in [\phi_1^\ell,\phi_2^\ell[, \\ \dfrac{1-\cos(\alpha(3h_\ell-t))}{4\sin^2\left(\frac{\alpha h_\ell}{2}\right)}, & t \in [\phi_2^\ell,\phi_3^\ell[, \\ 0, & otherwise. \end{cases}$$

We add several nodes at the extremities of the interval $[a,b]$ such that $\phi_{-2}^\ell = \phi_{-1}^\ell = \phi_0^\ell$ and $\phi_{m_\ell}^\ell = \phi_{m_\ell+1}^\ell = \phi_{m_\ell+2}^\ell$, the respective left and right-hand side boundary UAT B-splines of order three are given by

$$N_{-2,3}^{[\alpha,\ell]}(t) = \begin{cases} \dfrac{\cos(\alpha(h_\ell-t))-1}{\cos(\alpha h_\ell)-1}, & t \in [\phi_0^\ell,\phi_1^\ell[, \\ 0, & otherwise. \end{cases}$$

$$N_{m_\ell-1,3}^{[\alpha,\ell]}(t) = \begin{cases} \dfrac{\cos(\alpha(t-(m_\ell-1)h_\ell))-1}{\cos(\alpha h_\ell)-1}, & t \in [\phi_{m_\ell-1}^l,\phi_{m_\ell}^l[, \\ 0, & otherwise. \end{cases}$$

Then,

$$N_{-1,3}^{[\alpha,\ell]}(t)=\begin{cases}\dfrac{2\cos(\alpha h_\ell)-2\cos(\alpha(h-t))-\cos(\alpha t)+1}{2\cos(\alpha h_\ell)-2}, & t\in[\phi_0^\ell,\phi_1^\ell[,\\ \dfrac{\sin^2\left(\alpha h_\ell-\frac{\alpha t}{2}\right)}{2\sin^2\left(\frac{\alpha h_\ell}{2}\right)}, & t\in[\phi_1^\ell,\phi_2^\ell[,\\ 0, & otherwise.\end{cases}$$

$$N_{m_\ell-2,3}^{[\alpha,\ell]}(t)=\begin{cases}\dfrac{1-\cos(\alpha((m_\ell-2)h_\ell-t))}{4\sin^2\left(\frac{\alpha h}{2}\right)}, & t\in[\phi_{m_\ell-2}^l,\phi_{m_\ell-1}^l[,\\ \dfrac{\cos(\alpha(m_\ell h_\ell-t))-1}{+2\cos(\alpha(t-(m_\ell-1)h_\ell))-2\cos(\alpha h_\ell)}{4\sin^2\left(\frac{\alpha h}{2}\right)}, & t\in[\phi_{m_\ell-1}^l,\phi_{m_\ell}^l[,\\ 0, & \text{otherwise},\end{cases}$$

According to the theorem 2.3.1, we find that a uniform UAT B-spline curve can also be equivalently represented by another uniform UAT B-spline curve with knot intervals after bisection.

Theorem 3.2.1. *The UAT B-spline $N_{i,3}^{[\alpha,\ell]}(t)$, for all $i=-2,\cdots,m_\ell-1$, satisfy the following refinement equations.*

$$\begin{cases}N_{-2,3}^{[\alpha,\ell]}(t)=N_{-2,3}^{[\alpha,\ell+1]}(t)+\lambda_{b1}^{[3,\ell]}N_{-1,3}^{[\alpha,\ell]}(t),\\ N_{-1,3}^{[\alpha,\ell]}(t)=\lambda_{b2}^{[3,\ell]}N_{-1,3}^{[\alpha,\ell+1]}(t)+\lambda_1^{[3,\ell]}N_{0,3}^{[\alpha,\ell]}(t)+\lambda_0^{[3,\ell]}N_{1,3}^{[\alpha,\ell+1]}(t),\\ N_{i,3}^{[\alpha,\ell]}(t)=\lambda_0^{[3,\ell]}\left[N_{2i,3}^{[\alpha,\ell+1]}(t)+N_{2i+3,3}^{[\alpha,\ell+1]}(t)\right]+\lambda_1^{[3,\ell]}\left[N_{2i+1,3}^{[\alpha,\ell+1]}(t)+N_{2i+2,3}^{[\alpha,\ell+1]}(t)\right],\\ N_{m_\ell-2,3}^{[\alpha,\ell]}(t)=\lambda_0^{[3,\ell]}N_{m_\ell-4,3}^{[\alpha,\ell+1]}(t)+\lambda_1^{[3,\ell]}N_{m_\ell-3,3}^{[\alpha,\ell]}(t)+\lambda_{b2}^{[3,\ell]}N_{m_\ell-2,3}^{[\alpha,\ell+1]}(t),\\ N_{m_\ell-1,3}^{[\alpha,\ell]}(t)=\lambda_{b1}^{[3,\ell]}N_{m_\ell-2,3}^{[\alpha,\ell]}(t)+N_{m_\ell-1,3}^{[\alpha,\ell+1]}(t),\end{cases}\tag{3.2.2}$$

where

$$\lambda_0^{[3,\ell]}=\frac{1}{4}\sec^2\left(\frac{\alpha h_\ell}{4}\right),\ \lambda_1^{[3,\ell]}=1-\lambda_0^{[3,\ell]},$$
$$\lambda_{b1}^{[3,\ell]}=\frac{1}{\cos\left(\frac{\alpha h_\ell}{2}\right)+1},\ \lambda_{b2}^{[3,\ell]}=1-2\lambda_0^{[3,\ell]}.$$

Proof. On the one hand, we have

$$N_{i,3}^{[\alpha,\ell]}(t)=\frac{1}{h_\ell}\int_{t-h_\ell}^{t}N_{i,2}^{[\alpha,\ell]}(x)dx=\frac{1}{h_\ell}\int_{t-\frac{h_\ell}{2}}^{t}N_{i,2}^{[\alpha,\ell]}(x)dx+\frac{1}{h_\ell}\int_{t-h_\ell}^{t-\frac{h_\ell}{2}}N_{i,2}^{[\alpha,\ell]}(x)dx.$$

On the other hand, we can easily verify that the B-splines of order two verify the

following refinement equation.

$$N_{i,2}^{[\alpha,\ell]}(t) = \lambda_0^{[2,\ell]}\left[N_{2i,2}^{[\alpha,\ell+1]}(t) + N_{2i+2,2}^{[\alpha,\ell+1]}(t)\right] + N_{2i+1,2}^{[\alpha,\ell+1]}(t),$$

where $\lambda_0^{[2,\ell]} = \dfrac{1}{2\cos\left(\frac{\alpha h_\ell}{2}\right)}$, which implies

$$\begin{aligned}\frac{1}{h_\ell}\int_{t-\frac{h_\ell}{2}}^{t} N_{i,2}^{[\alpha,\ell]}(x)dx &= \frac{1}{h_\ell}\int_{t-\frac{h_\ell}{2}}^{t}\left[\lambda_0^{[2,\ell]}(N_{2i,2}^{[\alpha,\ell+1]}(x) + N_{2i+2,2}^{[\alpha,\ell+1]}(x)) + \lambda_1^{[2,\ell]}N_{2i+1,2}^{[\alpha,\ell+1]}(x)\right]dx,\\ &= \frac{\lambda_0^{[2,\ell]}}{2}\left[N_{2i,3}^{[\alpha,\ell+1]}(t) + N_{2i+2,3}^{[\alpha,\ell+1]}(t)\right] + \frac{\lambda_1^{[2,\ell]}}{2}N_{2i+1,3}^{[\alpha,\ell+1]}(t),\end{aligned}$$

and

$$\begin{aligned}\frac{1}{h_\ell}\int_{t-h_\ell}^{t-\frac{h_\ell}{2}} N_{i,2}^{[\alpha,\ell]}(x)dx &= \frac{1}{h_\ell}\int_{t-h_\ell}^{t-\frac{h_\ell}{2}}\left[\lambda_0^{[2,\ell]}(N_{2i,2}^{[\alpha,\ell+1]}(x) + N_{2i+2,2}^{[\alpha,\ell+1]}(x)) + N_{2i+1,2}^{[\alpha,\ell+1]}(x)\right]dx,\\ &= \frac{\lambda_0^{[2,\ell]}}{2}\left[N_{2i+1,3}^{[\alpha,\ell+1]}(t) + N_{2i+3,3}^{[\alpha,\ell+1]}(t)\right] + \frac{1}{2}N_{2i+2,3}^{[\alpha,\ell+1]}(t).\end{aligned}$$

Finally we obtain

$$\begin{aligned}N_{i,3}^{\alpha}(t) &= \frac{\lambda_0^{[2,\ell]}}{2}\left[N_{2i,3}^{[\alpha,\ell+1]}(t) + N_{2i+2,3}^{[\alpha,\ell+1]}(t)\right] + \frac{1}{2}N_{2i+1,3}^{[\alpha,\ell+1]}(t)\\ &+ \frac{\lambda_0^{[2,\ell]}}{2}\left[N_{2i+1,3}^{[\alpha,\ell+1]}(t) + N_{2i+3,3}^{[\alpha,\ell+1]}(t)\right] + \frac{1}{2}N_{2i+2,3}^{[\alpha,\ell+1]}(t),\\ &= \lambda_0^{[3,\ell]}\left[N_{2i,3}^{[\alpha,\ell+1]}(t) + N_{2i+3,3}^{[\alpha,\ell+1]}(t)\right] + \lambda_1^{[1,\ell]}\left[N_{2i+1,3}^{[\alpha,\ell+1]}(t) + N_{2i+2,3}^{[\alpha,\ell+1]}(t)\right],\end{aligned}$$

with

$$\lambda_0^{[3,\ell]} = \frac{\lambda_0^{[2,\ell]}}{2} = \frac{1}{4}\sec^2\left(\frac{\alpha h_\ell}{4}\right), \quad \lambda_1^{[3,\ell]} = \frac{\lambda_0^{[2,\ell]} + \lambda_1^{[2,\ell]}}{2} = 1 - \lambda_0^{[3,\ell]}.$$

□

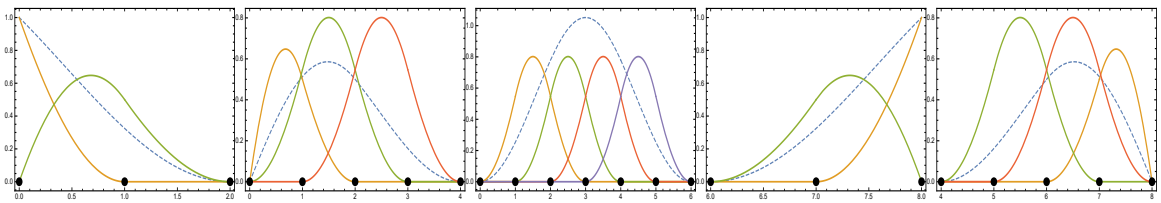

Figure 3.1 – Subdivision of UAT B-spline of order three. The blue dashed curves show the sum of the UAT B-splines.

Let $W_{\ell-1}$ be the orthogonal complement of $V_{\ell-1}$ in V_ℓ. In other words $W_{\ell-1}$ consists of all the functions in V_ℓ that are orthogonal to $V_{\ell-1}$, i.e.

$$W_{\ell-1} = \{N_{i,3}^{[\alpha,\ell]} \in V_\ell :< N_{i,3}^{[\alpha,\ell]}, N_{i-1,3}^{[\alpha,\ell-1]} >= 0 \text{ for all } N_{i-1,3}^{[\alpha,\ell-1]} \in V_{\ell-1}\} \tag{3.2.3}$$

Let $\tau^{\ell-1} = \{\tau_i^{\ell-1} = x_{2i-1}^{\ell}\}_{i=1}^{m_{\ell-1}}$ be a new knots sequences where $\Phi^\ell = \Phi^{\ell-1} \cup \tau^{\ell-1}$. It is clear that

$$\dim(W_{\ell-1}) = \dim(V_\ell) - \dim(V_{\ell-1}) = 2^{\ell+2} - 2^{\ell+1} = 2^{\ell+1} = m_{\ell-1}.$$

According to the Theorem 1.4.1, there exists for each $\tau_i^{\ell-1}$, $i = 1, ..., m_{\ell-1}$ one wavelet $\psi_{i,\ell-1} \in W_{\ell-1}$ with minimal support.

Theorem 3.2.2. *For all $i = 1, \ldots, m_{\ell-1}$, the αB-wavelettes $\psi_{i,\ell-1}$ is given by*

$$\begin{cases} \psi_{1,\ell-1} & = \sum_{i=0}^{5} p_i^{[3,\ell-1]} N_{i-2,3}^{[\omega,\ell]}, \\ \psi_{2,\ell-1} & = \sum_{i=0}^{6} q_i^{[3,\ell-1]} N_{i-1,3}^{[\omega,\ell]}, \\ \psi_{m_{\ell-1}-1,l-1} & = \sum_{i=0}^{6} q_i^{[3,\ell-1]} N_{m_\ell-2-i,3}^{[\omega,\ell]}, \\ \psi_{m_{\ell-1},l-1} & = \sum_{i=0}^{5} p_i^{[3,\ell-1]} N_{m_\ell-1-i,3}^{[\omega,\ell]}. \end{cases} \tag{3.2.4}$$

Then,

$$\psi_{i,\ell-1} = \mathcal{C}_i det \begin{bmatrix} < N_{i-5,3}^{[\omega,\ell-1]}, N_{2i-6,3}^{[\omega,\ell]} > & \cdots & < N_{i-5,3}^{[\omega,\ell-1]}, N_{2i+1,3}^{[\omega,\ell]} > \\ \vdots & \vdots & \vdots \\ < N_{i+1,3}^{[\omega,\ell-1]}, N_{2i-6,3}^{[\omega,\ell]} > & \cdots & < N_{i+1,3}^{[\omega,\ell-1]}, N_{2i+1,3}^{[\omega,\ell]} > \\ N_{2i-6,3}^{[\omega,\ell]} & \cdots & N_{2i+1,3}^{[\omega,\ell]} \end{bmatrix}, \tag{3.2.5}$$

$$= \sum_{j=0}^{7} r_j^{[3,\ell-1]} N_{2i+j-6,3}^{[\omega,\ell]}. \tag{3.2.6}$$

The expressions of $(p_i^{[3,\ell-1]})_{0\le i\le 5}$, $(q_i^{[3,\ell-1]})_{0\le i\le 6}$, and $(r_i^{[3,\ell-1]})_{0\le i\le 7}$ are given as follows

- $p_0^{[3,\ell-1]} = \frac{1}{945}\left(286 - \frac{49493\alpha^2 h_\ell^2}{52920} - \frac{48763327\alpha^4 h_\ell^4}{5601052800}\right) + O(h_\ell)^6,$
- $p_1^{[3,\ell-1]} = \frac{1}{945}\left(-\frac{1391}{4} + \frac{83803\alpha^2 h_\ell^2}{211680} + \frac{862315217\alpha^4 h_\ell^4}{22404211200}\right) + O(h_\ell)^6,$
- $p_2^{[3,\ell-1]} = \frac{1}{945}\left(\frac{4967}{24} - \frac{382183\alpha^2 h_\ell^2}{317520} - \frac{1129836137\alpha^4 h_\ell^4}{33606316800}\right) + O(h_\ell)^6,$

$\circ\ p_3^{[3,\ell-1]} = \frac{1}{945}\left(-\frac{2083}{24} - \frac{932861\alpha^2h_\ell^2}{635040} - \frac{2567850979\alpha^4h_\ell^4}{67212633600}\right) + O(h_\ell)^6,$

$\circ\ p_4^{[3,\ell-1]} = \frac{1}{945}\left(\frac{203}{12} + \frac{22973\alpha^2h_\ell^2}{22680} + \frac{191212499\alpha^4h_\ell^4}{4800902400}\right) + O(h_\ell)^6,$

$\circ\ p_5^{[3,\ell-1]} = \frac{1}{945}\left(-\frac{7}{12} - \frac{2399\alpha^2h_\ell^2}{45360} - \frac{6676853\alpha^4h_\ell^4}{2400451200}\right) + O(h_\ell)^6,$

and

$\star\ q_0^{[3,\ell-1]} = \frac{1}{171}\left(13 + \frac{1975\alpha^2h_\ell^2}{2736} + \frac{1345525\alpha^4h_\ell^4}{52399872}\right) + O(h_\ell)^6,$

$\star\ q_1^{[3,\ell-1]} = \frac{1}{171}\left(-\frac{56749}{1920} - \frac{20862787\alpha^2h_\ell^2}{36771840} - \frac{22197897427\alpha^4h_\ell^4}{1760635699200}\right) + O(h_\ell)^6,$

$\star\ q_2^{[3,\ell-1]} = \frac{1}{171}\left(\frac{98201}{1920} - \frac{30688837\alpha^2h_\ell^2}{36771840} - \frac{38255872777\alpha^4h_\ell^4}{1760635699200}\right) + O(h_\ell)^6,$

$\star\ q_3^{[3,\ell-1]} = \frac{1}{171}\left(-\frac{23509}{480} + \frac{4506331\alpha^2h_\ell^2}{4596480} + \frac{12359715533\alpha^4h_\ell^4}{440158924800}\right) + O(h_\ell)^6,$

$\star\ q_4^{[3,\ell-1]} = \frac{1}{171}\left(\frac{11291}{480} + \frac{1188331\alpha^2h_\ell^2}{4596480} + \frac{1057305533\alpha^4h_\ell^4}{440158924800}\right) + O(h_\ell)^6,$

$\star\ q_5^{[3,\ell-1]} = \frac{1}{171}\left(-\frac{8903}{1920} - \frac{1864705\alpha^2h_\ell^2}{7354368} - \frac{14909348009\alpha^4h_\ell^4}{1760635699200}\right) + O(h_\ell)^6,$

$\star\ q_6^{[3,\ell-1]} = \frac{1}{171}\left(\frac{307}{1920} + \frac{100505\alpha^2h_\ell^2}{7354368} + \frac{1148627341\alpha^4h_\ell^4}{1760635699200}\right) + O(h_\ell)^6,$

then

$*\ r_0^{[3,\ell-1]} = -r_7^{[3,\ell-1]} = \frac{1}{960}\left(1 + \frac{31\alpha^2h_\ell^2}{336} + \frac{67\alpha^4h_\ell^4}{13440}\right) + O(h_\ell)^6,$

$*\ r_1^{[3,\ell-1]} = -r_6^{[3,\ell-1]} = \frac{1}{960}\left(-29 - \frac{599\alpha^2h_\ell^2}{336} - \frac{983\alpha^4h_\ell^4}{13440}\right) + O(h_\ell)^6,$

$*\ r_2^{[3,\ell-1]} = -r_5^{[3,\ell-1]} = \frac{1}{960}\left(147 + \frac{291\alpha^2h_\ell^2}{112} + \frac{323\alpha^4h_\ell^4}{4480}\right) + O(h_\ell)^6,$

$*\ r_3^{[3,\ell-1]} = -r_4^{[3,\ell-1]} = \frac{1}{960}\left(-303 + \frac{501\alpha^2h_\ell^2}{112} + \frac{673\alpha^4h_\ell^4}{4480}\right) + O(h_\ell)^6.$

Proof. Since $\tau^{\ell-1}$ is the subsequence of Φ^ℓ such that $\Phi^\ell = \Phi^{\ell-1} \cup \tau^{\ell-1}$, then according to Theorem 5.1 introduced in [54], there exists for each $\tau_i^{\ell-1}$ a single wavelet $\psi_{i,\ell-1}$ with minimal support $[\phi_{r_i}^\ell, \phi_{\ell_i}^\ell]$. This wavelet is written according to the B-splines $N_{i,3}^{[\omega,\ell]}$ which are inside $[\phi_{r_i}^\ell, \phi_{\ell_i}^\ell]$ the support of $\psi_{i,\ell-1}$ at the same time it is orthogonal with the B-splines $N_{i,3}^{[\omega,\ell-1]}$ which are also inside $[\phi_{r_i}^\ell, \phi_{\ell_i}^\ell]$, Integers ℓ_i and r_i are

determined in such a way that they satisfy the conditions of Theorem 5.1 introduced in [54]. From the calculations we obtain the values of ℓ_i and r_i as follows:

$$\begin{cases} \ell_i = 1, \quad r_i = 7, & i = 1, \\ \ell_i = 1, \quad r_i = 9, & i = 2, \\ \ell_i = 2i-5, \quad r_i = 2i+2, & i = 3, ..., m_{\ell-1}-2, \\ \ell_i = m_\ell - 7, \quad r_i = m_\ell, & i = m_{\ell-1}-1, \\ \ell_i = m_\ell - 5, \quad r_i = m_\ell, & i = m_{\ell-1}. \end{cases}$$

□

Remark 6. The constants $\mathcal{C}_i$ are chosen such that $\|\psi_{i,\ell-1}\| = 1$.

The other side if we denote by $\psi_{\ell-1} = (\psi_{1,\ell-1}, \psi_{2,\ell-1}, \ldots, \psi_{m_{\ell-1},\ell-1})^T$ and

$$N_\ell^3 = (N_{-2,3}^{[\alpha,\ell]}, N_{-1,3}^{[\alpha,\ell]}, \ldots, N_{m_\ell-1,3}^{[\alpha,\ell]})^T,$$

we have the following theorem.

Theorem 3.2.1. *The family* $\{\psi_{1,\ell-1},\ i = 1, \ldots, m_{\ell-1}\}$ *form a basis for the wavelet space* $W_{\ell-1}$ *and satisfies the following equation.*

$$\psi_{\ell-1} = \mathcal{Q}_{3,\ell} N_\ell^3, \tag{3.2.7}$$

where $\mathcal{Q}_{3,\ell}$ *is a matrix of size* $(m_\ell + 2) \times m_{\ell-1}$ *defined as follows*

$$\mathcal{Q}_{3,\ell} = \begin{pmatrix}
p_0^{[3,\ell-1]} & & & & & & & & \\
p_1^{[3,\ell-1]} & q_0^{[3,\ell-1]} & & & & & & & \\
p_2^{[3,\ell-1]} & q_1^{[3,\ell-1]} & r_0^{[3,\ell-1]} & & & & & & \\
p_3^{[3,\ell-1]} & q_2^{[3,\ell-1]} & r_1^{[3,\ell-1]} & & & & & & \\
p_4^{[3,\ell-1]} & q_3^{[3,\ell-1]} & r_2^{[3,\ell-1]} & r_0^{[3,\ell-1]} & & & & & \\
p_5^{[3,\ell-1]} & q_4^{[3,\ell-1]} & r_3^{[3,\ell-1]} & r_1^{[3,\ell-1]} & \ddots & & & & \\
 & q_5^{[3,\ell-1]} & r_4^{[3,\ell-1]} & r_2^{[3,\ell-1]} & \ddots & r_0^{[3,\ell-1]} & & & \\
 & q_6^{[3,\ell-1]} & r_5^{[3,\ell-1]} & r_3^{[3,\ell-1]} & \ddots & r_1^{[3,\ell-1]} & & & \\
 & & r_6^{[3,\ell-1]} & r_4^{[3,\ell-1]} & \ddots & r_2^{[3,\ell-1]} & q_6^{[3,\ell-1]} & & \\
 & & r_7^{[3,\ell-1]} & r_5^{[3,\ell-1]} & \ddots & r_3^{[3,\ell-1]} & q_5^{[3,\ell-1]} & & \\
 & & & r_6^{[3,\ell-1]} & \ddots & r_4^{[3,\ell-1]} & q_4^{[3,\ell-1]} & p_5^{[3,\ell-1]} & \\
 & & & r_7^{[3,\ell-1]} & \ddots & r_5^{[3,\ell-1]} & q_3^{[3,\ell-1]} & p_4^{[3,\ell-1]} & \\
 & & & & \ddots & r_6^{[3,\ell-1]} & q_2^{[3,\ell-1]} & p_3^{[3,\ell-1]} & \\
 & & & & & r_7^{[3,\ell-1]} & q_1^{[3,\ell-1]} & p_2^{[3,\ell-1]} & \\
 & & & & & & q_0^{[3,\ell-1]} & p_1^{[3,\ell-1]} & \\
 & & & & & & & p_0^{[3,\ell-1]} &
\end{pmatrix}.$$

Where $(p_i^{[3,\ell-1]})_{0\le i\le 5}$, $(q_i^{[3,\ell-1]})_{0\le i\le 6}$ *and* $(r_i^{[3,\ell-1]})_{0\le i\le 7}$ *are calculated in the previous theorem.*

3.2.1 Gram matrix associated with bases $N_{i,3}^{[\omega,\ell]}$ and $\psi_{i,\ell}$

In the following sections, inner products of B-splines play a crucial role in constructing spline wavelets and implementing the corresponding algorithms. Therefore, we have decided to provide the reader with more detailed information about the computation of the integrals that form the entries of B spline Gram matrices. There is a standard formula for the inner product of B-splines of arbitrary order k involving divided differences (see for instance Theorem 4.25 in [78]). Still, in this section, we prefer to calculate the Gram matrix for $k = 3$ directly. The reason is a simplification of the general formula in our particular case, $k = 3$. As a straightforward consequence of the recursion formula for B-splines, the associated Gram matrix is the symmetric matrix of the general term

$$G_\ell = (< N_{i,3}^{[\alpha,\ell]}, N_{j,3}^{[\alpha,\ell]} >)_{-2\le i,j\le m_\ell-1},$$
$$H_\ell = (< \psi_{i,\ell}, \psi_{j,\ell} >)_{1\le i,j\le m_\ell},$$

be the Gram matrices of size $(m_\ell+2)\times(m_\ell+2)$ and $m_\ell\times m_\ell$ respectively. It is easy to see that G_ℓ and H_ℓ are symmetric. The linear independence of the basis functions implies that both G_ℓ and H_ℓ are positive definite and therefore non singular. On the other hand, it is simple to prove that $H_{\ell-1}$ can be written in the form

$$H_{\ell-1} = \mathcal{Q}_{3,\ell}^T G_\ell \mathcal{Q}_{3,\ell}. \tag{3.2.8}$$

Corollary 3.2.1. *For* $\ell \ge 1$, *The Gram matrices* G_ℓ *are given by*

$$G_\ell = \begin{pmatrix}
g_0^{[3,\ell]} & g_1^{[3,\ell]} & g_2^{[3,\ell]} & & & & & & & \\
g_1^{[3,\ell]} & g_3^{[3,\ell]} & g_4^{[3,\ell]} & g_5^{[3,\ell]} & & & & & & \\
g_2^{[3,\ell]} & g_4^{[3,\ell]} & g_6^{[3,\ell]} & g_7^{[3,\ell]} & g_5^{[3,\ell]} & & & & & \\
 & g_5^{[3,\ell]} & g_7^{[3,\ell]} & g_6^{[3,\ell]} & g_7^{[3,\ell]} & g_5^{[3,\ell]} & & & & \\
 & & g_5^{[3,\ell]} & g_7^{[3,\ell]} & g_6^{[3,\ell]} & g_7^{[3,\ell]} & g_5^{[3,\ell]} & & & \\
 & & & \ddots & \ddots & \ddots & \ddots & \ddots & & \\
 & & & & \ddots & \ddots & \ddots & \ddots & \ddots & \\
 & & & & g_5^{[3,\ell]} & g_7^{[3,\ell]} & g_6^{[3,\ell]} & g_7^{[3,\ell]} & g_5^{[3,\ell]} & \\
 & & & & & g_5^{[3,\ell]} & g_7^{[3,\ell]} & g_6^{[3,\ell]} & g_4^{[3,\ell]} & g_2^{[3,\ell]} \\
 & & & & & & g_5^{[3,\ell]} & g_4^{[3,\ell]} & g_3^{[3,\ell]} & g_1^{[3,\ell]} \\
 & & & & & & & g_2^{[3,\ell]} & g_1^{[3,\ell]} & g_0^{[3,\ell]}
\end{pmatrix}, \tag{3.2.9}$$

where

$$g_0^{[3,\ell]} = \frac{6\alpha h_\ell - 8\sin(\alpha h_\ell) + \sin(2\alpha h_\ell)}{16\alpha \sin^4\left(\frac{\alpha h_\ell}{2}\right)},$$

$$g_1^{[3,\ell]} = \frac{-4\alpha h_\ell + 7\sin(\alpha h_\ell) + \sin(2\alpha h) - 5\alpha h_\ell \cos(\alpha h_\ell)}{16\alpha \sin^4\left(\frac{\alpha h_\ell}{2}\right)},$$

$$g_2^{[3,\ell]} = \frac{\alpha h_\ell(\cos(\alpha h_\ell) + 2) - 3\sin(\alpha h_\ell)}{16\alpha \sin^4\left(\frac{\alpha h_\ell}{2}\right)},$$

$$g_3^{[3,\ell]} = \frac{14\alpha h_\ell - 12\sin(\alpha h_\ell) - 9\sin(2\alpha h_\ell) + 4\alpha h_\ell(3\cos(\alpha h_\ell) + \cos(2\alpha h_\ell))}{32\alpha \sin^4\left(\frac{\alpha h_\ell}{2}\right)},$$

$$g_4^{[3,\ell]} = \frac{-4\alpha h_\ell + 9\sin(\alpha h_\ell) + 3\sin(2\alpha h_\ell) - 11\alpha h_\ell \cos(\alpha h_\ell)}{32\alpha \sin^4\left(\frac{\alpha h_\ell}{2}\right)},$$

$$g_5^{[3,\ell]} = \frac{\alpha h_\ell(\cos(\alpha h_\ell) + 2) - 3\sin(\alpha h_\ell)}{32\alpha \sin^4\left(\frac{\alpha h_\ell}{2}\right)},$$

$$g_6^{[3,\ell]} = \frac{\alpha h_\ell(\cos(\alpha h_\ell) + 2\cos(2\alpha h_\ell)) - 3(-2\alpha h_\ell + \sin(\alpha h_\ell) + \sin(2\alpha h_\ell))}{16\alpha \sin^4\left(\frac{\alpha h_\ell}{2}\right)},$$

$$g_7^{[3,\ell]} = \frac{-2\alpha h_\ell + 6\sin(\alpha h_\ell) + 3\sin(2\alpha h_\ell) - 10\alpha h_\ell \cos(\alpha h_\ell)}{32\alpha \sin^4\left(\frac{\alpha h_\ell}{2}\right)}.$$

Remark 7. The above formulae of $g_i^{[3,\ell]}$ are not appropriate for small values of h_ℓ. To solve this problem, we can use the following Taylor expansions

$$g_0^{[3,\ell]} = \frac{h_\ell}{5} + \frac{\alpha^2 h_\ell^3}{105} + \frac{\alpha^4 h_\ell^5}{2100} + O\left(h_\ell^6\right),$$

$$g_1^{[3,\ell]} = \frac{7h_\ell}{60} - \frac{\alpha^2 h_\ell^3}{2520} - \frac{11\alpha^4 h_\ell^5}{50400} + O\left(h_\ell^6\right),$$

$$g_2^{[3,\ell]} = \frac{h_\ell}{60} + \frac{\alpha^2 h_\ell^3}{504} + \frac{\alpha^4 h_\ell^5}{7200} + O\left(h_\ell^6\right),$$

$$g_3^{[3,\ell]} = \frac{h_\ell}{3} - \frac{19\alpha^2 h_\ell^3}{1260} - \frac{\alpha^4 h_\ell^5}{5040} + O\left(h_\ell^6\right),$$

$$g_4^{[3,\ell]} = \frac{5h_\ell}{24} + \frac{17\alpha^2 h_\ell^3}{5040} - \frac{\alpha^4 h_\ell^5}{20160} + O\left(h_\ell^6\right),$$

$$g_5^{[3,\ell]} = \frac{h_\ell}{120} + \frac{\alpha^2 h_\ell^3}{1008} + \frac{\alpha^4 h_\ell^5}{14400} + O\left(h_\ell^6\right),$$

$$g_6^{[3,\ell]} = \frac{11h_\ell}{20} - \frac{3\alpha^2 h_\ell^3}{280} - \frac{\alpha^4 h_\ell^5}{5600} + O\left(h_\ell^6\right),$$

$$g_7^{[3,\ell]} = \frac{13h_\ell}{60} + \frac{11\alpha^2 h_\ell^3}{2520} + \frac{\alpha^4 h_\ell^5}{50400} + O\left(h_\ell^6\right).$$

In Fig. 3.2, we present the graphs of the five UAT spline wavelets, that form the basis of the space W_0, with different values of the parameter α.

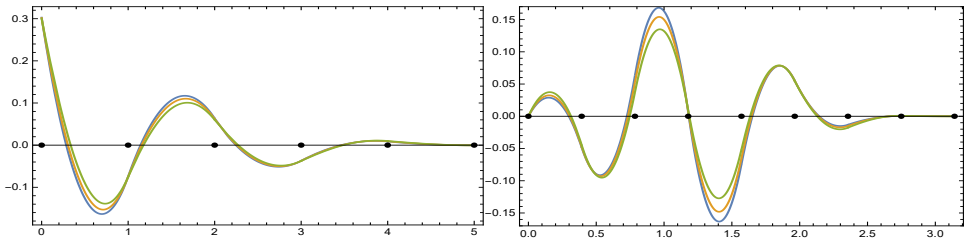

(a) $\psi_{-2,\ell-1}$. (b) $\psi_{-1,\ell-1}$.

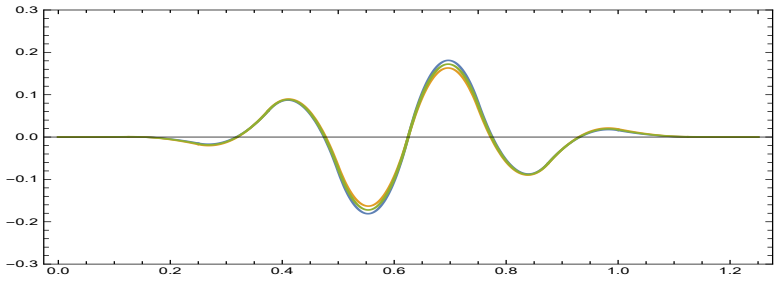

(c) $\psi_{i,\ell-1}, i = 0, \ldots, m_{\ell-1} - 3$.

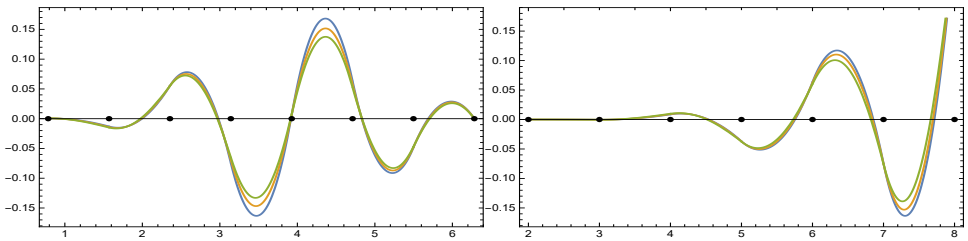

(d) $\psi_{m_{\ell-1}-2,\ell-1}$. (e) $\psi_{m_{\ell-1}-1,\ell-1}$.

Figure 3.2 – Graphs of UAT B-spline wavelets.

3.3 Quadratic UAH B-spline orthogonal wavelets

Similar to the trigonometric spline B-wavelets, in this section, we will determine the hyperbolic spline B-wavelets. Let $\tilde{V}_\ell$ be the space of quadratic UAH B-splines associated with subdivision Φ^ℓ.

$$\tilde{V}_\ell = \mathcal{S}_3([a,b], \Phi^\ell) = \{f \in C([a,b]) \ : f|_{[\phi_i^\ell, \phi_{i+1}^\ell]} \in \{1, \cosh(\alpha t), \sinh(\alpha t)\}\}. \quad (3.3.1)$$

Corollary 3.3.1. *The UAH B-spline functions $M_{i,3}^{[\alpha,\ell]}, -2 \le i \le m_\ell - 1$ of order 3 corresponding to the knot sequence Φ^ℓ are given by*

$$M_{0,3}^{[\alpha,\ell]}(t) = \begin{cases} \dfrac{\cosh(\alpha t) - 1}{4\sinh^2(\frac{\alpha h_\ell}{2})}, & t \in [\phi_0^\ell, \phi_1^\ell[, \\ -\dfrac{\cosh(\alpha(t - h_\ell)) + \cosh(\alpha(2h_\ell - t)) - 2\cosh(\alpha h_\ell)}{2(\cosh(\alpha h_\ell) - 1)}, & t \in [\phi_1^\ell, \phi_2^\ell[, \\ \dfrac{\cosh(\alpha(3h_\ell - t)) - 1}{4\sinh^2(\frac{\alpha h_\ell}{2})}, & t \in [\phi_2^\ell, \phi_3^\ell[, \\ 0, & \textit{otherwise.} \end{cases} \quad (3.3.2)$$

and

$$M_{i,3}^{[\alpha,\ell]}(t) = M_{0,3}^{[\alpha,\ell]}(t-\phi_i^\ell).$$

Then, the respective left and right hand side boundary hyperbolic UAH B-splines are

$$M_{-2,3}^{[\alpha,\ell]}(t) = \begin{cases} \dfrac{\cosh(\alpha(h_\ell - t)) - 1}{\cosh(\alpha h_\ell) - 1}, & t \in [\phi_0^\ell, \phi_1^\ell[, \\ 0, & otherwise. \end{cases}$$

$$M_{-1,3}^{[\alpha,\ell]}(t) = \begin{cases} \dfrac{2\cosh(\alpha h) - 2\cosh(\alpha(h-t)) - \cosh(\alpha t) + 1}{4sinh^2\left(\frac{\alpha h_\ell}{2}\right)}, & t \in [\phi_0^\ell, \phi_1^\ell[, \\ \dfrac{\sinh^2\left(\alpha h - \frac{\alpha t}{2}\right)}{2sinh^2\left(\frac{\alpha h_\ell}{2}\right)}, & t \in [\phi_1^\ell, \phi_2^\ell[, \\ 0, & otherwise, \end{cases}$$

and

$$M_{m_\ell-2,3}^{[\alpha,\ell]}(t) = \begin{cases} \dfrac{\cosh\left(\alpha\left(\left(m_\ell - 2\right)h_\ell - t\right)\right) - 1}{4\sinh^2\left(\frac{\alpha h_\ell}{2}\right)}, & t \in \left[\phi_{m_\ell-2}^\ell, \phi_{m_\ell-1}^\ell\right[, \\ 1 - \cosh\left(\alpha\left(m_\ell h_\ell - t\right)\right) & \\ \dfrac{-2\cosh\left(\alpha\left(t - \left(m_\ell - 1\right)h\right) + 2\cosh\left(\alpha h_\ell\right)\right.}{4\sinh^2\left(\frac{\alpha h_\ell}{2}\right)}, & t \in \left[\phi_{m_\ell-1}^\ell, \phi_{m\ell}^\ell\right[, \\ 0, & otherwise, \end{cases}$$

$$M_{m_\ell-1,3}^{[\alpha,\ell]}(t) = \begin{cases} \dfrac{\cosh(\alpha(t - (m_\ell - 1)h_\ell)) - 1}{\cosh(\alpha h_\ell) - 1}, & t \in [\phi_{m_\ell-1}^\ell, \phi_{m_\ell}^\ell[, \\ 0, & otherwise. \end{cases}$$

Theorem 3.3.1. *The UAH B-spline $M_{i,3}^{[\alpha,\ell]}(t)$, for all $i = -2, \cdots, m_\ell - 1$, satisfy the following refinement equations.*

$$\begin{cases} M_{-2,3}^{[\alpha,\ell]}(t) = M_{-2,3}^{[\alpha,\ell+1]}(t) + \lambda_{b1}^{[3,\ell]} M_{-1,3}^{[\alpha,\ell]}(t), \\ M_{-1,3}^{[\alpha,\ell]}(t) = \lambda_{b2}^{[3,\ell]} M_{-1,3}^{[\alpha,\ell+1]}(t) + \lambda_1^{[3,\ell]} M_{0,3}^{[\alpha,\ell]}(t) + \lambda_0^{[3,\ell]} M_{1,3}^{[\alpha,\ell+1]}(t), \\ M_{i,3}^{[\alpha,\ell]}(t) = \lambda_0^{[3,\ell]}\left[M_{2i,3}^{[\alpha,\ell+1]}(t) + M_{2i+3,3}^{[\alpha,\ell+1]}(t)\right] + \lambda_1^{[3,\ell]}\left[M_{2i+1,3}^{[\alpha,\ell+1]}(t) + M_{2i+2,3}^{[\alpha,\ell+1]}(t)\right], \\ M_{m_\ell-2,3}^{[\alpha,\ell]}(t) = \lambda_0^{[3,\ell]} M_{m_\ell-4,3}^{[\alpha,\ell+1]}(t) + \lambda_1^{[3,\ell]} M_{m_\ell-3,3}^{[\alpha,\ell]}(t) + \lambda_{b2}^{[3,\ell]} M_{m_\ell-2,3}^{[\alpha,\ell+1]}(t), \\ M_{m_\ell-1,3}^{[\alpha,\ell]}(t) = \lambda_{b1}^{[3,\ell]} M_{m_\ell-2,3}^{[\alpha,\ell]}(t) + M_{m_\ell-1,3}^{[\alpha,\ell+1]}(t), \end{cases} \tag{3.3.3}$$

where

$$\lambda_0^{[3,\ell]} = \frac{1}{4} sech^2\left(\frac{\alpha h_\ell}{4}\right),\ \lambda_1^{[3,\ell]} = 1 - \lambda_0^{[3,\ell]},$$

$$\lambda_{b1}^{[3,\ell]} = \frac{1}{\cosh\left(\frac{\alpha h_\ell}{2}\right) + 1},\ \lambda_{b2}^{[3,\ell]} = \frac{1}{2}\left(\tanh^2\left(\frac{\alpha h_\ell}{4}\right) + 1\right).$$

Theorem 3.3.2. *For all $i = 1, 2, m_{\ell-1} - 1, m_{\ell-1}$, the UAH B-wavelettes $\tilde{\psi}_{i,\ell-1}$ is given by*

$$\begin{cases} \tilde{\psi}_{1,\ell-1} & = \sum_{i=0}^{5} \alpha_i^{[3,\ell-1]} M_{i-2,3}^{[\alpha,\ell]}, \\ \tilde{\psi}_{2,\ell-1} & = \sum_{i=0}^{6} \beta_i^{[3,\ell-1]} M_{i-1,3}^{[\alpha,\ell]}, \\ \tilde{\psi}_{m_{\ell-1}-1,l-1} & = \sum_{i=0}^{6} \beta_i^{[3,\ell-1]} M_{m_\ell-2-i,3}^{[\alpha,\ell]}, \\ \tilde{\psi}_{m_{\ell-1},l-1} & = \sum_{i=0}^{5} \alpha_i^{[3,\ell-1]} M_{m_\ell-1-i,3}^{[\alpha,\ell]}. \end{cases} \tag{3.3.4}$$

Then, for $i = 3, ..., m_{\ell-1} - 2$ we have

$$\tilde{\psi}_{i,\ell-1} = \mathcal{C}_i det \begin{bmatrix} < M_{i-5,3}^{[\alpha,\ell-1]}, M_{2i-6,3}^{[\alpha,\ell]} > & \cdots & < M_{i-5,3}^{[\alpha,\ell-1]}, M_{2i+1,3}^{[\alpha,\ell]} > \\ \vdots & \vdots & \vdots \\ < M_{i+1,3}^{[\alpha,\ell-1]}, M_{2i-6,3}^{[\alpha,\ell]} > & \cdots & < M_{i+1,3}^{[\alpha,\ell-1]}, M_{2i+1,3}^{[\alpha,\ell]} > \\ M_{2i-6,3}^{[\alpha,\ell]} & \cdots & M_{2i+1,3}^{[\alpha,\ell]} \end{bmatrix} \tag{3.3.5}$$

$$= \sum_{j=0}^{7} \delta_j^{[3,\ell-1]} M_{2i+j-6,3}^{[\alpha,\ell]}. \tag{3.3.6}$$

Where,

$\circ\ \alpha_0^{[3,\ell-1]} = \frac{1}{945}\left(286 + \frac{49493\alpha^2 h_\ell^2}{52920} - \frac{48763327\alpha^4 h_\ell^4}{5601052800}\right) + O\left(h_\ell^6\right),$

$\circ\ \alpha_1^{[3,\ell-1]} = \frac{1}{945}\left(-\frac{1391}{4} - \frac{83803\alpha^2 h_\ell^2}{211680} + \frac{862315217\alpha^4 h_\ell^4}{22404211200}\right) + O\left(h_\ell^6\right),$

$\circ\ \alpha_2^{[3,\ell-1]} = \frac{1}{945}\left(\frac{4967}{24} + \frac{382183\alpha^2 h_\ell^2}{317520} - \frac{1129836137\alpha^4 h_\ell^4}{33606316800}\right) + O\left(h_\ell^6\right),$

$\circ\ \alpha_3^{[3,\ell-1]} = \frac{1}{945}\left(-\frac{2083}{24} + \frac{932861\alpha^2 h_\ell^2}{635040} - \frac{2567850979\alpha^4 h_\ell^4}{67212633600}\right) + O\left(h_\ell^6\right),$

$\circ\ \alpha_4^{[3,\ell-1]} = \frac{1}{945}\left(\frac{203}{12} - \frac{22973\alpha^2 h_\ell^2}{22680} + \frac{191212499\alpha^4 h_\ell^4}{4800902400}\right) + O\left(h_\ell^6\right),$

$\circ\ \alpha_5^{[3,\ell-1]} = \frac{1}{945}\left(-\frac{7}{12} + \frac{2399\alpha^2 h_\ell^2}{45360} - \frac{6676853\alpha^4 h_\ell^4}{2400451200}\right) + O\left(h_\ell^6\right),$

and

$\star\ \beta_0^{[3,\ell-1]} = \frac{1}{171}\left(13 - \frac{1975\alpha^2 h_\ell^2}{2736} + \frac{1345525\alpha^4 h_\ell^4}{52399872}\right) + O\left(h_\ell^6\right),$

$\star\ \beta_1^{[3,\ell-1]} = \frac{1}{171}\left(-\frac{56749}{1920} + \frac{20862787\alpha^2 h_\ell^2}{36771840} - \frac{22197897427\alpha^4 h_\ell^4}{1760635699200}\right) + O\left(h_\ell^6\right),$

$$\star\ \beta_2^{[3,\ell-1]} = \frac{1}{171}\left(\frac{98201}{1920} + \frac{30688837\alpha^2h_\ell^2}{36771840} - \frac{38255872777\alpha^4h_\ell^4}{1760635699200}\right) + O\left(h_\ell^6\right),$$

$$\star\ \beta_3^{[3,\ell-1]} = \frac{1}{171}\left(-\frac{23509}{480} - \frac{4506331\alpha^2h_\ell^2}{4596480} + \frac{12359715533\alpha^4h_\ell^4}{440158924800}\right) + O\left(h_\ell^6\right),$$

$$\star\ \beta_4^{[3,\ell-1]} = \frac{1}{171}\left(\frac{11291}{480} - \frac{1188331\alpha^2h_\ell^2}{4596480} + \frac{1057305533\alpha^4h_\ell^4}{440158924800}\right) + O\left(h_\ell^6\right),$$

$$\star\ \beta_5^{[3,\ell-1]} = \frac{1}{171}\left(-\frac{8903}{1920} + \frac{1864705\alpha^2h_\ell^2}{7354368} - \frac{14909348009\alpha^4h_\ell^4}{1760635699200}\right) + O\left(h_\ell^6\right),$$

$$\star\ \beta_6^{[3,\ell-1]} = \frac{1}{171}\left(\frac{307}{1920} - \frac{100505\alpha^2h_\ell^2}{7354368} + \frac{1148627341\alpha^4h_\ell^4}{1760635699200}\right) + O\left(h_\ell^6\right),$$

then

$$*\ \delta_0^{[3,\ell-1]} = -\delta_7^{[3,\ell-1]} = \frac{1}{960}\left(1 - \frac{31\alpha^2h_\ell^2}{336} + \frac{67\alpha^4h_\ell^4}{13440}\right) + O\left(h_\ell^6\right),$$

$$*\ \delta_1^{[3,\ell-1]} = -\delta_6^{[3,\ell-1]} = \frac{1}{960}\left(-29 + \frac{599\alpha^2h_\ell^2}{336} - \frac{983\alpha^4h_\ell^4}{13440}\right) + O\left(h_\ell^6\right),$$

$$*\ \delta_2^{[3,\ell-1]} = -\delta_5^{[3,\ell-1]} = \frac{1}{960}\left(147 - \frac{291\alpha^2h_\ell^2}{112} + \frac{323\alpha^4h_\ell^4}{4480}\right) + O\left(h_\ell^6\right),$$

$$*\ \delta_3^{[3,\ell-1]} = -\delta_4^{[3,\ell-1]} = \frac{1}{960}\left(-303 - \frac{501\alpha^2h_\ell^2}{112} + \frac{673\alpha^4h_\ell^4}{4480}\right) + O\left(h_\ell^6\right).$$

In Fig. 3.3, we present the graphs of the five UAH spline wavelets, that form the basis of the space $\tilde{W}_0$, with different values of the parameter α.

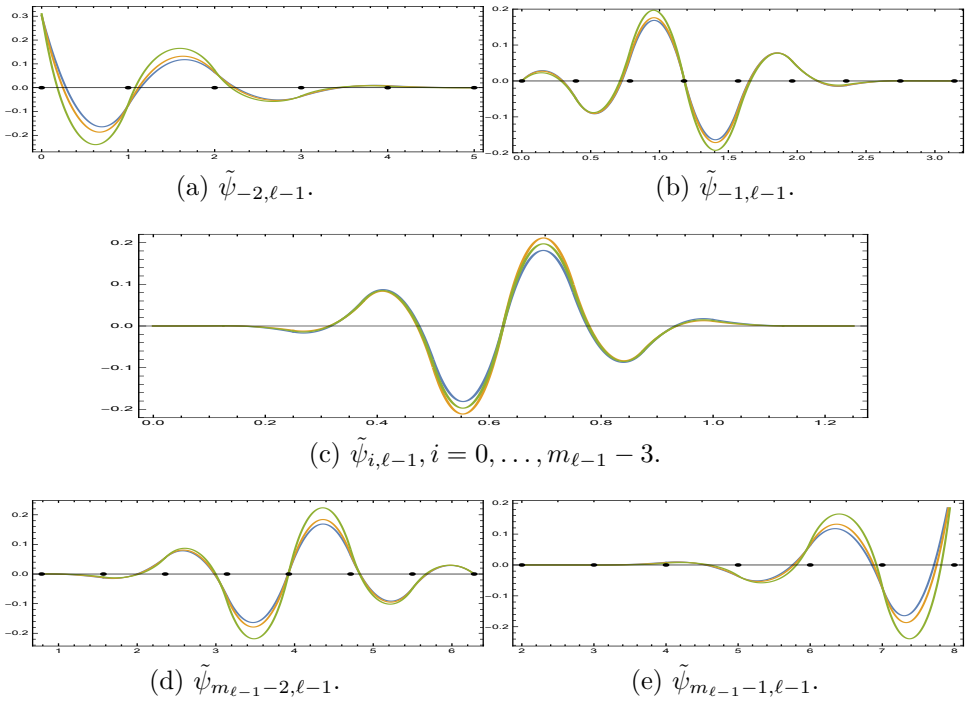

(a) $\tilde{\psi}_{-2,\ell-1}$. (b) $\tilde{\psi}_{-1,\ell-1}$.

(c) $\tilde{\psi}_{i,\ell-1}, i = 0, \ldots, m_{\ell-1} - 3$.

(d) $\tilde{\psi}_{m_{\ell-1}-2,\ell-1}$. (e) $\tilde{\psi}_{m_{\ell-1}-1,\ell-1}$.

Figure 3.3 – Graphs of UAT B-spline wavelets.

Theorem 3.3.1. *The family* $\{\tilde{\psi}_{1,\ell-1},\ i=1,\dots,m_{\ell-1}\}$ *form a basis for the wavelet space* $\tilde{W}_{\ell-1}$ *and satisfies the following equation.*

$$\tilde{\psi}_{\ell-1} = \tilde{\mathcal{Q}}_{3,\ell} M_{\ell}^{3}, \tag{3.3.7}$$

where $\tilde{\psi}_{\ell-1} = (\tilde{\psi}_{1,\ell-1}, \tilde{\psi}_{2,\ell-1}, \dots, \tilde{\psi}_{m_{\ell-1},\ell-1})^T$ *and* $\tilde{\mathcal{Q}}_{3,\ell}$ *is a matrix of size* $(m_\ell + 2) \times m_{\ell-1}$ *given by*

$$\tilde{\mathcal{Q}}_{3,\ell} = \begin{pmatrix}
\alpha_0^{[3,\ell-1]} & & & & & & & & \\
\alpha_1^{[3,\ell-1]} & \beta_0^{[3,\ell-1]} & & & & & & & \\
\alpha_2^{[3,\ell-1]} & \beta_1^{[3,\ell-1]} & \delta_0^{[3,\ell-1]} & & & & & & \\
\alpha_3^{[3,\ell-1]} & \beta_2^{[3,\ell-1]} & \delta_1^{[3,\ell-1]} & & & & & & \\
\alpha_4^{[3,\ell-1]} & \beta_3^{[3,\ell-1]} & \delta_2^{[3,\ell-1]} & \delta_0^{[3,\ell-1]} & & & & & \\
\alpha_5^{[3,\ell-1]} & \beta_4^{[3,\ell-1]} & \delta_3^{[3,\ell-1]} & \delta_1^{[3,\ell-1]} & \ddots & & & & \\
 & \beta_5^{[3,\ell-1]} & \delta_4^{[3,\ell-1]} & \delta_2^{[3,\ell-1]} & \ddots & \delta_0^{[3,\ell-1]} & & & \\
 & \beta_6^{[3,\ell-1]} & \delta_5^{[3,\ell-1]} & \delta_3^{[3,\ell-1]} & \ddots & \delta_1^{[3,\ell-1]} & & & \\
 & & \delta_6^{[3,\ell-1]} & \delta_4^{[3,\ell-1]} & \ddots & \delta_2^{[3,\ell-1]} & \beta_6^{[3,\ell-1]} & & \\
 & & \delta_7^{[3,\ell-1]} & \delta_5^{[3,\ell-1]} & \ddots & \delta_3^{[3,\ell-1]} & \beta_5^{[3,\ell-1]} & & \\
 & & & \delta_6^{[3,\ell-1]} & \ddots & \delta_4^{[3,\ell-1]} & \beta_4^{[3,\ell-1]} & \alpha_5^{[3,\ell-1]} & \\
 & & & \delta_7^{[3,\ell-1]} & \ddots & \delta_5^{[3,\ell-1]} & \beta_3^{[3,\ell-1]} & \alpha_4^{[3,\ell-1]} & \\
 & & & & \ddots & \delta_6^{[3,\ell-1]} & \beta_2^{[3,\ell-1]} & \alpha_3^{[3,\ell-1]} & \\
 & & & & & \delta_7^{[3,\ell-1]} & \beta_1^{[3,\ell-1]} & \alpha_2^{[3,\ell-1]} & \\
 & & & & & & \beta_0^{[3,\ell-1]} & \alpha_1^{[3,\ell-1]} & \\
 & & & & & & & \alpha_0^{[3,\ell-1]} &
\end{pmatrix}.$$

3.3.1 Gram matrix associated with bases $M_{i,3}^{[\omega,\ell]}$ and $\tilde{\psi}_{i,\ell}$

We had already given the definition of the Gram matrix in section (2), in the following we give directly the explicit expression of the matrices $\tilde{G}_\ell$ and $\tilde{H}_\ell$ associated to the bases $M_{i,3}^{[\omega,\ell]}$ and $\tilde{\psi}_{i,\ell}$ respectively. Using the special form of the piecewise linear UAH B-splines $M_{i,3}^{[\alpha,\ell]}$, we get

$$\tilde{G}_\ell = \begin{pmatrix}
\tilde{g}_0^{[3,\ell]} & \tilde{g}_1^{[3,\ell]} & \tilde{g}_2^{[3,\ell]} & & & & & & & \\
\tilde{g}_1^{[3,\ell]} & \tilde{g}_3^{[3,\ell]} & \tilde{g}_4^{[3,\ell]} & \tilde{g}_5^{[3,\ell]} & & & & & & \\
\tilde{g}_2^{[3,\ell]} & \tilde{g}_4^{[3,\ell]} & \tilde{g}_6^{[3,\ell]} & \tilde{g}_7^{[3,\ell]} & \tilde{g}_5^{[3,\ell]} & & & & & \\
 & \tilde{g}_5^{[3,\ell]} & \tilde{g}_7^{[3,\ell]} & \tilde{g}_6^{[3,\ell]} & \tilde{g}_7^{[3,\ell]} & \tilde{g}_5^{[3,\ell]} & & & & \\
 & & \tilde{g}_5^{[3,\ell]} & \tilde{g}_7^{[3,\ell]} & \tilde{g}_6^{[3,\ell]} & \tilde{g}_7^{[3,\ell]} & \tilde{g}_5^{[3,\ell]} & & & \\
 & & & \ddots & \ddots & \ddots & \ddots & \ddots & & \\
 & & & & \ddots & \ddots & \ddots & \ddots & \ddots & \\
 & & & & \tilde{g}_5^{[3,\ell]} & \tilde{g}_7^{[3,\ell]} & \tilde{g}_6^{[3,\ell]} & \tilde{g}_7^{[3,\ell]} & \tilde{g}_5^{[3,\ell]} & \\
 & & & & & \tilde{g}_5^{[3,\ell]} & \tilde{g}_7^{[3,\ell]} & \tilde{g}_6^{[3,\ell]} & \tilde{g}_4^{[3,\ell]} & \tilde{g}_2^{[3,\ell]} \\
 & & & & & & \tilde{g}_5^{[3,\ell]} & \tilde{g}_4^{[3,\ell]} & \tilde{g}_3^{[3,\ell]} & \tilde{g}_1^{[3,\ell]} \\
 & & & & & & & \tilde{g}_2^{[3,\ell]} & \tilde{g}_1^{[3,\ell]} & \tilde{g}_0^{[3,\ell]}
\end{pmatrix}, \tag{3.3.8}$$

where

$$\tilde{g}_0^{[3,\ell]} = \frac{6\alpha h_\ell - 8\sinh(\alpha h_\ell) + \sinh(2\alpha h_\ell)}{16\alpha \sinh^4\left(\frac{\alpha h_\ell}{2}\right)},$$
$$\tilde{g}_1^{[3,\ell]} = \frac{-4\alpha h_\ell + 7\sinh(\alpha h_\ell) + \sinh(2\alpha h_\ell) - 5\alpha h_\ell \cosh(\alpha h_\ell)}{16\alpha \sinh^4\left(\frac{\alpha h_\ell}{2}\right)},$$
$$\tilde{g}_2^{[3,\ell]} = \frac{\alpha h_\ell(\cosh(\alpha h_\ell) + 2) - 3\sinh(\alpha h_\ell)}{16\alpha \sinh^4\left(\frac{\alpha h_\ell}{2}\right)},$$
$$\tilde{g}_3^{[3,\ell]} = \frac{14\alpha h_\ell - 12\sinh(\alpha h_\ell) - 9\sinh(2\alpha h_\ell) + 4\alpha h_\ell(3\cosh(\alpha h_\ell) + \cosh(2\alpha h_\ell))}{32\alpha \sinh^4\left(\frac{\alpha h_\ell}{2}\right)},$$
$$\tilde{g}_4^{[3,\ell]} = \frac{-4\alpha h_\ell + 9\sinh(\alpha h_\ell) + 3\sinh(2\alpha h_\ell) - 11\alpha h_\ell \cosh(\alpha h_\ell)}{32\alpha \sinh^4\left(\frac{\alpha h_\ell}{2}\right)},$$
$$\tilde{g}_5^{[3,\ell]} = \frac{\alpha h_\ell(\cosh(\alpha h_\ell) + 2) - 3\sinh(\alpha h_\ell)}{32\alpha \sinh^4\left(\frac{\alpha h_\ell}{2}\right)},$$
$$\tilde{g}_6^{[3,\ell]} = \frac{\alpha h_\ell(\cosh(\alpha h_\ell) + 2\cosh(2\alpha h_\ell)) - 3(-2\alpha h_\ell + \sinh(\alpha h_\ell) + \sinh(2\alpha h_\ell))}{16\alpha \sinh^4\left(\frac{\alpha h_\ell}{2}\right)},$$
$$\tilde{g}_7^{[3,\ell]} = \frac{-2\alpha h_\ell + 6\sinh(\alpha h_\ell) + 3\sinh(2\alpha h_\ell) - 10\alpha h_\ell \cosh(\alpha h_\ell)}{32\alpha \sinh^4\left(\frac{\alpha h_\ell}{2}\right)}.$$

Then we have.

$$\tilde{H}_\ell = (< \tilde{\psi}_{i,\ell}, \tilde{\psi}_{j,\ell} >)_{1\le i,j\le m_\ell} = \tilde{\mathcal{Q}}_{3,\ell}^T \tilde{G}_\ell \tilde{\mathcal{Q}}_{3,\ell}.$$

Remark 8. The entries $\tilde{g}_i^{[3,\ell]}$ of the Gram matrix $\tilde{G}_\ell$ of UAH B-splines of order 3 admit the following Taylor representation.

$$\tilde{g}_0^{[3,\ell]} = \frac{h_\ell}{5} - \frac{\alpha^2 h_\ell^3}{105} + \frac{\alpha^4 h_\ell^5}{2100} + O\left(h_\ell^6\right),$$
$$\tilde{g}_1^{[3,\ell]} = \frac{7h_\ell}{60} + \frac{\alpha^2 h_\ell^3}{2520} - \frac{11\alpha^4 h_\ell^5}{50400} + O\left(h_\ell^6\right),$$
$$\tilde{g}_2^{[3,\ell]} = \frac{h_\ell}{60} - \frac{\alpha^2 h_\ell^3}{504} + \frac{\alpha^4 h_\ell^5}{7200} + O\left(h_\ell^6\right),$$
$$\tilde{g}_3^{[3,\ell]} = \frac{h_\ell}{3} + \frac{19\alpha^2 h_\ell^3}{1260} - \frac{\alpha^4 h_\ell^5}{5040} + O\left(h_\ell^6\right),$$
$$\tilde{g}_4^{[3,\ell]} = \frac{5h_\ell}{24} - \frac{17\alpha^2 h_\ell^3}{5040} - \frac{\alpha^4 h_\ell^5}{20160} + O\left(h_\ell^6\right),$$
$$\tilde{g}_5^{[3,\ell]} = \frac{h_\ell}{120} - \frac{\alpha^2 h_\ell^3}{1008} + \frac{\alpha^4 h_\ell^5}{14400} + O\left(h_\ell^6\right),$$
$$\tilde{g}_6^{[3,\ell]} = \frac{11h_\ell}{20} + \frac{3\alpha^2 h_\ell^3}{280} - \frac{\alpha^4 h_\ell^5}{5600} + O\left(h_\ell^6\right),$$
$$\tilde{g}_7^{[3,\ell]} = \frac{13h_\ell}{60} - \frac{11\alpha^2 h_\ell^3}{2520} + \frac{\alpha^4 h_\ell^5}{50400} + O\left(h_\ell^6\right).$$

3.4 Conclusion

In this chapter, we have given a method to construct explicitly the orthogonal wavelets associated with trigonometric and hyperbolic B-splines using a uniform knot sequence. Next, we provide the different steps for numerical processing.

Chapter 4

Trigonometric Hermite interpolation method for Fredholm linear integral equations

Contents

This chapter presents a new trigonometric composite Hermite interpolation method for solving Fredholm linear integral equations. This operator approximates locally both the function and its derivative, known on the subdivision nodes. Then, we derive a class of quadrature rules with endpoint corrections based on integrating the composite Hermite interpolant. We also provide error estimation and numerical examples to illustrate that this new operator could provide accurate results.

The results obtained in this chapter are presented in the preprint [7].

4.1 Introduction

During the last three decades, the use of spline function-based methods to solve Fredholm's linear integral equations has been the subject of several kinds of research, see e.g. [3, 4, 10, 11, 59, 71]. Many researchers are still interested in the development of these methods. Since their introduction in [18] and until now, B-spline functions are universally recognized as practical and powerful tools in approximation theory. The particularly quasi-interpolating method is very successfully used to approximate the integral equations' kernel [11]. A numerical approach to solve a Fredholm linear integral equation is an essential work in scientific research. Some methods for solving this type of equation are available in the open literature; for example, Projection methods-collocation [5, 45, 59] and Nyström methods [60] are among the most popular ones. In [3] and [4], the authors proposed a numerical method using spline quasi-interpolants. Borzabadi and Fard [9] used an iterative collocation method to find a numerical solution of nonlinear Fredholm integral equations. Superconvergent Nyström and degenerate kernel methods for Hammerstein equations with smooth kernel was studied in [1] and superconvergent projection methods for Hammerstein equations with smooth as well as less smooth kernels along the diagonal was proposed in [2]. Two methods based on the natural and quasi cubic spline interpolations in [10] for approximating the second kind Fredholm integral equations are discussed, and the convergence analysis is established. Most of the methods are based on quasi-interpolations of polynomial splines with the possibility to reproduce only polynomials, so they will be less efficient when the solution of the treated equation is trigonometric.

The construction of the classical Hermite interpolation problem was arising in many works in literature. Beginning with Schoenberg's seminal work [74]. Then, in [57], Mummy derived an explicit formula of B-spline control points for Hermite interpolation in terms of interpolation data. In [52], Lamnii et al. present a Hermite interpolation problem with B-splines of a high degree of smoothness. Many schemes available for constructing a Hermite interpolation preserving the form C^1 see for example [19, 53, 58, 76].

This work presents a general framework in which Hermite interpolation based on UAT B-splines is used to numerically solve the generalized Fredholm integral equations of the second kind using the Nyström method. In addition, explicit results for the quadratic spline functions of the interpolants are provided.

4.2 Uniform trigonometric algebraic quadratic B-splines

This section aims to present explicit formulas of the uniform algebraic trigonometric quadratic B-splines of order 3. Given a knot sequence $\Phi^\ell = \{\phi_i^\ell\}_{i=0}^{m_\ell}$ introduced in

1.2.1. The trigonometric B-splines space studied is defined by

$$S_3([a,b],\Phi^\ell)=\{s\in C([a,b]) : s|_{[\phi_j,\phi_{j+1}]}\in\Gamma_3,\ j=0,\dots,m_\ell-1\},$$

where $\Gamma_3=\text{span}\{1,\cos(x),\sin(x)\}$.
The third-order algebraic, trigonometric B-splines basis of the space $S_3([a,b],\Phi^\ell)$ noted here by $\{\mathcal{N}_{i,3}^\ell\}_{i=-2}^{m_\ell-1}$ is given by
For $i=0,1,\dots,m_\ell-3$,

$$\mathcal{N}_{i,3}^\ell(x)=\mathcal{N}_{0,3}^\ell(x-\phi_i^\ell), \tag{4.2.1}$$

with

$$\mathcal{N}_{0,3}^\ell(x)=\begin{cases}\dfrac{\cos(x)-1}{2\cos(h_\ell)-2}, & x\in[\phi_0^\ell,\phi_1^\ell[,\\ \dfrac{\cos(h_\ell-x)+\cos(2h_\ell-x)-2\cos(h_\ell)}{4\sin^2\left(\frac{h_\ell}{2}\right)}, & x\in[\phi_1^\ell,\phi_2^\ell[,\\ \dfrac{\cos(3h_\ell-x)-1}{2\cos(h_\ell)-2}, & x\in[\phi_2^\ell,\phi_3^\ell[,\\ 0, & otherwise,\end{cases} \tag{4.2.2}$$

and, if we put $\phi_{-2}^\ell=\phi_{-1}^\ell=\phi_0^\ell$ and $\phi_{m_\ell}^\ell=\phi_{m_\ell+1}^\ell=\phi_{m_\ell+2}^\ell$, the respective left and right-hand side boundary UAT B-splines are given by

$$\mathcal{N}_{-2,3}^\ell(x)=\begin{cases}\dfrac{\cos(h_\ell-x)-1}{\cos(h_\ell)-1}, & x\in[\phi_0^\ell,\phi_1^\ell[,\\ 0, & otherwise.\end{cases}$$

$$\mathcal{N}_{-1,3}^\ell(x)=\begin{cases}\dfrac{-2\cos(x-h_\ell)+2\cos(h_\ell)-\cos(x)+1}{2(\cos(h_\ell)-1)}, & x\in[\phi_0^\ell,\phi_1^\ell[,\\ \dfrac{\sin^2\left(h_\ell-\frac{x}{2}\right)}{2\sin^2(\frac{h_\ell}{2})}, & x\in[\phi_1^\ell,\phi_2^\ell[,\\ 0, & otherwise,\end{cases}$$

and

$$\mathcal{N}_{m_\ell-2,3}^\ell(x)=\begin{cases}-\dfrac{\cos(x-(m_\ell-2)h_\ell)-1}{4\sin^2\left(\frac{h_\ell}{2}\right)}, & x\in[\phi_{m_\ell-2}^\ell,\phi_{m_\ell-1}^\ell[,\\ \dfrac{1}{2}+\dfrac{\cos(x-m_\ell h_\ell)+2\cos(x-(m_\ell-1)h_\ell)-\cos(h_\ell)-2}{4\sin^2(\frac{h_\ell}{2})}, & x\in[\phi_{m_\ell-1}^\ell,\phi_{m_\ell}^\ell[,\\ 0, & otherwise.\end{cases}$$

$$\mathcal{N}_{m_\ell-1,3}^\ell(x)=\begin{cases}\dfrac{\cos(x-(m_\ell-1)h_\ell)-1}{\cos(h_\ell)-1}, & x\in[\phi_{m_\ell-1}^\ell,\phi_{m_\ell}^\ell[,\\ 0, & otherwise.\end{cases}$$

Proposition 4.2.1. *The family $\mathcal{N}_{i,3}^\ell$ generates the space $S_3([a,b],\Phi^\ell)$. Moreover,*

we have

$$(\mathcal{N}_{i,3}(x))' = \delta_{i,2}\mathcal{N}^{\ell}_{i,2}(x) - \delta_{i+1,2}\mathcal{N}^{\ell}_{i+1,2}(x),\ i = 0, ..., m_\ell - 3,$$

where

$$\delta_{i,2} = \left(\int_{-\infty}^{+\infty} \mathcal{N}_{i,2}(t, h_\ell)dt\right)^{-1},$$

and for $i = 0, \ldots, m_\ell - 3$,

$$\mathcal{N}^{\ell}_{i,2}(x) = \mathcal{N}^{\ell}_{0,2}(x - \phi^{\ell}_i),$$

with

$$\mathcal{N}^{\ell}_{i,2}(x) = \begin{cases} \dfrac{\sin(x)}{\sin(h_\ell)}, & x \in [\phi^{\ell}_0, \phi^{\ell}_1[, \\ \dfrac{\sin(2h_\ell - x)}{\sin(h_\ell)}, & x \in [\phi^{\ell}_1, \phi^{\ell}_2[, \\ 0, & \textit{otherwise.} \end{cases}$$

Then, for $i = -2, -1, m_\ell - 2, m_\ell - 1$, *the derivative of UAT B-splines* $\mathcal{N}^{\ell}_{i,3}$ *are given by*

$$\begin{cases} (\mathcal{N}^{\ell}_{-2,3}(x))' = -\cot(\dfrac{h}{2})\mathcal{N}^{\ell}_{-1,2}(x), \\ (\mathcal{N}^{\ell}_{-1,3}(x))' = \cot(\dfrac{h}{2})\mathcal{N}^{\ell}_{-1,2}(x) - \dfrac{1}{2}\cot(\dfrac{h}{2})\mathcal{N}^{\ell}_{0,2}(x), \\ (\mathcal{N}^{\ell}_{m_\ell-2,3}(x))' = \dfrac{1}{2}\cot(\dfrac{h}{2})\mathcal{N}^{\ell}_{m_\ell-2,2}(x) - \cot(\dfrac{h}{2})\mathcal{N}^{\ell}_{m_\ell-1,2}(x), \\ (\mathcal{N}^{\ell}_{m_\ell-1,3}(x))' = \cot(\dfrac{h}{2})\mathcal{N}^{\ell}_{m_\ell-1,2}(x), \end{cases} \tag{4.2.3}$$

where

$$\mathcal{N}^{\ell}_{-1,2}(x) = \begin{cases} \dfrac{\sin(h_\ell - x)}{\sin(h)}, & x \in [\phi^{\ell}_0, \phi^{\ell}_1[, \\ 0, & \textit{otherwise.} \end{cases}$$

$$\mathcal{N}^{\ell}_{m_\ell-1,2}(x) = \begin{cases} \dfrac{\sin(x - (m_\ell - 1)h_\ell)}{\sin(h)}, & x \in [\phi^{\ell}_{m_\ell-1}, \phi^{\ell}_{m_\ell}[, \\ 0, & \textit{otherwise.} \end{cases}$$

4.3 Algebraic trigometric Hermite interpolant and error estimates

4.3.1 Construction of Hermite interpolant

In this subsection, we are interested in constructing a new trigonometric Hermite interpolant into space $S_3([a, b], \Phi^\ell)$. The process of Hermite interpolation by using the quadratic UAT B-splines is as follows. For a given function f, we can construct

a trigonometric Hermite interpolant of the form:

$$Q_3[f](x) = \sum_{i=-2}^{m_\ell - 1} \mu_i(f) \mathcal{N}_{i,3}^{\ell}(x), \tag{4.3.1}$$

where the coefficients $\mu_i(f)$ are defined as linear combinations of some values of f and f' in the support of $\mathcal{N}_{i,3}$. Therefore, the operator $Q_3[f]$ is constructed to be exact on Γ_3, i.e. $Q_3[f] = f$, for all $f \in \Gamma_3$. The problem of interpolation is finding the coefficients $\mu_i(f)$ such that: for all $i = -2, \ldots, m_\ell - 1$,

$$\begin{cases} Q_3[f](\phi_i^\ell) & = f(\phi_i^\ell), \\ Q_3[f]'(\phi_i^\ell) & = f'(\phi_i^\ell). \end{cases} \tag{4.3.2}$$

Theorem 4.3.1. *The coefficient functionals $\mu_i(f)$ are respectively defined by the following formulas:*

$$\begin{aligned}
\mu_{-2}(f) &= \frac{1}{2}\left[f_0 + f_1 - \tan(\frac{h_\ell}{2})(f_0' + f_1')\right], \\
\mu_{-1}(f) &= f_1 - \tan(\frac{h_\ell}{2}) f_1', \\
\mu_i(f) &= \frac{1}{2}\left[f_{i+1} + f_{i+2} + \tan(\frac{h_\ell}{2})(f_{i+1}' - f_{i+2}')\right], \quad i = 0, \ldots, m_{\ell-3}, \\
\mu_{m_\ell - 2}(f) &= f_{m_{\ell-1}} + \tan(\frac{h_\ell}{2}) f_{m_{\ell-1}}', \\
\mu_{m_\ell - 1}(f) &= \frac{1}{2}\left[f_{m_{\ell-1}} + f_{m_\ell} + \tan(\frac{h_\ell}{2})(f_{m_{\ell-1}}' + f_{m_\ell}')\right],
\end{aligned}$$

with $f_i = f(\phi_i^\ell)$ and $f_i' = f'(\phi_i^\ell)$.

Proof. According to (4.2.3) and (4.3.2), and we make the substitution $x = \phi_0$ in (4.3.1), we deduce that $\mu_{-2}(f)$ can be written in the form

$$\begin{cases} \mu_{-2}(f) & = f(\phi_0^\ell), \\ \mu_{-2}(f) & = -\cot\left(\dfrac{h_\ell}{2}\right)\mu_{-2}(f) + \cot\left(\dfrac{h_\ell}{2}\right)\mu_{-1}(f), \end{cases}$$

as a result

$$\mu_{-2}(f) = \frac{1}{2}\left(\mu_{-1}(f) - \tan\left(\frac{h_\ell}{2}\right) f'(\phi_0) + f(\phi_0)\right). \tag{4.3.3}$$

Repeating the same technique by taking $x = \phi_1$, we obtain

$$\begin{cases} f(\phi_1^\ell) & = \dfrac{1}{2}\left(\mu_{-1}(f) + \mu_0(f)\right), \\ f'(\phi_1^\ell) & = \dfrac{1}{2}\cot\left(\dfrac{h_\ell}{2}\right)\left(\mu_0(f) - \mu_{-1}(f)\right). \end{cases}$$

Moreover,

$$\mu_{-1}(f) = f(\phi_1^\ell) - \tan\left(\frac{h_\ell}{2}\right) f'(\phi_1).$$

Consequently (4.3.3) becomes

$$\mu_{-2}(f) = \frac{1}{2}\left(f(\phi_0^\ell) + f(\phi_1^\ell) - \tan(\frac{h_\ell}{2})(f'(\phi_0^\ell) + f'(\phi_1^\ell))\right).$$

Now treating the general case, on one hand let $x = \phi_i$, $i = 0, \ldots, m_\ell - 3$, then we have

$$Q_3[f](\phi_i^\ell) = \sum_{i=-2}^{m_\ell - 1} \mu_i(f) M_{i,3}^\ell(\phi_i),$$

thus

$$\begin{aligned} f(\phi_i^\ell) &= \mu_{i-2}(f) M_{i-2,3}^\ell(\phi_i) + \mu_{i-1}(f) M_{i-1,3}^\ell(\phi_i), \\ &= \frac{1}{2}\left(\mu_{i-2}(f) + \mu_{i-1}(f)\right). \end{aligned} \tag{4.3.4}$$

On the other hand,

$$Q_3[f]'(\phi_i^\ell) = \sum_{i=-2}^{m_\ell - 1} \mu_i(f)\left(\delta_{i,2} M_{i,2}^\ell(\phi_i^\ell) - \delta_{i+1,2} M_{i+1,2}^\ell(\phi_i)\right),$$

therefore $\delta_{i,2} = \delta_{i+1,2} = \frac{1}{2}\cot\left(\frac{h_\ell}{2}\right)$, with a change of index we get

$$f'(\phi_i^\ell) = \frac{1}{2}\cot\left(\frac{h_\ell}{2}\right)(\mu_{i-1}(f) - \mu_{i-2}(f)), \tag{4.3.5}$$

from (4.3.4) and (4.3.5) we obtain the following system

$$\begin{cases} f(\phi_i^\ell) = \frac{1}{2}\left(\mu_{i-2}(f) + \mu_{i-1}(f)\right), \\ f'(\phi_i^\ell) = \frac{1}{2}\cot(\frac{h_\ell}{2})(\mu_{i-1}(f) - \mu_{i-2}(f)), \end{cases}$$

which implies,

$$\begin{cases} \mu_{i-1}(f) = f(\phi_i^\ell) + \tan(\frac{h_\ell}{2}) f'(\phi_i^\ell), \\ \mu_{i-2}(f) = f(\phi_i^\ell) - \tan(\frac{h_\ell}{2}) f'(\phi_i^\ell). \end{cases} \tag{4.3.6}$$

With a change of index we find

$$\begin{cases} \mu_i(f) = f(\phi_{i+1}^\ell) + \tan(\dfrac{h_\ell}{2}) f'(\phi_{i+1}^\ell), \\ \mu_i(f) = f(\phi_{i+2}^\ell) - \tan(\dfrac{h_\ell}{2}) f'(\phi_{i+2}^\ell). \end{cases}$$

The solution is to take the average of the two coefficient functionals; hence we have

$$\mu_i(f) = \frac{1}{2}\left(f_{i+1} + f_{i+2} + \tan(\frac{h}{2})(f'_{i+1} - f'_{i+2}) \right).$$

Similarly, we can prove the last two equations, which concludes the proof. □

4.3.2 Hermite basis of space $S_3([a,b], \Phi^\ell)$

We now establish a Hermite basis for $\Omega_3([a,b], \Phi^\ell)$ using the interpolation problem (4.3.2). More specifically, let φ_i and ψ_i be the solution functions of the problem (4.3.2) in $S_3([a,b], \Phi^\ell)$, which satisfy the following interpolation conditions:

$$\begin{aligned} &\varphi_i(\phi_j^\ell) = \delta_{i,j}, \quad \varphi_i'(\phi_j^\ell) = 0, \quad j = 0, \dots, m_\ell, \\ &\psi_i(\phi_j^\ell) = 0, \quad \psi_i'(\phi_j^\ell) = \delta_{i,j}, \quad j = 0, \dots, m_\ell, \end{aligned}$$

where $\delta_{i,j}$ stands for the Kronecker symbol.
We can easily verify that the supports of φ_i and ψ_i are given by $\mathrm{supp}(\varphi_i) = \mathrm{supp}(\psi_i) = [\phi_{i-1}^\ell, \phi_{i+1}^\ell]$, and the solution spline $Q_3[f]$ of the problem (4.3.2) can be written as

$$Q_3[f](x) = \sum_{i=0}^{m_\ell} \left(f_i \varphi_i(x) + f_i' \psi_i(x) \right). \tag{4.3.7}$$

According to (4.3.6) we have

$$\begin{cases} \varphi_0(x) & = \mathcal{N}_{-2,3}(x), \\ \varphi_1(x) & = \mathcal{N}_{-1,3}(x) + \mathcal{N}_{0,3}(x), \\ \varphi_i(x) & = \mathcal{N}_{i-2,3}(x) + \mathcal{N}_{i-1,3}(x), \quad i = 2, \dots, m_\ell - 2, \\ \varphi_{m_\ell-1}(x) & = \mathcal{N}_{m_\ell-2,3}(x) + \mathcal{N}_{m_\ell-3,3}(x), \\ \varphi_{m_\ell}(x) & = \mathcal{N}_{m_\ell-1,3}(x), \end{cases}$$

and

$$\begin{cases} \psi_0(x) & = 0, \\ \psi_1(x) & = \mathcal{N}_{0,3}(x) - \mathcal{N}_{-1,3}(x), \\ \psi_i(x) & = \mathcal{N}_{i-2,3}(x) - \mathcal{N}_{i-1,3}(x), \quad i = 2, \dots, m_\ell - 2, \\ \psi_{m_\ell-1}(x) & = \mathcal{N}_{m_\ell-2,3}(x) - \mathcal{N}_{m_\ell-3,3}(x), \\ \psi_{m_\ell}(x) & = 0. \end{cases}$$

Furthermore, the functions φ_i and ψ_i for $i = 0, \ldots, m_\ell$, constitute the Hermite basis of the space $S_3([a,b], \Phi^\ell)$. This basis presents a major disadvantage which is the instability caused by the non-positivity of its elements. Consequently, it is in practice undesirable especially in the construction of approximants.

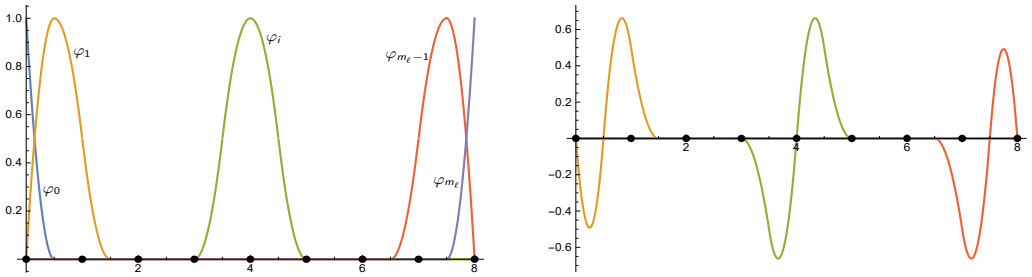

(a) Hermite basis elements φ_i. (b) Hermite basis elements ψ_i.

Figure 4.1 – Hermite basis of $\Omega_3([a,b], \phi^\ell)$.

4.3.3 Error estimates

In this subsection, we provide how to use the algebraic, trigonometric Taylor expansion for establishing the error estimation of our operator $Q_3[f]$. To do this, we will rewrite our operator in an appropriate form, so

$$Q_3[f](x) = \sum_{i=-2}^{m_\ell - 1} \left(\sum_{s=0}^{1} \beta_{i,s} f(\tau_{i,s}) + \sum_{s=0}^{1} \gamma_{i,s} f'(\tau_{i,s}) \right) \mathcal{N}_{i,3}^{\ell}, \tag{4.3.8}$$

where $\beta_{i,0} = \beta_{i,1} = \dfrac{1}{2}$, $\gamma_{i,0} = \dfrac{1}{2}\tan(\dfrac{h_\ell}{2})$, $\gamma_{i,1} = -\dfrac{1}{2}\tan(\dfrac{h_\ell}{2})$, $\tau_{i,0} = \phi_{i+1}$ and $\tau_{i,1} = \phi_{i+2}$.

Our objective is to establish an error bound for $Q_3[f]$. For the sake of simplicity and without losing the generality, we use the same manner and notation as in [31, 32]. More precisely, let

$$L_1^3[a,b] = \left\{ f \,:\, \mathbf{D}^2 f \text{ is absolutely continuous on } [a,b] \text{ and } \mathbf{D}^2 f \in L_1[a,b] \right\}.$$

Let $\mathbf{L}_3 = \mathbf{D}\left(\mathbf{D}^2 + 1\right)$ be a differential operator, its null space is Γ_3, i.e,

$$\mathbf{L}_3 f = 0, \qquad \forall f \in \Gamma_3. \tag{4.3.9}$$

The differential operator $\mathbf{L}_3$ will play an essential role in defining the algebraic, trigonometric Taylor expansion, which we will use to establish the estimation error bounds for quadratic splines interpolant operator. The Green functions are given by:

$$\begin{cases} G_3(x;y) &= 1 - \cos(x-y)_+, \\ G_4(x;y) &= (x-y)_+ - \sin(x-y)_+. \end{cases} \tag{4.3.10}$$

This Green's function plays an essential role in defining a B-spline basis for the space of algebraic trigonometric B splines. The following theorem shows that it is also the kernel for a useful generalized Taylor expansion.

Theorem 4.3.2. *[32] (Algebraic, trigonometric Taylor expansion). Let $f \in L_1^3[a,b]$. Then for any point $t \in [a,b]$,*

$$f(x) = s_f(x) + \int_t^x G_3(x;y)\,\mathbf{L}_3 f(y)\,dy, \tag{4.3.11}$$

where s_f is the unique element in Γ_3, such that

$$\mathbf{D}^j f(t) = \mathbf{D}^j s_f(t), \qquad j = 0,\ldots,2.$$

s_f is called an algebraic, trigonometric Taylor expansion of f about the point t. The following result gives an increase of the UAT B-splines $\mathcal{N}_{i,3}^{\ell}$, and the demonstration of this result is almost similar to the one of Theorem 10 in [31].

Theorem 4.3.3. *There exist a constant C such that*

$$\|D^j \mathcal{N}_{i,3}^{\ell}\| \le C h_{\ell}^{-j}, \quad j = 0,1,2. \tag{4.3.12}$$

Theorem 4.3.4. *The functionals $\beta_{i,s}$ and $\gamma_{i,s}$ in (4.3.8) satisfy,*

$$\left|\sum_{s=0}^{1}\beta_{i,s}f(\tau_{i,s}) + \sum_{s=0}^{1}\gamma_{i,s}f'(\tau_{i,s})\right| \le 2^{\frac{1}{q}-1}\left[\|f\|_{L^p[\phi_{i+1},\phi_{i+2}]} + \tan\left(\tfrac{h_\ell}{2}\right)\|f'\|_{L^p[\phi_{i+1},\phi_{i+2}]}\right]$$

for all $1 \le p,\ q \le \infty$.

Proof. Applying the Cauchy-Schwarz inequality, we obtain,

$$\begin{aligned}\left|\sum_{s=0}^{1}\beta_{i,s}f(\tau_{i,s}) + \sum_{s=0}^{1}\gamma_{i,s}f'(\tau_{i,s})\right| &\le \left|\sum_{s}\beta_{i,s}f(\tau_{i,s})\right| + \left|\sum_{s}\gamma_{i,s}f'(\tau_{i,s})\right| \\ &\le \left(\sum_{s}|\beta_{i,s}|^q\right)^{\frac{1}{q}}\left(\sum_{s}|f(\tau_{i,s})|^p\right)^{\frac{1}{p}} \\ &\quad + \left(\sum_{s}|\gamma_{i,s}|^q\right)^{\frac{1}{q}}\left(\sum_{s}|f'(\tau_{i,s})|^p\right)^{\frac{1}{p}}\end{aligned}$$

with $\dfrac{1}{p} + \dfrac{1}{q} = 1$ (Hölder inequality).
On the other hand,

$$\left(\sum_{s=0}^{1}|\beta_{i,s}|^q\right)^{\frac{1}{q}} = 2^{\frac{1}{q}}\frac{1}{2} = 2^{\frac{1}{q}-1}, \qquad \left(\sum_{s=0}^{1}|\gamma_{i,s}|^q\right)^{\frac{1}{q}} = 2^{\frac{1}{q}-1}\tan\left(\tfrac{h_\ell}{2}\right),$$

and,

$$\left(\sum_{s=1}^{2}|f(\tau_{i,s})|^p\right)^{\frac{1}{p}} \leq \left(\int_{\tau_{i,0}}^{\tau_{i,1}}|f|^p\right)^{1/p}, \qquad \left(\sum_{s=1}^{2}|f'(\tau_{i,s})|^p\right)^{\frac{1}{p}} \leq \left(\int_{\tau_{i,0}}^{\tau_{i,1}}|f'|^p\right)^{1/p}.$$

Which concludes the proof. □

The following theorem provides a general approach that allows obtaining the approximation errors for the Hermite interpolant reproducing the space of quadratic algebraic trigonometric functions.

Theorem 4.3.5. *There exists a constant C_1 such that for all $f \in L_1^3([a,b])$ and for all partitions Φ^ℓ of $[a,b]$,*

$$\|f - Q_3[f]\|_\infty \leq C_1 h_\ell^3 \|\mathbf{L}_3 f\|_\infty. \tag{4.3.13}$$

Proof. Let t be in neighbor of x, then we have

$$f = s_f + \int_t^x G_3(x,y)\mathbf{L}_3 f(y)dy$$

$$\|f - s_f\| \leq \|\mathbf{L}_3 f\|_\infty \left|\int_t^x G_3(x,y)dy\right|$$

where the function s_f is the unique element in Γ_3, that satisfy $\mathbf{D}^{j-1}f(t) = \mathbf{D}^{j-1}s_f(t)$, for $j = 0, 1, 2$.
We note that

$$\int_t^x G_3(x,y)dy = G_4(x,t).$$

Hence for $t = x - h_\ell$, we have $G_4(x,t) = h_\ell - \sin(h_\ell)$.
On the other hand, for small values of h_ℓ, we replace $\sin(h_\ell)$ by $h_\ell - \dfrac{h_\ell^3}{3!} + O(h_\ell^3)$.
Thus we have

$$|G_4(x,t)| \leq \frac{h_\ell^3}{3!} + O(h_\ell^3). \tag{4.3.14}$$

This completes the proof. □

4.4 Quadratic quadrature formulae based on $Q_3[f]$

As an application of the previous results, we will construct a quadrature formula approximating a definite integral of a function f, in terms of a weighted linear combination of function evaluations at the knots ϕ_i^ℓ. The idea is to integrate the Hermite interpolant $Q_3[f]$ instead of f. Indeed, if we denote this new quadrature

formula by $\mathcal{I}_{Q_3}^{\ell}$ we have

$$\mathcal{I}_{Q_3}^{\ell}(f) = \int_a^b Q_3[f](x)dx = \sum_{i=-2}^{m_\ell - 1} \omega_i \mu_i(f), \tag{4.4.1}$$

where $\omega_i = \int_a^b \mathcal{N}_{i,3}(x)dx$ are the weights of the quadrature formula $\mathcal{I}_{Q_3}^{\ell}$ given explicitly by:

$$\begin{cases} \omega_{-2} = \omega_{m_\ell - 1} = \dfrac{h_\ell - \sin(h_\ell)}{2 - 2\cos(h_\ell)}, \\ \omega_{-1} = \omega_{m_\ell - 2} = \dfrac{h_\ell + \sin(h_\ell) - 2h_\ell \cos(h_\ell)}{2 - 2\cos(h_\ell)}, \\ \omega_i = h_\ell, \quad i = 0, \ldots, m_\ell - 3. \end{cases}$$

In the following, we proceed analogously to Subsection 3.2. To summarize, we have the following theorem.

Theorem 4.4.1. *There exists a constant C_2 such that for all $f \in L_1^3([a,b])$. The error $\mathcal{E}_{Q_3} = \int_a^b f(x)dx - \int_a^b Q_3[f](x)dx$ associated with the quadrature formula based on $Q_3[f]$ is given by,*

$$|\mathcal{E}_{Q_3}(f,[a,b])| \leq C_2 h_\ell^4 \|\mathbf{L}_3 f\|_\infty. \tag{4.4.2}$$

Proof. The proof can be immediately deducted from Theorem 4.3.5. □

4.5 Solution of Fredholm linear integral equations

4.5.1 Description of the method

This section describes an application method based on the quadrature formula's rules, introduced in the previous section, to solve numerically Fredholm integral equations of the second kind. The particular numerical way which we use is involved in [71]. The equation in which we are interested is given by

$$u(x) - \int_a^b k(x,t)u(t)dt = f(x), \tag{4.5.1}$$

where $k(x,t) \in \mathcal{C}([a,b] \times [a,b])$ and $f \in \mathcal{C}([a,b])$ are known functions and u is the function to be determined.
Now if we put $\mathcal{K}u = \int_a^b k(x,t)u(t)dt$, the equation (4.5.1) becomes

$$u - \mathcal{K}u = f. \tag{4.5.2}$$

The classical approach consists of approaching the integral operator $\mathcal{K}$ with $\mathcal{K} = \mathcal{K}_\ell + Q_3[\mathcal{K}] - Q_3[\mathcal{K}_\ell]$, this scheme leads to simpler and less expensive computations. Then, the Nyström operator associated with our Hermite interpolant is given by

$$\mathcal{K}_\ell u(x) = \int_a^b Q_3[k(x,\cdot)u(\cdot)](t)dt = \sum_{i=-2}^{m_\ell-1} \omega_i u(\phi_i^\ell)\mu_i(k(x,\phi_i^\ell)). \tag{4.5.3}$$

Let us consider u_ℓ the approximate solution of u and replacing u in Eq. (4.5.2), we get

$$u_\ell - (\mathcal{K}_\ell + Q_3[\mathcal{K}] - Q_3[\mathcal{K}_\ell])u_\ell = f. \tag{4.5.4}$$

Now we can present the main result of this section.

Theorem 4.5.1. *Let V and W be the vectors with components*

$$V_i = \mathcal{K}f(\phi_i^\ell), \qquad W_i = f(\phi_i^\ell),$$

and let A, B, C, D be the matrices with coefficients

$$A_{i,j} = \mathcal{K}\mathcal{N}_{j,3}^\ell(\phi_i^\ell), \quad B_{i,j} = \omega_j \overline{k}_j(\phi_i^\ell), \quad C_{i,j} = \omega_j k_j^*(\phi_i^\ell), \quad D_{i,j} = \mathcal{N}_{j,3}^\ell(\phi_i^\ell),$$

where $\overline{k}_j = \mu_j(k(\cdot,\phi_j^\ell))$ and $k_j^* = \mathcal{K}\overline{k}_j$.
Then the approximate solution is given by

$$u_\ell = f + \sum_{i=-2}^{m_\ell-1} X_i \mathcal{N}_{i,3}^\ell + \sum_{i=-2}^{m_\ell-1} \omega_i Y_i \overline{k}_i, \tag{4.5.5}$$

where $Z = [X\ Y]^T$ is the solution of the following linear system of size $2m_\ell + 4$

$$(\mathcal{I} - F)Z = G,$$

with $F = \begin{bmatrix} A & C-B \\ D & B \end{bmatrix}$ *and* $G = \begin{bmatrix} V \\ W \end{bmatrix}$.

Proof. According to (4.3.1) and (4.5.3) we have

$$Q_3[\mathcal{K}u] = \sum_{i=-2}^{m_\ell-1} \mu_i(\mathcal{K}u)\mathcal{N}_{i,3}^\ell = \sum_{i=-2}^{m_\ell-1} X_i' \mathcal{N}_{i,3}^\ell,$$
$$\mathcal{K}_\ell u = \sum_{i=-2}^{m_\ell-1} \omega_i u(\phi_i^\ell)\mu_i(k(x,\phi_i^\ell)) = \sum_{i=-2}^{m_\ell-1} \omega_i Y_i' \mu_i(k(x,\phi_i^\ell)),$$

where $X_i' = \mu_i(\mathcal{K}u)$ and $Y_i' = u(\phi_i^\ell)$ for $i = -2, \ldots, m_\ell - 1$ are constants.

Then

$$Q_3[\mathcal{K}_\ell u] = \sum_{i=-2}^{m_\ell-1}\left(\sum_{j=-2}^{m_\ell-1}\omega_j Y_j'\mu_j(k(x,\phi_j^\ell))\right)\mathcal{N}_{i,3}^\ell.$$

We deduce that the approximate solution can be written as

$$u_\ell = f + \sum_{i=-2}^{m_\ell-1} X_i\mathcal{N}_{i,3}^\ell + \sum_{i=-2}^{m_\ell-1}\omega_i Y_i\overline{k}_i,$$

where X_i and Y_i for $i=-2,\ldots,m_\ell-1$ are constants.
By using the expression of u_ℓ we obtain

$$Q_3[\mathcal{K}u_\ell] = \sum_{i=-2}^{m_\ell-1}\mu_i(\mathcal{K}u_\ell)\mathcal{N}_{i,3}^\ell = \sum_{i=-2}^{m_\ell-1}\left(\mathcal{K}f(\phi_i^\ell) + \sum_{k=-2}^{m_\ell-1}X_k\tilde{\mathcal{N}}_k(\phi_i^\ell) + \sum_{l=-2}^{m_\ell-1}\omega_\ell Y_\ell k_\ell^*(\phi_i^\ell)\right)\mathcal{N}_{i,3}^\ell, \tag{4.5.6}$$

where

$$\begin{aligned}
\mathcal{K}f(\phi_i^\ell) &= \int_a^b k(\phi_i,t)f(t)dt,\\
\tilde{\mathcal{N}}_k(\phi_i^\ell) &= \mathcal{K}\mathcal{N}_{k,3}(\phi_i^\ell) = \int_{\phi_k}^{\phi_k+3} k(\phi_i^\ell,t)\mathcal{N}_{k,3}^\ell(t)dt,\\
k_\ell^*(\phi_i^\ell) &= \mathcal{K}\mu_\ell(k(\cdot,\phi_\ell))(\phi_i^\ell) = \mu_\ell(k(\cdot,\phi_\ell))\int_a^b k(\phi_i,t)dt.
\end{aligned}$$

On the other hand,

$$\mathcal{K}_\ell u_\ell = \sum_{i=-2}^{m_\ell-1}\omega_i\left(f(\phi_i^\ell) + \sum_{k=-2}^{m_\ell-1}X_k\mathcal{N}_k(\phi_i^\ell) + \sum_{l=-2}^{m_\ell-1}\omega_\ell Y_\ell\overline{k}_\ell(\phi_i^\ell)\right)\mu_i(k(\cdot,\phi_i^\ell)), \tag{4.5.7}$$

$$Q_3[\mathcal{K}_\ell u_\ell] = \sum_{i=-2}^{m_\ell-1}\left[\sum_{j=-2}^{m_\ell-1}\omega_j\left(f(\phi_j^\ell) + \sum_{k=-2}^{m_\ell-1}X_k\mathcal{N}_k(\phi_j^\ell) + \sum_{l=-2}^{m_\ell-1}\omega_\ell Y_\ell\overline{k}_\ell(\phi_j^\ell)\right)\mu_i(k(\cdot,\phi_j^\ell))\right]\mathcal{N}_{i,3}^\ell. \tag{4.5.8}$$

According to (4.5.6)−(4.5.8) and by identifying the coefficients of $\{\mathcal{N}_{i,3}^\ell\}_{i=-2}^{m_\ell-1}$ and $\mu_i(k(\cdot,\phi_i^\ell))$ respectively, we obtain

$$\begin{cases} X = V + AX + CY - B(W + DX + BY),\\ Y = W + DX + BY. \end{cases}$$

By replacing Y by its value in the first equation, we deduce that

$$\begin{cases} X = V + AX + (C-B)Y,\\ Y = W + DX + BY. \end{cases}$$

Witch completes the proof. □

4.5.2 Error estimates

Here, we give the error estimates for this type of application. The order of convergence of the approximate solution to the exact solution is the sum of the order of convergence of the quadrature rule and the order of convergence of the Hermite interpolant operator on which this rule is based. Let C be a generic constant, which can take various values in different situations but is independent of ℓ. Therefore, we have the following theorem.

Theorem 4.5.2. *For $\ell > 0$, we have*

$$\|u - u_\ell\|_\infty \leq C\|(I - Q_3)[\mathcal{K} - \mathcal{K}_\ell]\|_\infty,$$

where C is a constant independent of ℓ.

Proof. We denote by $\tilde{\mathcal{K}}_\ell = \mathcal{K}_\ell + Q_3[\mathcal{K}] - Q_3[\mathcal{K}_\ell]$, then we have

$$\|\mathcal{K} - \tilde{\mathcal{K}}_\ell\|_\infty = \|(\mathcal{I} - Q_3)[\mathcal{K} - \mathcal{K}_\ell]\|_\infty,$$

which converges to 0 if ℓ tends to infinity.
Then we deduce that for all large ℓ, $(\mathcal{I} - \tilde{\mathcal{K}}_\ell)$ is invertible and $\|(\mathcal{I} - \tilde{\mathcal{K}}_\ell)^{-1}\|_\infty \leq C$, where C is a constant independent of ℓ.
Furthermore we have

$$u - u_\ell = (I - \tilde{\mathcal{K}}_\ell)^{-1}(\mathcal{K} - \tilde{\mathcal{K}}_\ell)u.$$

Thus

$$\|u - u_\ell\|_\infty \leq C\|(I - Q_3)[\mathcal{K} - \mathcal{K}_\ell]\|_\infty.$$

This complete the proof. □

Theorem 4.5.3. *Let $u \in C([a, b])$. Then for ℓ large enough, the approximate solution satisfies*

$$\|u - u_\ell\|_\infty = O(h_\ell^7). \tag{4.5.9}$$

Proof. According to (4.3.13), we can easily show that

$$\|(I - Q_3)[f]\|_\infty \leq C_1 h_\ell^3 \|\mathbf{L}_3 f\|_\infty, \tag{4.5.10}$$

where C_1 is a constant independent of ℓ and $\|.\|_\infty$ is the maximum norm.
Which implies that,

$$\|(I - Q_3)[\mathcal{K} - \mathcal{K}_\ell]y\|_\infty \leq C_1 \|\mathbf{L}_3(\mathcal{K} - \mathcal{K}_\ell)\|_\infty h_\ell^3,$$

with

$$(\mathcal{K} - \mathcal{K}_\ell)y = \int_a^b (I - Q_3)[k(x, t)]y(t)dt.$$

Thus,

$$\mathbf{L}_3(\mathcal{K}-\mathcal{K}_\ell)y=\int_a^b (I-Q_3)[\mathbf{L}_3k(x,t)]y(t)dt.$$

Then, from (4.4.2) we deduce that,

$$\|\mathbf{L}_3[\mathcal{K}-\mathcal{K}_\ell]\|_\infty = O(h_\ell^4). \tag{4.5.11}$$

Combining (4.5.10) and (4.5.11) we deduce that

$$\|(I-Q_3)[\mathcal{K}-\mathcal{K}_\ell]y\|_\infty = O(h_\ell^7),$$

hence by using Theorem 4.5.2, we deduce (4.5.9). □

4.6 Numerical Examples and Application

In order to show the accuracy and effectiveness of our proposed method, we will present some numerical experiment tests.

Example 4.6.1. We consider three integrals

$$\begin{aligned}
\mathcal{I}_1 &= \int_0^1 (\sin(x)+\cos(x))dx = 1.30116867893976,\\
\mathcal{I}_2 &= \int_0^1 (1+x+\cos(x))dx = 2.34147098480790,\\
\mathcal{I}_3 &= \int_{-1}^1 \frac{1}{1+16x^2}dx = 0.66290883183401.
\end{aligned}$$

For different values of ℓ, we present in tables 4.1, 4.2 and 4.3 the maximum errors of the approximate integrals $\mathcal{I}_1$, $\mathcal{I}_2$ and $\mathcal{I}_3$ using the quadratic formula $\mathcal{I}_{Q_3}^\ell$ described in this paper, rule introduced in [31, 71] and Simpson's rule. More precisely, Column 2 of each table contains the number of nodes discretizing the interval $[0,1]$.

Table 4.1 – The maximum error for approximating $\mathcal{I}_1$ using $\mathcal{I}_{Q_3}^\ell$, rule introduced in [31, 71] and Simpson's rule.

ℓ	m_ℓ	$\mathcal{I}_{Q_3}^\ell$	Eddargani [31]	Sablonniére [71]	Simpson's rule
3	8	0	1.5959×10^{-6}	3.1771×10^{-9}	1.7681×10^{-6}
4	16	0	1.1208×10^{-7}	6.4059×10^{-11}	1.1035×10^{-7}
5	32	0	7.3830×10^{-9}	1.1104×10^{-12}	6.8946×10^{-9}
6	64	0	4.7312×10^{-10}	1.7541×10^{-14}	4.3088×10^{-10}

Table 4.2 – The maximum error for approximating $\mathcal{I}_2$ using $\mathcal{I}^{\ell}_{Q_3}$, rule introduced in [31, 71] and Simpson's rule.

ℓ	m_ℓ	$\mathcal{I}^{\ell}_{Q_3}$	Eddargani [31]	Sablonniére [71]	Simpson's rule
3	8	0	1.0321×10^{-6}	2.0546×10^{-9}	1.1434×10^{-6}
4	16	0	7.2482×10^{-8}	4.1427×10^{-11}	7.1365×10^{-8}
5	32	0	4.7746×10^{-9}	7.1809×10^{-13}	4.4587×10^{-9}
6	64	0	3.0597×10^{-10}	1.1990×10^{-14}	2.7865×10^{-10}

Table 4.3 – The maximum error for approximating $\mathcal{I}_3$ using $\mathcal{I}^{\ell}_{Q_3}$, rule introduced in [31, 71] and Simpson's rule.

ℓ	m_ℓ	$\mathcal{I}^{\ell}_{Q_3}$	Eddargani [31]	Sablonniére [71]	Simpson's rule
6	64	2.2129×10^{-9}	3.0203×10^{-8}	1.8408×10^{-9}	7.3029×10^{-10}
7	128	1.3823×10^{-10}	9.5883×10^{-10}	1.5503×10^{-11}	4.566×10^{-11}
8	256	0	3.0712×10^{-11}	1.2345×10^{-13}	2.8540×10^{-12}
9	512	0	1.0051×10^{-12}	9.9920×10^{-16}	1.7800×10^{-13}
10	1024	0	3.4233×10^{-14}	0	1.1000×10^{-14}

Example 4.6.2. We consider the following Fredholm integral equation of the second kind quoted from [71]

$$u(x) - \int_0^{\frac{\pi}{2}} \sin(30x)\cos(31t)u(t)dt = \sin(x) + \frac{\sin(30x)}{30},$$

where the exact solution is given by $u(x) = \sin(x)$. The result has been shown for different values of ℓ in Table 4.4. Where the Numerical Convergence Order (NCO) are computed by the formula $\log\left(\frac{e_\ell}{e_{2\ell}}\right)/\log(2)$, with e_ℓ is maximum error of a given operator using m_ℓ equally spaced knots.

Table 4.4 – Absolute errors of example 2.

ℓ	m_ℓ	Our method	NCO	Sablonniére [71]	NCO
5	32	3.1247×10^{-08}	–	1.17×10^{-05}	–
6	64	2.1312×10^{-10}	7.28671	1.16×10^{-8}	9.9782
7	128	9.5186×10^{-13}	7.7159	4.18×10^{-11}	8.11641
8	256	4.0015×10^{-15}	7.89406	9.39×10^{-14}	8.79816

Example 4.6.3. We consider the following second Fredholm integral equation.

$$u(x) - \int_0^1 (x^{25} - 1)(t^{50} + t^{25} - 1)u(t)dt = f(t),$$

where $f(x)$ is defined such that the exact solution is $u(x) = \cos(50x)$. The results for different values of ℓ are summarized in Table 4.5.

Table 4.5 – Absolute errors of example 3.

ℓ	m_ℓ	Our method	NCO	Sablonniére [71]	NCO
5	32	2.8513×10^{-09}	–	1.77×10^{-06}	–
6	64	4.2735×10^{-11}	6.0601	8.82×10^{-9}	7.05151
7	128	3.5462×10^{-13}	6.9130	2.24×10^{-11}	8.62114
8	256	1.6150×10^{-15}	7.7786	7.53×10^{-14}	8.21663

According to the above three examples, we remark that the operator described here is preferable to approximate a large class of functions. As the numerical results show, it is clear that our approach is more appropriate for approximating integrals that contain algebraic, trigonometric functions.

4.7 Conclusion

In this work, we have given the explicit expression of the Hermite interpolant scheme that reproduce algebraic and trigonometric functions. We have also proposed an efficient method to solve the integral Fredholm equations of the second type based on spline interpolation. Numerical comparison with some known rules of the same order shows the efficiency of the proposed quadrature rules.

Conclusion and perspectives

The conclusion of this report begins with a look back at the research's goals and methodology. Although particular results are obtained, there are still numerous unanswered questions. Then it gives an overview of the manuscript's key findings to open the way for future research.

Overview of the contributions

We review the principal outcomes of this thesis.

In Chapter 2, we provided the refinement equation of B-splines of order k associated with the uniform sequence of the interval $[a, b]$. As a consequence, we constructed the subdivision formula for UAH B-splines curves. Furthermore, this chapter introduced a new inverse subdivision approach for multiresolution, called "Smooth Reverse Subdivision", to create fair coarse models.

In Chapter 3, we have constructed quadratic orthogonal wavelets based on trigonometric and hyperbolic B-splines using a uniform node sequence over the interval $[a, b]$.

Chapter 4 proposed a quadrature formula based on integrating the Hermite trigonometric composite interpolation adapted to a uniform subdivision of a bounded interval. Due to the simplicity of these formulas, we obtained significant and encouraging performances compared to classical quadrature formulas such as the Simpson method and the Gauss-Legendre method. Then, we are interested in the solution of Fredholm integral equations of the second kind using modified Nyström methods. This method is constructed to approach the kernel of the integral correspondent operator. Our work aims to build an approximate solution of linear integral equations using Nyström methods based on quadratic UAT B-splines. We illustrate our results with numerical examples.

Future research suggestions

The actuality of this domain is very extensive: splines, wavelets, and interpolation/approximation curves are used everywhere. Just choose an object at random it is probable that one of the concepts studied in this work has been used. A similar perspective is to continue constructing wavelets for hyperbolic or trigonometric

B-splines of degrees greater than or equal to four and use it for the resolution of differential or integral equations to exploit it in image processing. Each of these chapters opens many perspectives:

All of the obtained results in Chapters 2 and 3 for curves can be easily extended to multiresolution surfaces using the tensor products of UAH and UAT B-splines. On the other hand, the wavelet basis constructed in this thesis can be proposed to develop a complete approximation method for the numerical solution of integral and integrodifferential equations.

The results of the 4th Chapter can be extended to obtain spline interpolants based on higher-order B-spline functions. Then, we can be extended to nonlinear integral and integrodifferential equations and other classes of singular integral equations. Consequently, in the direct continuity of our thesis work, the previous method can be applied to Volterra integral equations and integrodifferential equations, but some modifications are necessary.

Bibliography

[1] C. Allouch, D. Sbibih, M. Tahrichi, *Superconvergent Nyström and degenerate Kernel methods for Hammerstein integral equations*, J. Comput. Appl. Math, 258 (2014), 30-41.

[2] C. Allouch, D. Sbibih, M. Tahrichi, *Superconvergent projection methods for Hammerstein integral equations*, J. Integral Equations Applic., in press.

[3] C. Allouch, P. Sablonniére, *Iteration methods for Fredholm integral equations of the second kind based on spline quasi-interpolants*, Math. Comput. Simul, 99 (2014), 19-27.

[4] C. Allouch, P. Sablonniére, D. Sbibih, *Solving Fredholm integral equations by approximating kernels by spline quasi-interpolants,* Numer. Algorithm, 56 (2011), 437-453.

[5] K.E. Atkinson, G. Chandler, *The collocation method for solving the radiosity equation for unoccluded surfaces,* J. Integral Eqs. Appl, 10 (1998), 253-290.

[6] M. Ajeddar and A. Lamnii, *Smooth reverse subdivision of uniform algebraic hyperbolic B-splines and wavelets,* International Journal of Wavelets, Multiresolution and Information Processing, (2021), 2150018.

[7] M. Ajeddar and A. Lamnii, *Trigonometric Hermite interpolation method for Fredholm linear integral equations,* Journal of Applied Analysis, 10 (2021), 253-290.

[8] K.E. Atkinson, *Numerical solution of fredholm integral equations of the second kind,* Theoretical Numerical Analysis. Springer, New York, NY, (2009), 473-549.

[9] A.H. Borzabadi, O.S. Fard, *A numerical scheme for a class of nonlinear Fredholm integral equations of the second kind,* Journal of Computational and Applied Mathematics, 232 (2009), 449-454.

[10] A. Bellour, D. Sbibih and A. Zidna, *Two cubic spline methods for solving Fredholm integral equations,* Applied Mathematics and Computation, 276 (2016), 1-11.

[11] D. Barrera, F. Elmokhtari and D. Sbibih, *Two methods based on bivariate spline quasi-interpolants for solving Fredholm integral equations,* Applied Numerical Mathematics, 127 (2018), 127, 78-94.

[12] R. H. A. Bartels, J. C. A. Beatty, and B. A. A. Barsky, *An introduction to splines for use in computer graphics and geometric modeling,* Morgan Kaufmann Series in Computer Graphics and Geometric Modeling. Morgan Kaufmann, (1987).

[13] C.T.H. Baker, *The Numerical Treatment of Integral Equations,* Clarendon Press, Oxford, (1977).

[14] R.H. Bartels, H. Richard, and F. Samavati, *Reversing subdivision rules: Local linear conditions and observations on inner products,*Journal of Computational and Applied Mathematics, 119.1-2 (2000), 29-67.

[15] E. Bournay, *Seismic image segmentation by texture analysis and nonlinear filtering,* DEA report in Applied Mathematics, Joseph Fourier University, June (1993).

[16] E. E. Catmull and J. H. Clark, *Recursevely generated b-spline surfaces on topological meshes,* Computer Aided Design, 19 (1978), 350-355.

[17] A. S. Cavaretta, W. Dahmen and C. A. Micchelli, *Stationary subdivision*, Memoirs of the American Mathematical Society, 453 (1991), 346-349.

[18] H. B. Curry and I. J. Schoenberg, *On spline distributions and their limits-the polya distribution functions,* Amer. Math. Soc, (1947), 1114-1114

[19] C. Conti and R. Morandi, *Piecewise C^1-shape-preserving Hermite interpolation,* Computing, 56 (1996), 56, 323-341.

[20] J. A. Cottrell, T.J.R. Hughes and Y. Bazilevs, *Isogeometric analysis: toward integration of CAD and FEA,* John Wiley and Sons, (2009).

[21] G. M. Chaikin, *An algorithm for high-speed curve generation,* Computer graphics and image processing, 3.4 (1974), 346-349.

[22] C.K. Chui, *Wavelets,* Department of mathematics Texas A and M univercity College Station, Texas (1992).

[23] W. Dahmen and C. A. Micchelli, *On the theory and application of exponential splines,* Topics in Multivariate Approximation. Academic Press, (1987), 37-46.

[24] N. A. Dodgson and M. F. Hassan, *Reverse Subdivision*, Advances in Multiresolution for Geometric Modelling, (2005), 271-283.

[25] D. Doo and M. Sabin, *Behaviour of recursive division surface near extraordinay points,* Computer Aided Design, 19 (1978), 356-360.

[26] N. Dyn, *Subdivision schemes in computer aided geometric design,* Computer Aided Geometric Design, 20 (1992), 36-3104.

[27] N. Dyn, J. A. Gregory and D. Levin, *A four-point interpolatory subdivision scheme for curve design,* Computer Aided Geometric Design, 04 (1987), 257-268.

[28] G. Delauriers and S. Dubuc, *Symmetric iterative interpolation processes,* Constructive Appoximation, 05 (1989), 49-68.

[29] C. De Boor, *Cutting corners always works,* Computer Aided Geometric Design, 4.1-2 (1987), 125-131.

[30] S. Eddargani, A. Lamnii, M. Lamnii, D. Sbibih, A. Zidna: *Algebraic hyperbolic spline quasi-interpolants and applications,* J. Comput Appl Math, 347 (2019), 196-209.

[31] S. Eddargani, A. Lamnii, M. Lamnii, D. Sbibih and A. Zidna, *Algebraic hyperbolic spline quasi-interpolants and applications,* J. Comput Appl Math, 347 (2019), 196-209.

[32] S. Eddargani, A. Lamnii and M. Lamnii, *On algebraic trigonometric integro splines,* ZAMM-Journal of Applied Mathematics and Mechanics/Zeitschrift für Angewandte Mathematik und Mechanik, vol. 100, no 2, p. e201900262, (2020).

[33] J. Feng, J. Shao, X. Jin, Q. Peng and A. R. Forrest, *Multiresolution free-form deformation with subdivision surface of arbitrary topology.* The Visual Computer, 22 (2006), 28-42.

[34] M. E. Fang, W. Ma and G. Wang, *A generalized curve subdivision scheme of arbitrary order with a tension parameter.* Computer Aided Geometric Design, 27.9 (2010), 720-733.

[35] K. Foster, M. C. Sousa, F. F. Samavati and B. Wyvill, *Polygonal silhouette error correction: a reverse subdivision approach.* International Journal of Computational Science and Engineering, 3.1 (2007), 53-70.

[36] S. Hajji, B. Danouj and A. Lamnii, *UAT B-Splines of Order 4 for Reconstructing the Curves and Surfaces.* Applied Mathematical Sciences, 12.21 (2018), 1007-1020.

[37] S. Holtz, T. Rohwedder, R. Schneider, *The alternating linear scheme for tensor optimization in the tensor train format.* SIAM Journal on Scientific Computing, 34.2 (2012), A683–A713.

[38] X. Han, *Quadratic trigonometric polynomial curves with a shape parameter,* Computer Aided Geometric Design, 19 (2002), 503–512.

[39] X. Han, *Cubic trigonometric polynomial curves with a shape parameter,* Computer Aided Geometric Design, 21 (2004), 535–548.

[40] W. Hackbusch, *Integral Equations: Theory and Numerical Treatment,* Rabinowitz, Methods of Numerical Integration Academic Press, Orlando Florida (1984).

[41] E. K. Kulikov, A. A. Makaro, *On approximation by hyperbolic splines,* J. Math. Sci. (N.Y.), 240 (2019), 822-832.

[42] B. I. Kvasov, *On the construction of hyperbolic interpolation splines,* Comput. Math. Math. Phys, 48 (2008), 539-548.

[43] B.I. Kvasov, P. Sattayatham, *GB-splines of arbitrary order,* Journal of Computational and Applied Mathematics, 104 (1999), 63-88.

[44] M. Kallay, *General B-spline Hermite interpolation,* Computer aided geometric design, 8 (1991), 159-161.

[45] S. Kumar, I.H. Sloan, *A new collocation-type method for Hammerstein integral equations,* Math. Comp, 48 (1987), 585-593.

[46] R. Kress, *Linear Integral Equations,* Math. Springer-Verlag, 2nd edition, Berlin, (1999).

[47] A. Lamnii, H. Mraoui, D. Sbibih and A. Zidna, *Uniform tension algebraic trigonometric spline wavelets of class C^2 and ordre four,* Mathematics and Computers in Simulation, 87, (2013), 68-86.

[48] J. M. Lane and R. F. Riesenfeld, *A theoretical development for the computer generation and display of piecewise polynomial surfaces,* IEEE Transactions on Pattern Analysis and Machine Intelligence, 1 (1980), 35.

[49] Y. Lü, G. Wang and X. Yang, *Uniform hyperbolic polynomial B-spline curves,* Computer Aided Geometric Design, 19.6 (2002), 379.

[50] G. Lavoué, F. Dupont and A. Baskurt, *High rate compression of CAD meshes based on subdivision inversion,* Annals of Telecommunications, 60 (2005), 1286-1310.

[51] Y. Lü, G. Wang and X. Yang, *Uniform trigonometric polynomial B-spline curves,* Science in China Series F Information Sciences, 45.5 (2002), 335-343.

[52] A. Lamnii, F. Oumellal, *Computation of Hermite interpolation in terms of B-spline basis using polar forms,* Mathematics and Computers in Simulation, 134 (2017), 17-27.

[53] A. Lahtinen, *Shape preserving interpolation by quadratic splines,* Journal of computational and applied mathematics, 29 (1990), 15-24.

[54] T. Lyche and L. Schumaker, *L-Spline Wavelets,*(1994).

[55] M. Fang, W. Ma and G. Wang, *A generalized curve subdivision scheme of arbitrary order with a tension parameter,* Computer Aided Geometric Design 27 (2010) 720-733.

[56] L. Mündermann, P. MacMurchy, J. Pivovarov, and P. Prusinkiewicz, *Modeling lobed leaves,* In Computer Graphics International, (2003). Proceedings, pages 60-65, july 2003.

[57] M. S. Mummy, *Hermite interpolation with B-splins,* Computer aided geometric design, 6 (1989), 177-179.

[58] C. Manni, C^1 *comonotone Hermite interpolation via parametric cubics,* Journal of computational and applied mathematics, 69 (1996), 143-157.

[59] S. Micula, G. Micula, *On the superconvergent spline collocation methods for the Fredholm integral equations on surfaces,* Math. Balkanica, 19 (2005), 155-166.

[60] G. Mastroianni, G.V. Milanovic, D. Occorsio, *Nyström method for Fredholm integral equations of the second kind in two variables on a triangle,* Appl. Math. Comp, 14 (2013), 7653-7662.

[61] Y. Meyer, *Ondelettes, fonctions splines et analyses graduées,* In Cahiers du Ceremade, number 8703, Université Paris-Dauphine, 1987.

[62] S. G. Mallat, *A theory for multiresolution signal decomposition: the wavelets representation,* IEEE Trans. Patt. Anal. Mach. Intelly, 11 (1989), 974-693.

[63] K. Nguyen-Tan, R. Raffin, M. Daniel and C. Le, *Reconstruction de surface B-spline par subdivision non-uniforme inverse,* Proceedings of GTMG, 9 (2009), 67-76.

[64] A. Ron, *Exponential box splines,* Constructive Approximation, 4 (1988), 357-378.

[65] B. Sauvage, *Déformation de courbes et surfaces multirésolution sous contraintes,* Diss. Institut National Polytechnique de Grenoble (INPG), (2005), 03-19.

[66] J. Sadedhi and F. F. Samavati, *Smooth reverse subdivision,* Computers and Graphics, 33 (2009), 217-225.

[67] J. Sadedhi and F. F. Samavati, *Smooth reverse Loop and Catmull-Clark subdivision,* Graphical Models, 73 (2011), 202-217.

[68] M. Sakai and R. A. Usmani, *On exponential splines,* J. Approx. Theory, 47 (1986), 122-131.

[69] S. S. Siddiqi, W. us Salam and K. Rehan, *Construction of binary four and five point non-stationary subdivision schemes from hyperbolic B-splines,* Applied Mathematics and Computation, 280 (2016) 30-38.

[70] E. J. Stollnitz, T. D. DeRose and D. H. Salesin, *Wavelets for computer graphics,* San Francisco; Morgan Kaufmann Publishers, (1996).

[71] P. Sablonniére, D. Sbibih, M. Tahrichi, *High-order quadrature rules based on spline quasi-interpolants and application to integral equations,* Applied Numerical Mathematics, 62 (2012), 507-520.

[72] P. Sablonniére, D. Sbibih, M. Tahrichi, *Superconvergent Nyström and degenerate kernel methods for Hammerstein integral equations,* Journal of Computational and Applied Mathematics, 258 (2014), 30-41.

[73] P. Sablonniére, *A quadrature formula associated with a univariate spline quasi interpolant,* BIT Numerical Mathematics, 47 (2007), 825-837.

[74] I. J. Schoenberg and A. Sharma, *Cardinal interpolation and spline fucntions V. The B-splines for cardinal Hermite interpolation,* Linear Algebra and its Applications, 7 (1973), 1-42.

[75] H. P. Seidel, *On Hermite interpolation with B-splines,* Computer Aided Geometric Design, 8 (1991), 439-441.

[76] L. L. Schumaker, *On shape preserving quadratic spline interpolation,* SIAM Journal on Numerical Analysis, 20 (1983), 854-864.

[77] I. J. Schoenberg and A. Sharma, *Contributions to the problem of approximation of equidistant data by analytic functions,* IJ Schoenberg Selected Papers. Springer, (1988), 3–57.

[78] L. L. Schumaker, *Spline Functions: Basic Theory, John Willey and Sons,* Inc. New York, (1981).

[79] M. Unser and T. Blu, *Cardinal exponential splines: Part I–Theoryandfiltering algorithms,* IEEE Trans. Signal Process, 53.4 (2005) 1425-1438.

[80] M. Unser, A. Aldroubi and M. Eden, *On the asymptotic convergence of B-spline wavelets to Gabor functions,* IEEE transactions on information theory, 38.2 (1992), 864–872.

[81] S. Valette, J. Rossignac and R. Prost, *An efficient subdivision inversion for wavemesh-compression of 3D triangle meshes,* IEEE International Conference on Image Processing (ICIP'03), 1 (2003), 777-780.

[82] V.G. Zakharov, *Operator adapted wavelets: connection with Strang–Fix conditions,* Int. J. Wavelets Multiresolut. Inf. Process. 10 (2012), 1250006.

[83] G. Wang and Y. Li, *Optimal properties of the uniform algebraic trigonometric B-splines,* Computer Aided Geometric Design, 23 (2006), 226-238.

[84] Y. Xu, *Recursions for Tchebycheff B-splines and their jumps,* Approximation theory, wavelets and applications (Maratea, 1994), 543-555, NATO Adv. Sci. Inst. Ser. C Math. Phys. Sci., 454, Kluwer Acad. Publ., Dordrecht, (1995).

[85] J. Zhang, *C-Bézier curves and surfaces,* Graphical Models and Image Processing, 61.1 (1999), 2-15.

FICHE PRÉSENTATIVE DE LA THÈSE

▷ **Nom et Prénom de l'auteur : Mohamed Ajeddar**

▷ **Intitulé du travail**: *A study of non-polynomial splines and their Numerical applications*

▷ **Encadrant : Abdellah Lamnii**, Professeur à la Faculté des Sciences et Techniques, Settat, Maroc.

▷ **Lieux de réalisation des travaux** (laboratoires, institution,...):

∗ *Laboratoire de Mathématiques, Informatique et Sciences de l'ingénieur, Faculté des Sciences et Techniques, Settat, Maroc.*

▷ **Période de réalisation du travail de thèse**: Novembre 2017–Mars 2022.

▷ **Rapporteurs** (nom, prénom, grade, institution) :

• **Mohamed Louzar**, Professeur de l'enseignement supérieur, Faculté des Sciences et Techniques, Université Hassan I, Maroc.
• **Mohammed Mestari**, Professeur de l'enseignement supérieur, ENSET Mohammedia, Université Hassan II, Maroc.
• **Aziz Ikemakhen**, Professeur de l'enseignement supérieur, Faculté des Sciences et Techniques, Université Cadi Ayyad, Maroc.

Liste des publications

1. M. Ajeddar, A. Lamnii, *Smooth reverse subdivision of uniform algebraic hyperbolic B-splines and wavelets*, , International Journal of Wavelets, Multiresolution and Information Processing. (2021): 2150018. https://doi.org/10.1142/S0219691321500181.

2. M. Ajeddar, A. Lamnii, *Trigonometric Hermite interpolation method for Fredholm linear integral equations*, Journal of Applied Analysis, (2021).

3. M. Ajeddar, A. Lamnii, *An efficient computation of Wavelets based on UAT B-splines reverse subdivision*, Springer (1st International Conference in Applied Mathematics to Finance, Marketing and Economics), (2022).

Communications orales

- M. Ajeddar, A. Lamnii, Uniform hyperbolic polynomial B-spline curves, *International Conference on Technology, Engineering and Mathematics (TEM)*, 26-27 March 2018, ENSA Kenitra.
- M. Ajeddar, A. Lamnii, Uniform algebraic hyperbolic B-spline curves with a tension parameter α, *3ème Journée Scientifique sur les Méthodes de Modélisation en Sciences Physiques et Mathématiques Appliquées*, 27 décembre 2018, FST Mohammedia.
- M. Ajeddar, A. Lamnii, Smooth reverse subdivision of UAT B-spline curves and wavelets, *International Conference on Fixed Point Theory and Applications (ICFPTA'19)*, 30 November 2019, Mohammedia-Maroc.
- M. Ajeddar, A. Lamnii, Uniform algebraic Trigonometric spline Quasi-interpolants and the integral equations, *3nd International Conference on Mathematics and Its Applications (ICMACASA2020)*, 28-29 Février 2020, FSAC Casablanca.
- M. Ajeddar, A. Lamnii, Trigonometric Hermite interpolation method for Fredholm integral equations, *The* 1^{st} *Conference in Applied Mathematics: Finance, Marketing and Economics (ICAMFME'20)* , 26-27 October 2020, ENCG EL Jadida.
- M. Ajeddar, A. Lamnii, Trigonometric Hermite interpolation method for Fredholm linear integral equations, *8ème édition de la Journée Doctorant du CEDoc STSM*, 08 juillet 2021, FST Settat.

Communications affichées

- M. Ajeddar, A. Lamnii, Uniform algebraic hyperbolic B-spline curves and subdivision scheme, 7 ème édition de la *"Journée Doctorant"*, 2 Mai 2018, FST Settat.